DNA-damage-induced apoptosis in stem and cancer cells

Citation

Permanent link

Terms of Use

Share Your Story

DNA-damage-induced apoptosis in stem and cancer cells

A dissertation presented

by

Julia Chang Liu

to

The Committee on Higher Degrees in Biophysics

in partial fulfillment of the requirements

for the degree of

Doctor of Philosophy

in the subject of

Biophysics

Harvard University

Cambridge, Massachusetts

January 2014

Dissertation Advisor: Professor Galit Lahav   Julia Chang Liu

DNA-damage-induced apoptosis in stem and cancer cells

ABSTRACT

This work comprises analyses of cell fate decision-making in response to DNA damage. DNA damage is a ubiquitous threat to genomic stability, and depending on the type and extent of the damage, can lead to widespread changes in cell function as well as cell death. How apoptosis, or programmed cell death, is triggered in damaged cells was studied in different cell types for different types of damage.

Cell fate decisions are the outcome of information processing in signaling networks. When cells are challenged by DNA damage, the p53 network plays an important role in regulating diverse responses, including DNA repair, cell cycle arrest, senescence, and apoptosis. The function of the p53 network in human embryonic stem cells (hESCs) and their differentiated progeny was characterized. Unexpectedly, little distinction in the p53 response between hESCs and differentiated cells was found. Instead, higher damage sensitivity in hESCs compared with differentiated cells was discovered to be determined by mitochondrial priming.

Heterogeneity in cellular damage responses was further explored in cancer cells in response to the chemotherapy drug cisplatin. p53 dynamics were analyzed in single cells after cisplatin-induced DNA damage. While half the population underwent apoptosis and half survived, both apoptotic and surviving cells reached similar levels of p53. However, cells that entered apoptosis accumulated p53 faster than cells that survived cisplatin treatment. Hence, a "dynamic threshold" model for p53-dependent apoptosis was proposed, suggesting the threshold level p53 must reach to induce apoptosis increases with time. Computational modeling was used to explore possible mechanisms by which faster p53 increase could lead to

apoptosis.

A new flow cytometry method to concurrently detect progression through apoptosis simultaneously with cell cycle phase across a population of cells was developed. This technique, using the vital dye DyeCycle Violet and the apoptotic stain YOPRO, allows quick and easy assessment of apoptosis and cell cycle arrest in multiple conditions.

Overall, this set of experiments and analyses demonstrates the importance of signaling networks and their interactions in determining cell state and damage sensitivity. Using systems biology approaches to study cellular decision-making may contribute to scientific understanding and clinical impact.

Contents

List of Figures

Dedicated to my grandmother.

has been a blessing to have such solid support from these and many other people. All the people in the Systems Biology department truly make it a friendly and engaging environment to work and learn.

I owe a huge thank you to my Dissertation Advisory Committee: Stephen Elledge, George Daley, and Suzanne Gaudet. Their guidance has been invaluable and they truly exemplify the finest quality of the Harvard faculty. Thank you also to my Thesis Committee: George Daley, Suzanne Gaudet, and Derrick Rossi.

I thank my roommates, Ashley Wolf, Sarah Pfau, Emily Capra, and Julie Kim, for the wonderful years we've lived together in Cambridge. They have made our apartment truly a warm and loving home and have been my family throughout graduate school.

I am so grateful to have had my parents with me every step of the way. My family has given me every opportunity and have always believed in me, and their love and support mean the world to me.

Finally, I would like to thank Eric Batchelor. He is a fantastic scientist, a patient and careful reader of multiple drafts of this thesis, and most importantly, my best friend.

The text is typeset in LaTeX using Andrew Leifer's modified version of Jordan Suchow's template, available at:

`http://github.com/aleifer/LaTeX-template-for-Harvard-dissertation`.

Page intentionally left blank.

Yet, our problem is the living organization and therefore our interest will not be in properties of components, but in processes and relations between processes realized through components.

Humberto Maturana and Francisco Varela, 1980

1

Introduction

LIVING ORGANISMS, AND THE CELLS COMPRISING THEM, are not static objects. They exist in complex and constantly changing environments, and must respond appropriately to a variety of internal and external stimuli. To survive in such changing conditions, cells must detect signals and then process that information to adapt their cellular state to the new condition, for instance by altering gene expression or metabolism. Hence, cells are able to sense and respond to beneficial changes in environment, such as availability of a nutrient, or deleterious changes,

such as starvation. The signaling networks responsible for cellular information processing are composed of interacting proteins and genes that jointly coordinate cellular functions.

Signaling networks respond to numerous cellular stresses, including DNA damage. In the absence of a proper damage response, cellular proliferation without repair of DNA strand breaks can lead to the detrimental accumulation of mutations. Mutations that facilitate deregulated proliferation or predispose cells to acquire further mutations are often associated with the development of cancer. Hence, cells protect themselves from genomic instability by activating the DNA damage response, which ensures that the cell will stop dividing and initiate DNA repair. In cases of significant or irreparable damage, the DNA damage response will lead the cell to undergo irreversible cell fates such as senescence (permanent cell cycle arrest) or apoptosis (programmed cell death). Thus, determining the appropriate response for the level and type of damage is critical.

1.1 THE P53 NETWORK RESPONDS TO DNA DAMAGE

The tumor suppressor p53 is a central protein in mammalian biological networks that respond to stress. p53 is one of the most frequently mutated proteins in human cancers, and somatic mutations in p53 have been found in half of human tumors (Greenblatt et al., 1994). Moreover, in tumors that retain wild-type p53, mutations in p53-associated pathways often render p53 inactive. Inheritance of p53 mutations causes propensity to development of rare tumors in childhood and predisposition to early-onset common cancers in adulthood. Such germline p53 mutations define the condition known as Li-Fraumeni syndrome. Consistent with p53's function as a barrier to tumor progression, restoration of wild-type p53 can

promote the regression of tumors in vivo (Ventura et al., 2007, Xue et al., 2007). For the above reasons, p53 is commonly known as the "guardian of the genome" (Lane, 1992).

The p53 network is relatively well characterized (Figure 1.1). Under basal conditions, p53 is expressed at low levels, primarily due to a negative feedback loop through the E3 ubiquitin ligase Mdm2. p53 activates transcription of Mdm2, which negatively regulates p53 by targeting it for ubiquitination and degradation. Upstream of p53, damage-sensing kinases such as ataxia telengiectesia mutated (ATM) and checkpoint kinase 2 (Chk2) are activated by phosphorylation upon formation of DNA double-strand breaks (DSBs) caused by gamma irradiation. Transcription of the p53 gene remains constant; instead, active ATM-P and Chk2-P phosphorylate the p53 protein, leading to its stabilization and accumulation. After DNA damage, p53 and Mdm2 show pulses. These pulsatile dynamics were originally characterized as damped oscillations from population-averaging studies, but were later shown to be pulses of fixed amplitude and duration in single-cell experiments. The negative feedback loop between p53 and its negative regulator Mdm2 was found to be insufficient for recurrent p53 pulses; rather, there is a second negative feedback loop from p53 to the upstream signaling kinases via the phosphatase Wip1 (Batchelor et al., 2008, Geva-Zatorsky et al., 2010). Wip1 is a transcriptional target of p53 and can dephosphorylate p53 as well as ATM-P and Chk2-P, shutting down their activity (Fujimoto et al., 2006, Lu et al., 2005, Shreeram et al., 2006). As a result of these feedbacks, p53 pulses after DSB induction show excitability (Batchelor et al., 2008, Loewer et al., 2010). Similar to an action potential in a neuron, a pulse of p53 will complete its full excitation once activated, even if the stimulus is inhibited during the pulse. Furthermore, each pulse
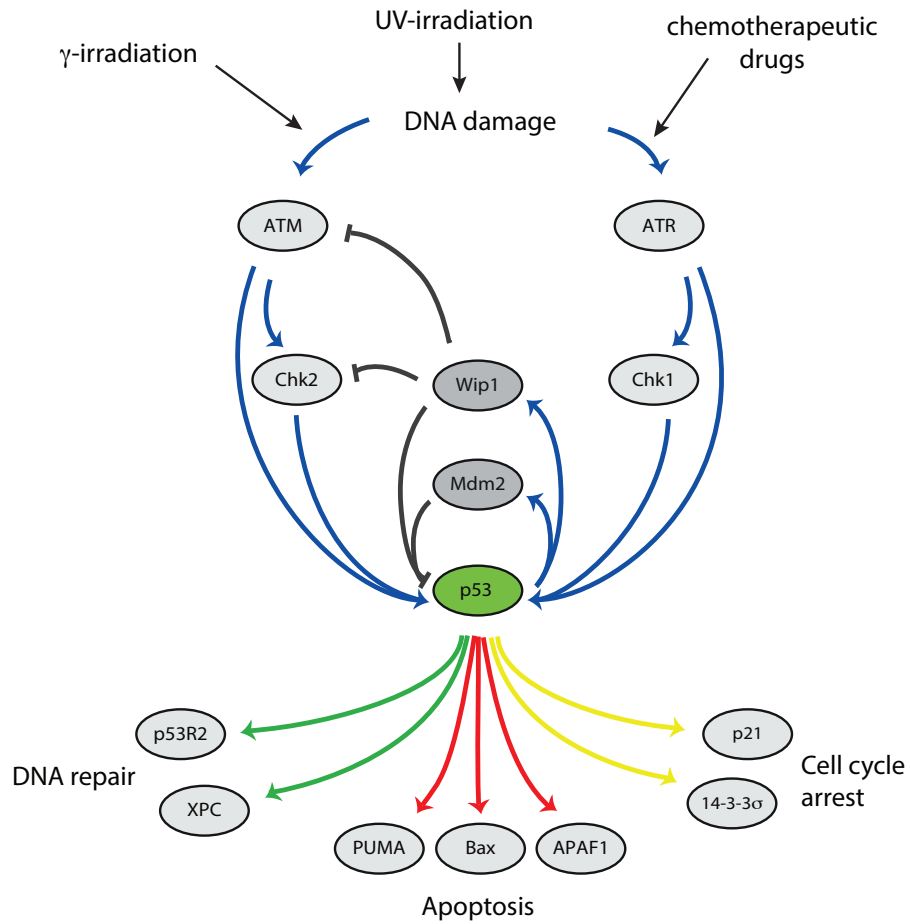
Figure 1.1: The p53 network. Schematic of the upstream and downstream interactions involved in the p53 response to damage. For simplicity, not all known interactions are shown; inhibitory arrows from ATM and ATR to Mdm2 and from Wip1 to Chk1 have been omitted for clarity. Adapted from Alexander Loewer and Eric Batchelor.

of p53 has nearly uniform amplitude and duration independent of the dose of damage, and it is the number of pulses that correlates with the damage dose (Lahav et al., 2004). Based on these findings, our current understanding of post-DSB p53 dynamics is that p53 behavior is more closely analogous to successively triggered pulses rather than autonomous oscillations. This model is termed recurrent initiation (Batchelor et al., 2008).

Different types of damage can lead to different patterns of p53 dynamics. As mentioned, gamma irradiation leads to DSBs, activating ATM and a series of undamped pulses of p53. In contrast, UV irradiation induces different types of DNA lesions, two classes of which are cyclobutane–pyrimidine dimers (CPDs) and 6–4 photoproducts (6–4PPs, which are pyrimidine adducts) (Sinha and Häder, 2002). Repair of these lesions via nucleotide excision repair and base excision repair transiently produces single-stranded DNA. Single-stranded DNA (ssDNA) induced by UV irradiation leads to the activation of the ataxia telangiectasia and Rad3 related (ATR) protein kinase and a single dose-dependent p53 pulse (Batchelor et al., 2011). This single p53 pulse, unlike the pulses triggered by DSBs, is not excitable, as inhibition of ATR shortly following UV irradiation attenuates the accumulation of p53, suggesting that the p53 pulse is dependent on continuous ATR activation. Excitability of the p53 response to DSBs and not to ssDNA was shown to be dependent on several differences in two pathways, including feedback from Wip1 on ATM and not ATR, and rapid degradation of Mdm2 upon its phosphorylation by ATM. Hence, network architecture contributes to a graded-amplitude p53 response to UV irradiation that is distinct from the pulsatile p53 response to gamma irradiation (Batchelor et al., 2011). That the dynamics of p53 are dependent on the stimulus and that different stimuli – gamma versus UV irradiation – activate

distinct targets of p53 (Zhao et al., 2000), suggest that p53 dynamics could be important for the regulation of cell fate decisions.

Of clinical relevance, many drugs used to treat cancers cause DNA damage but in functionally different ways from gamma or UV irradiation. For instance, the chemotherapy drug cisplatin has been used to treat solid tumors, including testicular and ovarian cancers (Kelland, 2007). A platinum complex, it forms both interstrand and intrastrand DNA crosslinks. The DNA adducts caused by cisplatin are detected by various DNA damage-sensing and repair pathways (Helleday et al., 2008), and also lead to a p53 response. The dynamics of p53 and subsequent cellular responses following cisplatin treatment will be discussed in Chapter 3.

One possible response to DNA damage is transient cell cycle arrest and DNA repair. In this case, cells survive, repair DNA breaks induced by the damage, and then re-enter the cell cycle. p53 is an important mediator of cell cycle arrest and DNA repair and activates the transcription of genes involved in both processes. For instance, CDKN1A, SFN, and CDC25C are p53 target genes involved in cell cycle arrest, and DDB2, GADD45A, and XPC are p53 targets associated with repair (Purvis et al., 2012, Riley et al., 2008). In single cells, pulses of p53 triggered by DNA DSBs have been observed to correlate with the number of DSBs induced (Loewer et al., 2013). Higher levels of damage lead to more p53 pulses, suggesting that the extent of DNA repair is monitored and that persistent damage will continue to trigger p53.

p53 also has target genes involved in permanent cell cycle arrest, termed senescence. One example is the CDKN1A gene, encoding the protein p21, which has important roles in both temporary arrest and senescence. The cell fate decision between arrest and senescence is dependent on p53 dynamics after damage. When

pulses of p53 after gamma irradiation were altered to create a sustained level of p53 activation, the expression of downstream target genes of p53 changed (Purvis et al., 2012). Notably, p21 levels were significantly higher in sustained p53 conditions. Consistent with that observation, sustained p53 led to a greater fraction of cells that underwent senescence, instead of transient cell cycle arrest and re-entry into the cell cycle (Purvis et al., 2012). These findings suggest that p53 dynamics might encode information to specifically select a particular cell fate.

1.2   THE APOPTOTIC PATHWAY IN DAMAGED CELLS

The most acute terminal response to DNA damage is apoptosis. Comprising multiple stages, apoptosis is a highly stereotyped mode of cell death (Elmore, 2007). It plays an important role not only in defense against damage but also in development, aging, and homeostasis, and is considered a type of "programmed" cell death. In contrast to necrosis, or uncontrolled cell death that is often the result of injury or trauma, apoptosis does not trigger inflammation and an immune response. It is characterized morphologically by cell shrinkage, chromatin condensation, and nuclear fragmentation (Taylor et al., 2008). The plasma membrane exhibits "blebbing" – formation of bulges and protrusions – and portions of the cell are encapsulated into membrane-bound vesicles named apoptotic bodies, which contain cytoplasm, organelles, and nuclear fragments. Apoptotic bodies are recognized and engulfed by phagocytes such as macrophages, and hence apoptosis does not generate an immune response (Kerr et al., 1972).

Unlike the extrinsic apoptotic pathway, which occurs via the binding of extracellular death ligands to transmembrane receptors, the intrinsic pathway is non-receptor-mediated and relies on intracellular signaling, for instance the DNA

damage response. Both pathways converge upon the mitochondria, the sites of apoptotic initiation. Mitochondrial outer membrane permeabilization (MOMP) is one of the first steps in apoptosis and occurs when Bax (Bcl-2-associated X protein) and/or Bak (Bcl-2-antogonist/killer-1) become activated via conformational changes and oligomerize at the mitochondrial outer membrane (Dewson and Kluck, 2009). Following MOMP, multiple events occur, including the release of cytochrome c from the mitochondrial intermembrane space into the cytoplasm, where it can trigger the formation of the apoptosome. The apoptosome is a large protein complex assembled from cytochrome c and Apaf-1 (apoptotic protease-activating factor-1), which recruits pro-caspase-9 and results in the allosteric activation of caspase-9 (Acehan et al., 2002).

Caspases (cysteine aspartic acid-specific proteases) are a family of highly specific proteases, subdivided into initiators and effectors (Nicholson, 1999). Caspase-9, for instance, is an initiator caspase and can auto-activate and activate other caspases through proteolytic processing. Thus, active caspase-9 propagates a cascade of downstream caspase activation. Caspase-3, -6, and -7 are the effector caspases responsible for cleavage of the majority of substrates during apoptosis, including cytoskeletal proteins such as actins, tubulins, and associated proteins (Taylor et al., 2008). Caspases also activate endonucleases that mediate DNA fragmentation and chromatin condensation. A multitude of proteins involved in various cellular functions are also attacked by caspases, including poly(ADP-ribose) polymerase (PARP) (Duriez and Shah, 1997). PARP cleavage serves as a hallmark of apoptosis and caspase activation, and its presence is often used experimentally for detection of apoptosis.

In addition to the identification of cleavage products of caspases, there are

many other methods to detect apoptosis. Caspase activation can be assayed by Western blot or other antibody-based techniques. Other features of apoptosis that serve to identify it experimentally include DNA fragmentation, which can be detected by the TUNEL (Terminal dUTP Nick End-Labeling) method (Gavrieli et al., 1992, Kressel and Groscurth, 1994). Membrane-based assays take advantage of biochemical properties of apoptotic cells, including the movement of phosphatidylserine from the inner leaflet of the plasma membrane, where it resides in healthy cells, to the outer membrane leaflet as a signal for phagocytosis. When phosphatidylserine is thus exposed, it can be detected by Annexin V, a recombinant phosphatidylserine-binding protein (Koopman et al., 1994). Assays to detect apoptosis will be discussed in more detail in the Appendix.

Control and regulation of apoptotic mitochondrial permeabilization are the responsibility of the Bcl-2 family of proteins (Figure 1.2). These proteins, defined by conserved sequence motifs known as Bcl-2 homology domains (BH1 to BH4), include both pro-apoptotic and pro-survival members (Youle and Strasser, 2008). Bcl-2 itself and its close relatives Bcl-xL, Bcl-w, and Mcl-1 contain all four BH domains and are anti-apoptotic. The pro-apoptotic proteins of this family can be divided into the Bax-like subfamily, including Bax, Bak, and Bok, which have BH1, BH2, and BH3 but lack BH4, and the BH3-only subfamily, which have homology only within the BH3 motif, which is essential for pro-death function. Bax and Bak as mentioned above are required for triggering MOMP, and their activation, allosteric conformational change, and oligomerization are induced by the "activator" BH3-only proteins Bid and Bim (Chipuk et al., 2010). The other BH3-only proteins, including Bad, Puma, and Noxa among others, are termed "sensitizers," as they do not induce activation of Bax/Bak directly. Instead, they promote apopto-
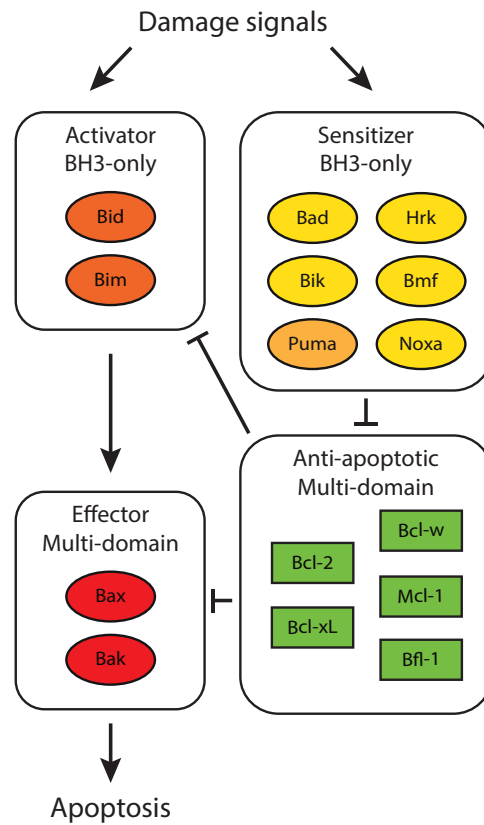
Figure 1.2: The Bcl-2 family of pro-apoptotic and anti-apoptotic proteins. In response to damage, activators activate effectors, causing mitochondrial permeabilization and commitment to death. Anti-apoptotic proteins sequester activators, and sensitizers act as selective inhibitors of anti-apoptotic proteins. Pro-apoptotic proteins are shown in ovals and anti-apoptotic proteins in rectangles. Puma is colored differently to indicate that it may also act as an activator (Kim et al., 2006). Adapted from Deng et al., 2007.

sis by occupying and inhibiting the anti-apoptotic proteins, freeing the activators. There is evidence that Puma can also function as an activator (Kim et al., 2006). In short, anti-apoptotic Bcl-2 family members bind and sequester pro-apoptotic BH3-only proteins and also block activation of Bax and Bak. In response to damage, the stabilization, increased transcription, or modification of BH3-only proteins counteract and overwhelm the reserve of anti-apoptotic proteins, leading to Bax and Bak activation and MOMP (Huang and Strasser, 2000).

At least two major roles for p53 in regulating cell-intrinsic apoptosis have been described. p53 mediates the transcription of multiple target genes whose protein products are known to be involved in apoptosis, such as Puma, Noxa, Bax, and Apaf1 (Oda et al., 2000a, Riley et al., 2008). After damage, synthesis of these pro-apoptotic proteins can be upregulated dependent on transcription by p53. In addition, multiple studies show that p53 can promote apoptosis by directly interacting with mitochondrial proteins (Green and Kroemer, 2009, Speidel, 2010). p53 was shown to bind and antagonize anti-apoptotic proteins such as Bcl-2 and Bcl-xL, resulting in MOMP and cytochrome c release (Mihara et al., 2003, Tomita et al., 2006). Other studies have demonstrated that p53 can directly activate Bax and also release other pro-apoptotic proteins from Bcl-xL (Chipuk et al., 2004). This role of p53 as a direct activator of Bax could be complemented by joint function of p53's transcriptional target Puma as a sensitizer, relieving p53 from binding with Bcl-xL (Chipuk et al., 2005). p53 function as an activator may also pertain to Bak as well as Bax, as p53 has been observed to disrupt Bak sequestration by Mcl-1, leading to oligomerization and activation of Bak (Leu et al., 2004, Pietsch et al., 2007). p53 may also act as a sensitizer, as Tet-inducible p53 can displace the BH3-only activator Bim from anti-apoptotic proteins including Mcl-1, Bcl-2,

and Bcl-xL (Han et al., 2010). Taken together, it is clear that p53 potentially has multiple protein-protein interactions with pro-apoptotic and anti-apoptotic Bcl-2 family members. Hence, p53 exhibits both transcription-dependent and transcription-independent activity in promoting apoptosis.

1.3 THE DNA DAMAGE RESPONSE IN STEM CELLS

Different cell types favor different responses to cellular stress, ranging from cell cycle arrest and DNA repair to senescence or apoptosis. Human embryonic stem cells (hESCs) are known to be acutely sensitive to DNA damage. As an important cell population that gives rise to all tissues in the body, hESCs are expected to undergo apoptosis after damage to prevent damaged cells from compromising the genomic integrity of the organism. Conversely, adult stem cells may need to be resistant to DNA damage, as unchecked apoptosis might compromise tissue and organ structure. Hence stem cells are caught between two opposing needs: on one hand they should block the propagation of mutations to their progeny cells, yet on the other hand they have a responsibility to preserve existing tissue organization.

Multiple studies have shown that hESCs have higher rates of apoptosis after damage than differentiated cells (Filion et al., 2009, Grandela et al., 2008, Qin et al., 2006), yet this phenomenon is still incompletely understood. Several distinct mechanisms have been proposed to explain how the regulatory networks that control apoptosis might have unique functions in hESCs (Figure 1.3). Not only is p53 well-known regulator of cell fate decisions in somatic cells (Vousden and Lane, 2007), it is also induced after various types of damage in hESCs. Furthermore, apoptosis of hESCs was shown to be dependent on p53 (Grandela et al., 2008, Qin et al., 2006). However, multiple studies suggest diverse roles for p53 in

promoting apoptosis in hESCs. Consistent with its transcription factor activity, p53 was found to translocate to the nucleus of hESCs upon treatment with etoposide, an inhibitor of topoisomerase II (Grandela et al., 2008). In contrast, in hESCs treated with UV irradiation p53 does not transcribe target genes but instead activates apoptosis through the mitochondrial pathway (Qin et al., 2006). More recently, the pro-apoptotic protein Bax, a transcriptional target of p53, was shown to be a major activator of rapid apoptosis in hESCs. hESCs, unlike differentiated cells, maintain Bax in its active conformation at the Golgi apparatus (Dumitru et al., 2012). Upon DNA damage caused by etoposide, Bax rapidly localizes to the mitochondria and initiates apoptosis. While Bax translocation is also observed to be dependent on p53, the exact mechanism generating the translocation remains unclear. Interestingly, the basal level of active Bax varies substantially among different hESC lines, and is not detectable in at least one line (H1) (Dumitru et al., 2012). Nonetheless, H1 cells show the typical hESC sensitivity to DNA damage, suggesting that apoptosis can also be induced by other mechanisms (Liu et al., 2013).

In Chapter 2, we will thoroughly discuss our investigations on DNA damage-induced apoptosis in hESCs in comparison with their differentiated progeny (Liu et al., 2013). Briefly, activation of apoptosis was dependent on p53, consistent with previous findings. The transcription of apoptotic target genes of p53, including PUMA, APAF1, and FAS, was induced after damage in hESCs. However, these same genes were also upregulated in differentiated cells, suggesting that p53 transcriptional activity does not distinguish hESCs from differentiated cells. p53 was observed in the cytoplasm of hESCs, and a cytoplasm-confined mutant p53 confirmed that cytoplasmic p53 alone is able to induce apoptosis. However, cy-
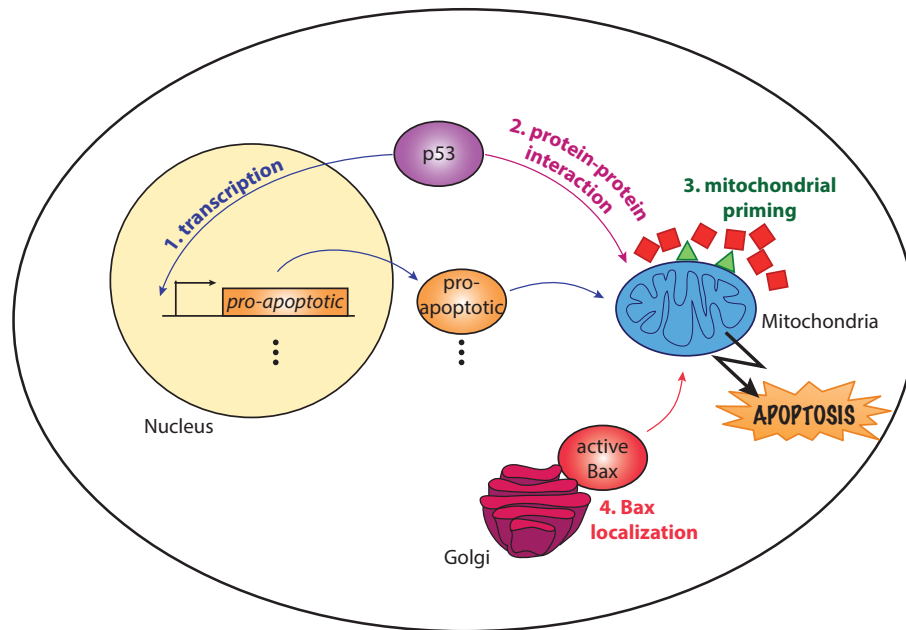
Figure 1.3: Multiple pathways contribute to hESC sensitivity to DNA damage.
1) The tumor suppressor protein p53 acts as a transcription factor, activating transcription of pro-apoptotic target genes. The pro-apoptotic protein products proceed to induce apoptosis at the mitochondria. 2) p53 also has transcription-independent direct interactions with pro-apoptotic and anti-apoptotic proteins in the cytoplasm that promote apoptosis. 3) High mitochondrial priming, implying a high ratio of pro-apoptotic to anti-apoptotic proteins, maintains hESCs close to the apoptotic threshold. 4) The apoptotic protein Bax is localized in its active conformation at the Golgi apparatus in some hESCs, poised to induce rapid apoptosis after damage-induced translocation to the mitochondria.

toplasmic p53 was also present in differentiated cells. These results led to the hypothesis that while p53 signaling appeared similar in hESCs and differentiated cells, the internal environment of the two cell types differs and explains their differential sensitivity to DNA damage.

Recent studies have shown that sensitivity to DNA damaging drugs could be predicted by a cellular property termed mitochondrial priming. Mitochondrial priming is determined by the balance between pro-apoptotic and anti-apoptotic Bcl-2 family proteins (Certo et al., 2006). As described above, the functions of the anti-apoptotic proteins Bcl-2, Bcl-xL, Mcl-1, etc. are to antagonize Bak and Bax activation and oligomerization, whereas pro-apoptotic BH3-only proteins promote Bak and Bax activation, in many cases by inhibiting the anti-apoptotic proteins. The relative abundance and impact of the pro-apoptotic and anti-apoptotic proteins can be measured by BH3 profiling (Ni Chonghaile et al., 2011). BH3 profiling quantifies the magnitude of mitochondrial depolarization, representing MOMP, upon exposure to a panel of pro-apoptotic, promiscuously interacting BH3 peptides. Greater sensitivity to the BH3 peptides indicates closer proximity to the apoptotic threshold, as MOMP can be initiated more readily. Moreover, some BH3-only proteins (for example, Bid and Bim) interact with effectively all anti-apoptotic Bcl-2 proteins, whereas others (for example, Noxa) interact only with certain Bcl-2-family members. Due to differential binding of anti-apoptotic proteins to the different BH3-only proteins, BH3 profiling can be used to probe which anti-apoptotic proteins contribute more or less to blocking apoptosis in a particular cell line or tissue (Deng et al., 2007). Consistent with their higher damage sensitivity, hESCs exhibited higher mitochondrial priming for all BH3 peptides than their differentiated progeny and hence were closer to the apoptotic

15

threshold. We concluded that in different cellular environments, the function of the same signaling pathway - the p53-regulated DNA damage response - produces a dramatic difference in cell fate between hESCs and differentiated cells.

Altogether, the problem of how multiple networks interact and sum together to produce the appropriate cellular response to a given stimulus is complex and not fully understood. This thesis discusses some processes known to contribute to the DNA damage response in several cell types. In particular, the p53 protein plays a prominent role in the regulation of downstream pathways leading to different cell fates, including apoptosis. In Chapter 2, we discuss our investigation of the function of p53 in hESCs. We show that while DNA-damage-induced apoptosis is p53-dependent, mitochondrial priming determines hESCs' sensitivity to damage. In Chapter 3, we analyze quantifiable characteristics of p53 behavior that influence the cell fate decision of colon cancer cells in response to the chemotherapy drug cisplatin. Finally, we include an Appendix describing the flow cytometry assay we developed to measure the effects of a drug or other perturbation on both cell cycle phase and apoptosis. Together, this work presents examples of how regulatory networks interact to commit to a particular cell fate. Using a variety of methods, from population to single cell assays, we develop greater insight into individual molecular mechanisms regulating cell fate decisions, as well as the interconnected relationships among the mechanisms.

He whose eye happens to look down into the yawning abyss be-
comes dizzy.

Søren Kierkegaard

2

High mitochondrial priming sensitizes hESCs

to DNA damage

OF THE DIVERSE ARRAY OF POSSIBLE CELLULAR RESPONSES TO DNA DAMAGE - in-
cluding DNA repair, cell cycle arrest, senescence, and apoptosis - human embry-
onic stem cells (hESCs) primarily undergo apoptosis (Momcilovic et al., 2010, Wil-
son et al., 2010). hESCs are able to self-renew indefinitely and can differentiate
into all cell lineages in the body, making it particularly important that they main-

tain genomic integrity. Their high sensitivity to DNA damage and ability to differentiate make them a good model system for studying the regulatory networks that control apoptosis and how they differ between hESCs and their differentiated progeny.

One important protein controlling cell fate decisions in response to DNA damage is the tumor suppressor protein p53 (Vogelstein et al., 2000, Vousden and Lane, 2007). p53 was previously shown to be induced in response to DNA damage in hESCs, primarily triggering apoptosis (Filion et al., 2009, Grandela et al., 2008, Qin et al., 2006). In somatic cells, p53 is known to contribute to cell death through two primary mechanisms. First, nuclear p53 activates the transcription of pro-apoptotic proteins, such as PUMA, Bax, and NOXA (Villunger et al., 2003). Second, cytoplasmic p53 directly interacts with mitochondrial proteins, acting either as a direct activator of Bak and/or Bax oligomerization, or as a sensitizer, by sequestering anti-apoptotic proteins (Green and Kroemer, 2009). In hESCs, there is evidence that p53 triggers apoptosis exclusively through the mitochondrial pathway after UV irradiation (Qin et al., 2006). However, other work showed that p53 not only associates with mitochondria but also translocates to the nucleus in response to DNA breaks caused by the topoisomerase II-poison etoposide, suggesting that induction of apoptosis by p53 involves a transcription dependent pathway (Grandela et al., 2008). Additionally, the genome-wide transcriptome of hESCs after gamma irradiation revealed altered gene expression of primarily p53-dependent, pro-apoptotic transcripts (Sokolov et al., 2011).

The cellular responses of differentiated cells to DNA damage differ widely depending on the tissue of origin. For example, tissues vary drastically in their survival ability after irradiation: some tissues, including those comprising bone mar-

row, small intestine, thymus, and spleen, are acutely affected by even low doses of radiation, while tissues from kidney, heart, liver, and lung are relatively resistant (Gudkov and Komarova, 2003). While it is thought that sensitivity to DNA damage tends to be characteristic of highly proliferating cells, some rapidly dividing tumors are resistant to chemotherapy while other slowly dividing tumors are chemosensitive, suggesting that additional factors affect the cellular damage response (Gudkov and Komarova, 2003). Distinct p53 expression and activity in cells from different tissues can be a factor contributing to differential tissue sensitivity to DNA damage (Komarova, 1997). In addition, recent studies have found that cells' relative mitochondrial priming affects their sensitivity to DNA damaging drugs (Certo et al., 2006, Ni Chonghaile et al., 2011, Vo et al., 2012). Mitochondrial priming denotes the intrinsic potential of cells to undergo apoptosis due to the balance of pro- and anti-apoptotic Bcl-2 family proteins at the mitochondria, and can be assessed by BH3 profiling (Ni Chonghaile et al., 2011). This assay measures mitochondrial outer membrane permeabilization (MOMP) after mitochondria are exposed to pro-apoptotic promiscuously interacting BH3 peptides. Higher mitochondrial priming determined by BH3 profiling has been shown to correlate with clinical response in several cancers (Ni Chonghaile et al., 2011) as well as increased chemosensitivity (Vo et al., 2012).

Here we determined the origin of the sensitivity of hESCs to DNA damage compared with their differentiated progeny. Specifically we investigated whether the p53 pathway is differentially induced in hESCs and differentiated cells or whether other intrinsic cellular properties can explain the difference in sensitivity. We found that DNA damage rapidly induced p53-dependent apoptosis in hESCs. p53 target genes were also induced; however, inhibition of p53's transcriptional activ-
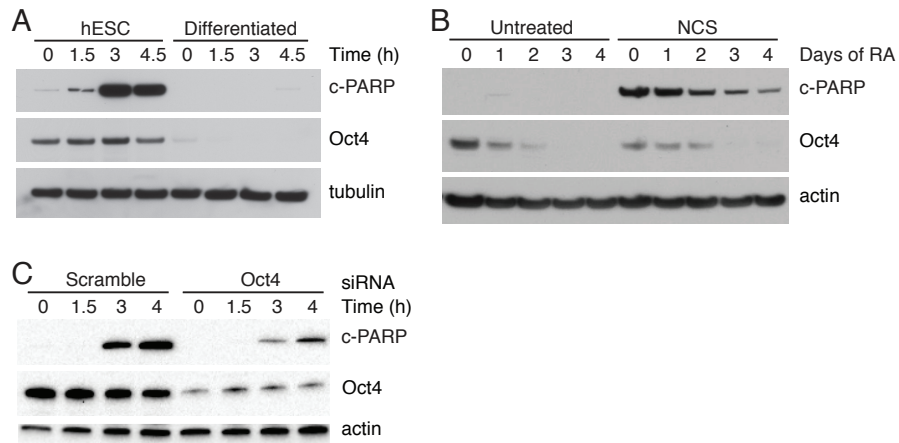
Figure 2.1: DNA damage leads to rapid apoptosis in undifferentiated hESCs but not in differentiated cells. A. Immunoblot of c-PARP and Oct4 in hESCs and differentiated cells treated with 100 ng/ml of NCS. B. Immunoblot of c-PARP and Oct4 of cells differentiated with $1\,\mu M$ RA for 0, 1, 2, 3, and 4 days, before and after NCS treatment for 3 hours. C. Immunoblot of c-PARP and Oct4 in hESCs transfected with scramble or Oct4 siRNA and treated with NCS.

ity or expression of exclusively cytoplasmic p53 did not prevent apoptosis, suggesting that p53's cytoplasmic function is the main contributor to apoptosis of hESCs. p53 was also induced in differentiated cells. Its localization and function did not differ between hESCs and differentiated cells. Instead, we found that differential mitochondrial priming, measured by BH3 profiling, determined the sensitivity of hESCs to DNA damage. hESCs showed high mitochondrial priming relative to their differentiated progeny. Increasing the low priming of differentiated cells increased their sensitivity to DNA damage and led to apoptosis.

2.1 DNA DAMAGE LEADS TO RAPID P53-DEPENDENT APOPTOSIS IN hESCs BUT NOT IN DIFFERENTIATED CELLS

We first characterized the response of hESCs to DNA damage and compared their behavior with that of differentiated cells from the same background. DNA damage was induced using the radiomimetic drug neocarzinostatin (NCS), which creates double-stranded DNA breaks (DSBs) within five minutes following its addition to cell culture medium (Shiloh et al., 1983). Cells were differentiated with 1 μM retinoic acid (RA) for 4 days (Andrews, 1984), and differentiation was confirmed using an antibody against Oct4, one of the key pluripotency genes in hESCs (Niwa et al., 2000). Induction of apoptosis was measured using an antibody against the 89-kDa fragment of cleaved PARP (c-PARP), which is cleaved during apoptosis by caspase-3. We found that hESCs accumulated c-PARP within 3 hours after DNA damage. In contrast, differentiated cells exhibited no c-PARP (Figure 2.1A). Treatment of hESCs with RA for shorter periods allowed us to investigate cells in the process of differentiation. We observed that decrease in Oct4 during RA treatment was correlated with reduction of c-PARP after damage (Figure 2.1B). We further demonstrated the strong connection between pluripotency and induction of apoptosis by silencing Oct4. Oct4 knockdown cells show a drastic reduction in c-PARP levels after damage in comparison with hESCs treated with scramble siRNA (Figure 2.1C). Sensitivity to DNA damage was confirmed in two additional hESC lines (Figure 2.2A,B), suggesting that the differential sensitivity between stem and differentiated cells is not limited to one specific line. Furthermore, the higher induction of c-PARP in hESCs compared with their differentiated progeny was consistently reproduced in response to additional DNA damage-inducing agents, includ-
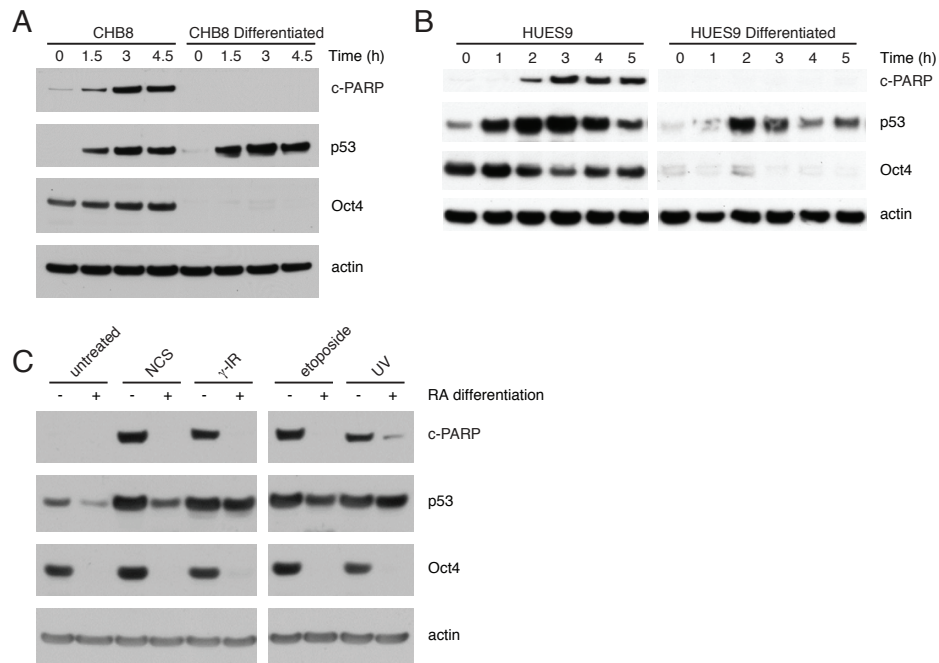
Figure 2.2: DNA damage leads to rapid apoptosis in undifferentiated hESCs but not in differentiated cells. A. Immunoblot of c-PARP, p53, and Oct4 in CHB8 hESCs and CHB8 cells differentiated with 1 μM RA for 4 days, treated with 100 ng/ml of NCS. B. Immunoblot of c-PARP, p53, and Oct4 in HUES9 hESCs and HUES9 cells differentiated with RA for 4 days, treated with NCS. C. Immunoblot of c-PARP, p53, and Oct4 in hESCs and differentiated cells, untreated or treated for 3 h with NCS, 2.5 Gy γ-irradiation, 5 μM etoposide, or 10 J/m² UV.

ing γ-irradiation, UV radiation and etoposide (Figure 2.2C).

Annexin V measurements confirmed that hESCs, but not differentiated cells, undergo apoptotic death after DNA damage (Figure 2.3A). Consistently, cell cycle analysis showed that the sub-G1 fraction of the population, which represents dead cells, increases rapidly in undifferentiated cells (Figure 2.3B). Over 50% of cells died within 3 hours after damage. In contrast, the sub-G1 fraction of the differentiated cells remained low following DNA damage. We noticed that a small fraction of hESCs survived the damage. To determine whether these were resistant stem cells, or spontaneously differentiated cells, we monitored the levels of Oct4 and c-PARP in the surviving cells 24 hours after damage. We found that the remaining cells were no longer Oct4-positive (Figure 2.3C), suggesting that they had already differentiated in culture or in response to the damage. These surviving differentiated cells were also c-PARP-negative, supporting pluripotency as a determinant of sensitivity to damage. In agreement, immunofluorescence (IF) experiments revealed that in a colony comprising both undifferentiated (Oct4-positive) and spontaneously differentiated (Oct4-negative) cells, c-PARP was only detectable in the undifferentiated cells (Figure 2.3D). This difference in sensitivity was not due to different extents of DNA damage incurred by NCS since the levels of γ-H2AX, the canonical marker for double strand breaks (Löbrich et al., 2010), were comparable between undifferentiated and differentiated cells (Figure 2.4). Taken together, these results show that hESCs, unlike their differentiated progeny, respond to DNA damage by rapidly undergoing apoptosis. This highly sensitive damage response is linked to pluripotency.

We next determined whether p53 plays a role in the induction of apoptosis in

23
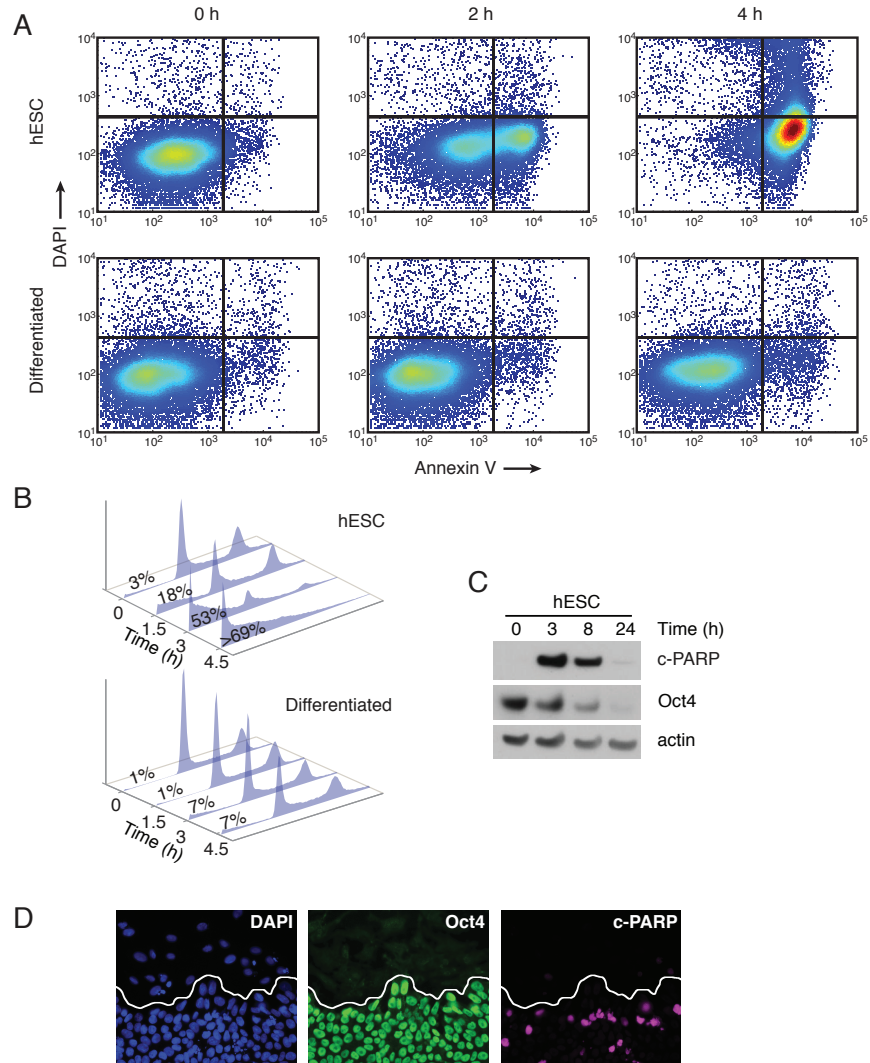
Figure 2.3: Confirmation of apoptotic cell death in hESCs but not differentiated cells. (**A**). Plots of DAPI incorporation (measuring cell permeabilization) versus Annexin V staining, of hESCs (top row) and differentiated cells (bottom row) treated with NCS for 0, 2, and 4 hours. (**B**). DNA content (propidium iodide incorporation) measured by flow cytometry of hESCs and differentiated cells, treated with NCS. The percentage of cells in the sub-G1 fraction is marked. (**C**). Immunoblot of c-PARP and Oct4 in hESCs at later time points after NCS treatment. (**D**). Immunofluorescence images of an hESC colony co-stained with DAPI and antibodies against Oct4 and c-PARP, fixed 2.5 hours after damage with NCS.

24
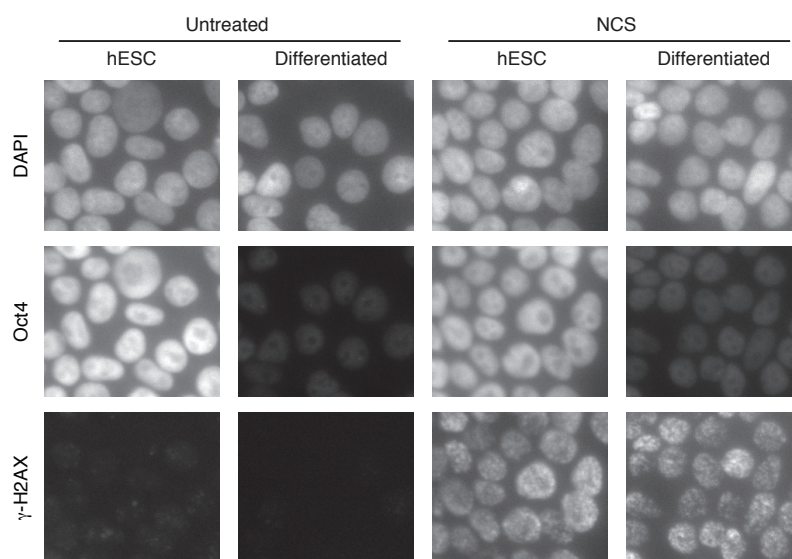
Figure 2.4: Undifferentiated and differentiated cells experience similar levels of NCS-induced DNA damage. Immunofluorescence images of hESCs and differentiated cells before and 15min after treatment with NCS. Cells were co-stained with DAPI and antibodies against Oct4 and γ-H2AX.
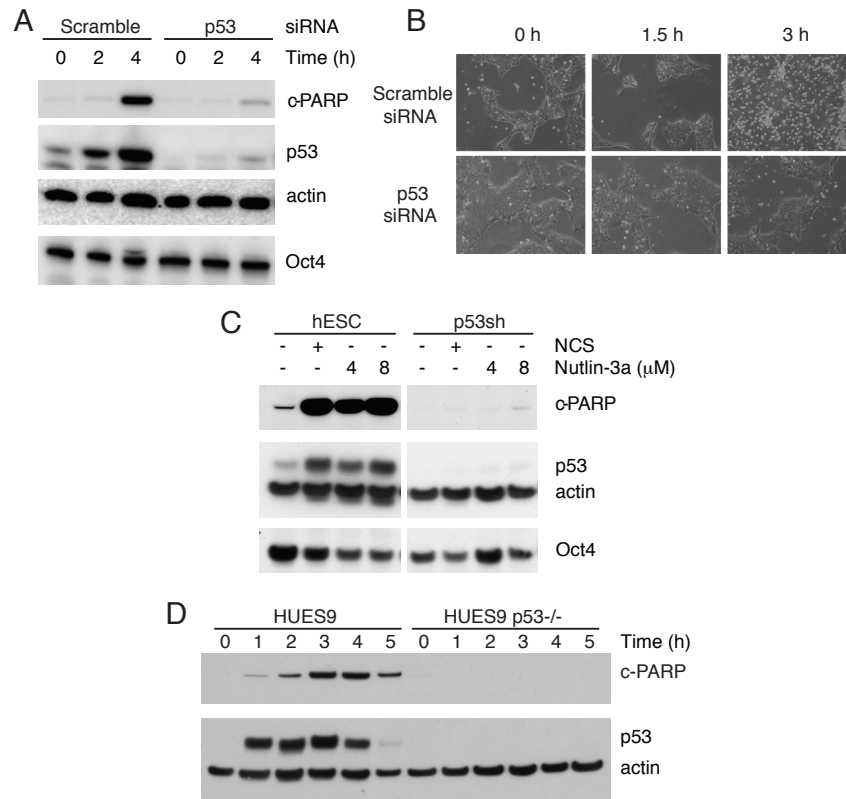
Figure 2.5: Apoptosis in hESCs is p53 dependent. (**A**). Immunoblot of c-PARP, p53, and Oct4 in hESCs transfected with scramble or p53 siRNA and treated with NCS. (**B**). Brightfield images of hESC colonies treated with either scramble or p53 siRNA, damaged with NCS for 0, 1.5, and 3 hours. (**C**). Immunoblot of c-PARP, p53, and Oct4 in hESCs and p53shRNA hESCs after 3 hours of NCS or 3 hours of Nutlin-3a treatment at the indicated concentrations. (**D**). Immunoblot of c-PARP and p53 in HUES9 and HUES9 p53-/- hESCs treated with NCS.

hESCs in response to DNA damage. p53 levels were induced in hESCs following DSBs (Figure 2.5A). Knocking down p53 using siRNA abrogated the c-PARP response (Figure 2.5A). In addition, cultures treated with siRNA against p53 did not show the colony shrinkage or the floating cells observed in damaged hESC cultures (Figure 2.5B). This shows that p53 is required for activation of the apoptotic pathway in hESCs in response to DNA damage. To determine whether apoptosis in hESCs can be triggered solely by elevation of p53 and independently of DNA damage we treated cells with Nutlin-3a. Nutlin-3a is a small molecule that inhibits the binding of Mdm2, a major negative regulator of p53, to p53, thereby increasing p53 stability (Vassilev et al., 2004). Nutlin-3a led to accumulation of p53 and c-PARP to levels comparable to those observed in response to DNA damage (Figure 2.5C). The ability of Nutlin-3a to trigger apoptosis in hESCs suggests that stabilization of p53 is sufficient to induce apoptosis without requiring additional damage-dependent post-translational modifications. To further strengthen the dependency of cell death on p53 we used a short hairpin RNA (shRNA) against p53 that is stably integrated into hESCs via lentiviral infection. Cells carrying the p53shRNA lost induction of p53 and showed no c-PARP after DNA damage and Nutlin-3a treatments (Figure 2.5C). Similar results were obtained when we used a different hESC line, HUES9, and compared c-PARP levels after NCS treatment between wild-type and p53-/- cells (Figure 2.5D).

p53 activates transcription of pro-apoptotic genes in both hESCs and differentiated cells. In somatic cells, p53 acts as a transcription factor activating many target genes, including pro-apoptotic genes (Riley et al., 2008). We asked whether p53 also activates transcription of pro-apoptotic genes in damaged hESCs, potentially contributing to their death in response to DNA damage. We used qRT-PCR
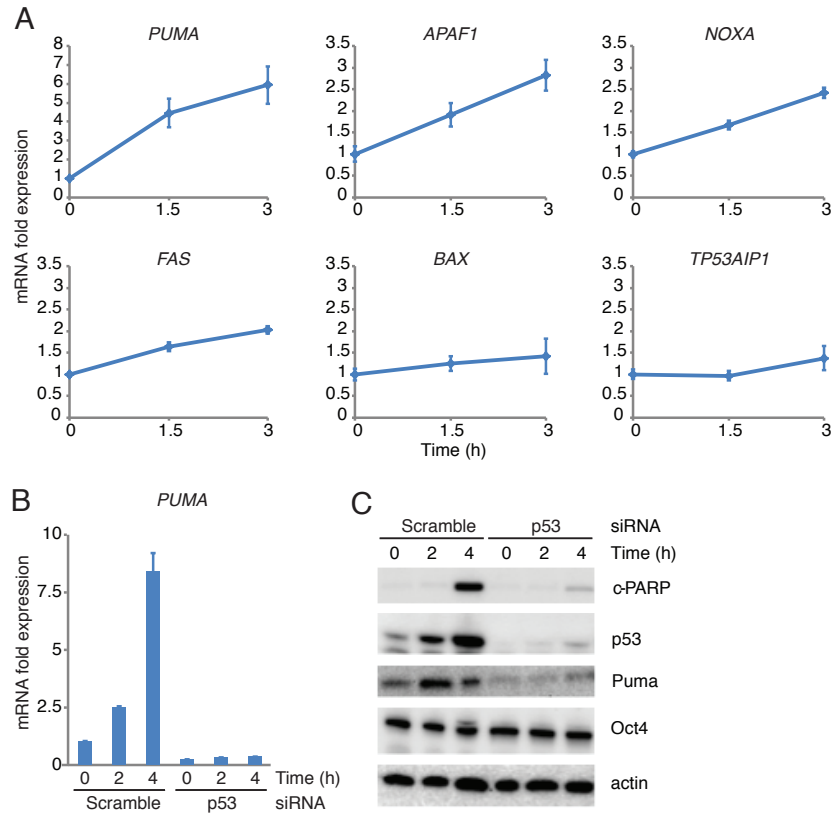
Figure 2.6: p53 transcriptional activity is induced after DNA damage. (A).
Relative mRNA expression of pro-apoptotic p53 target genes in hESCs treated
with 100 ng/ml NCS, as measured by RT-qPCR. mRNA levels were normalized
to GAPDH. (**B**). Relative PUMA mRNA expression after treatment with NCS in
hESCs transfected with scramble or p53 siRNA. (**C**). Immunoblots of c-PARP, p53,
PUMA, and Oct4 after treatment with NCS in hESCs transfected with scramble or
p53 siRNA. Data are represented as mean +/- SD.
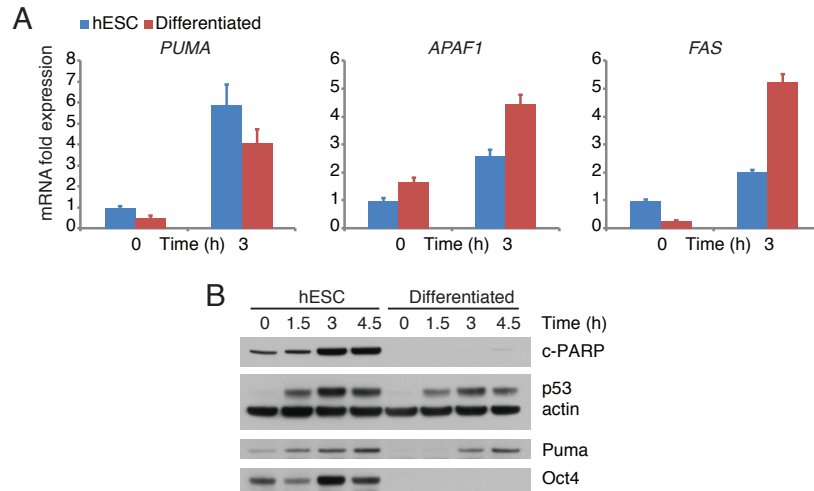
Figure 2.7: p53 transcriptional activity is not distinct between undifferentiated and differentiated cells. (**A**). Relative mRNA expression of pro-apoptotic p53 target genes in hESCs and differentiated cells, undamaged and after 3 hours of NCS. For all genes in both hESCs and differentiated cells, pre- and post-damage mRNA levels were statistically significant ($p<0.05$) as determined by Student's t-test. (**B**). Immunoblot of c-PARP, p53, PUMA, and Oct4 in hESCs and differentiated cells, damaged with NCS. Data are represented as mean $+/-$ SD.

to measure mRNA levels in hESCS of known p53 transcriptional targets involved in apoptosis (Müller et al., 1998, Nakano and Vousden, 2001, Oda et al., 2000a,b, Riley et al., 2008, Robles et al., 2001, Thornborrow et al., 2002). Two genes (BAX and TP53AIP1) showed almost no induction (Figure 2.6A). Three genes (FAS, APAF1, and NOXA) showed between 2- to 3-fold induction 3 hours after damage. Notably, PUMA, a gene encoding a pro-apoptotic BH3-only protein that inhibits anti-apoptotic proteins (Chipuk et al., 2005), showed more than 6-fold induction in mRNA level following DNA damage. PUMA mRNA and protein levels were significantly reduced in cells silenced for p53 suggesting that activation of PUMA following DNA damage is p53-dependent (Figure 2.6B,C).

Why do differentiated cells, which originated from the stem cell population, show such a remarkable difference in their sensitivity to DNA damage? One possibility is that p53 does not activate transcription of pro-apoptotic genes in differentiated cells. We compared mRNA levels of three pro-apoptotic p53 target genes (PUMA, APAF1, and FAS) between undifferentiated and differentiated cells. We found that these pro-apoptotic genes were induced in both undifferentiated and differentiated cells (Figure 2.7A). In the case of APAF1 and FAS, mRNA levels in differentiated cells even exceeded those in undifferentiated cells. Moreover, PUMA protein levels in differentiated cells reached comparable levels to those in undifferentiated cells, though the accumulation was slightly delayed in differentiated cells (Figure 2.7B). Taken together, these results show that p53 activates the transcription of pro-apoptotic genes in both differentiated and undifferentiated cells. Therefore, p53's transcriptional activity cannot explain the high sensitivity of hESCs to DNA damage compared with differentiated cells.

2.2   CYTOPLASMIC P53 CONTRIBUTES TO APOPTOSIS IN HESCS

It has been shown that in addition to acting as a transcription factor, p53 can also activate apoptosis through other mechanisms, for example by interacting with mitochondrial proteins in the cytoplasm (Green and Kroemer, 2009). To determine whether such transcription-independent mechanisms contribute to apoptosis in hESCs we used the RNA polymerase-II poison α-amanitin to inhibit transcription during the DNA damage response. Surprisingly we found that hESCs still activated apoptosis after DNA damage (Figure 2.8A) even when p53 target genes were not induced (Figure 2.8B). This apoptosis was p53-dependent, since the p53sh hESCs did not activate c-PARP following damage and α-amanitin treat-
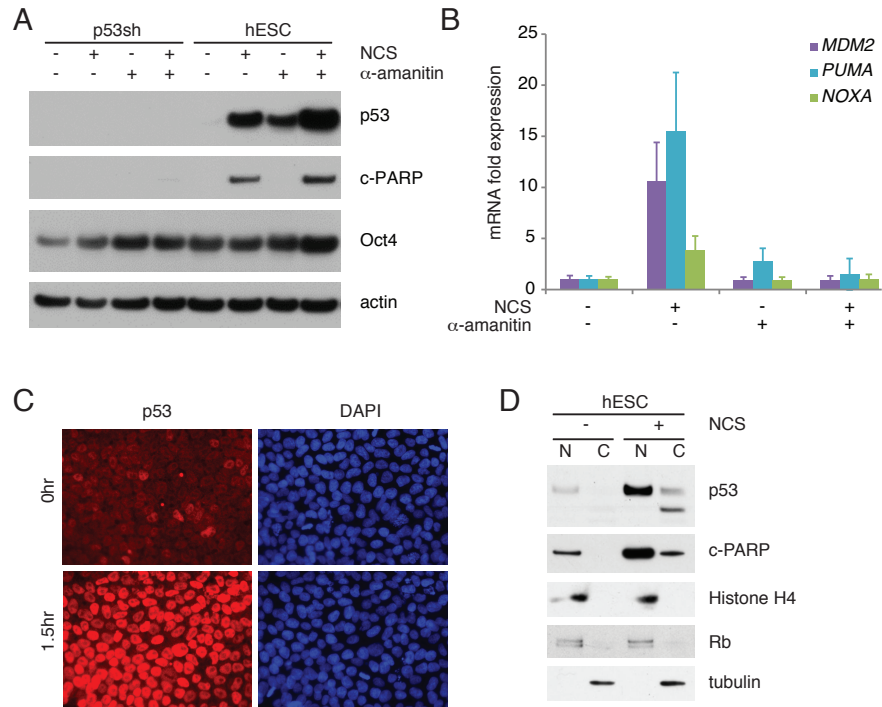
Figure 2.8: p53-induced apoptosis occurs even during inhibition of transcriptional activity. (**A**). Immunoblot of c-PARP, p53, and Oct4 in hESCs and a p53shRNA hESC line after 3 hours of 100 ng/ml NCS and/or 4 hours of 15 µg/ml α-amanitin treatment (1 hour pre-treatment when combined with NCS). (**B**). Relative Mdm2, PUMA, and NOXA mRNA expression of hESCs after 3 hours of NCS and/or 4 hours of α-amanitin treatment (1 hour pre-treatment when combined with NCS). Data are represented as mean +/- SD. (**C**). p53 and DAPI immunofluorescence images of hESCs fixed at the indicated times after treatment with NCS. (**D**). Immunoblot of p53 and c-PARP in the nuclear and cytoplasmic fractions of hESCs. Cells were undamaged or damaged with NCS for 3 hours. Histone H4 and the transcription factor Rb serve as nuclear markers, and tubulin as a cytoplasmic marker. N = nuclear, C = cytoplasmic.

ment (Figure 2.8A). These results show that even though p53 target genes are upregulated in damaged hESCs, p53 transcriptional activity is not the main contributor to the rapid apoptosis seen in these cells. We therefore checked whether the cytoplasmic activity of p53 contributes to the apoptotic response in hESCs. Using IF to probe the localization of p53 in damaged hESCs, we found that p53 appeared primarily nuclear (Figures 2.3D and 2.8C). However, by separating cell lysates into nuclear and cytoplasmic fractions, we found that a fraction of p53 (about 20%) resided in the cytoplasm following DNA damage (Figure 2.8D). These low levels of cytoplasmic p53 may be below the detection threshold of IF. To determine whether cytoplasmic p53 can activate apoptosis in hESCs, we expressed a mutant form of p53 confined to the cytoplasm and tested its ability to activate apoptosis. p53 contains a bipartite nuclear localization signal (NLS), part of which includes Lys305 and Arg306. The two amino acid substitutions K305A and R306A cause p53 to be excluded from the nucleus (O'Keefe et al., 2003). We cloned the K305A and R306A mutant p53 and fused it with an mVenus fluorescent tag. Using lentiviral infection, we introduced this mutant p53 (cytop53) into hESCs expressing p53shRNA. Cytop53 contains synonymous substitutions that render it resistant to shRNA knockdown. Cytop53 was exclusively expressed in the cytoplasm (Figure 3E) and showed no transcriptional activity (Figure 3F), in contrast to a wild-type p53-mVenus (wtp53). We found that cells expressing cytop53 successfully induced c-PARP after damage (Figure 3G). These results show that cytoplasmic p53 contributes to the activation of apoptosis in hESCs. The levels of c-PARP were lower in cells expressing cytop53 in comparison to cells expressing wtp53. This may result from reduced cytoplasmic function or misfolding due to the inserted mutations.
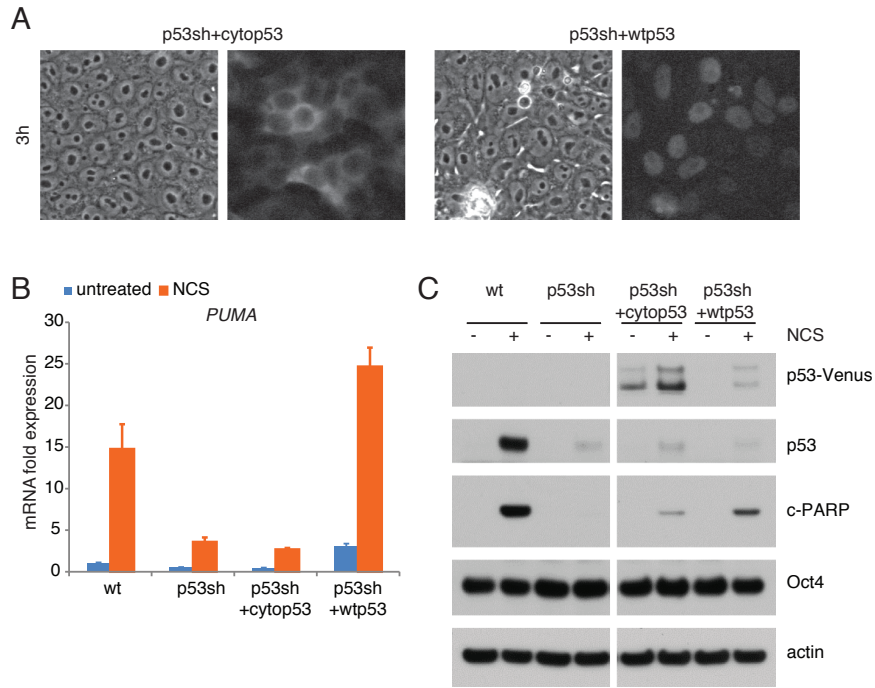
Figure 2.9: Residual cytoplasmic p53 is active in contributing to apoptosis in hESCs. (**A**). Phase and fluorescent images of p53shRNA hESC lines with re-introduced p53-mVenus (wtp53) and p53K305A,R306A-mVenus (cytop53) after 3 hours of damage with NCS. These cells were then collected for the immunoblots in (C). (**B**). Relative PUMA mRNA expression in parental hESCs (wt), p53shRNA hESCs (p53sh), and p53shRNA hESC lines with re-introduced p53-mVenus (wtp53) and p53K305A,R306A-mVenus (cytop53) before and after treatment with NCS. Data are represented as mean +/- SD. (**C**). Immunoblot of p53-Venus, p53, c-PARP, and Oct4 in parental hESCs (wt), p53shRNA hESCs (p53sh), and p53shRNA hESC lines with re-introduced p53-mVenus (wtp53) and p53K305A,R306A-mVenus (cytop53).

2.3 HESCs, UNLIKE DIFFERENTIATED CELLS, ARE HIGHLY PRIMED TO- WARD APOPTOSIS INDEPENDENTLY OF P53

Since p53's transcriptional activity is similar between hESCs and differentiated cells and cytoplasmic p53 can activate apoptosis in hESCs, we next examined two potential mechanisms that might explain the p53-dependent apoptosis observed only in undifferentiated cells. The first is that cytoplasmic p53 is active exclusively in undifferentiated cells. The second is that cytoplasmic p53 is active in both differentiated and undifferentiated cells, but other intrinsic properties of hESCs affect their sensitivity to damage. Specifically, recent studies showed that mitochondrial priming determines the survival of various cancer cells (Ni Chonghaile et al., 2011, Vo et al., 2012). We therefore first explored whether undifferentiated cells are intrinsically more "primed" for apoptosis than differentiated cells. Using BH3 profiling to measure MOMP induced by pro-apoptotic BH3-only peptides (Chonghaile et al., 2011), we found that undifferentiated cells underwent MOMP more readily than differentiated cells in response to each peptide in the panel, at all concentrations (Figure 2.10A). To better connect mitochondrial priming with differentiation we measured the priming level during the course of RA differentiation. Our results show a consistent trend: mitochondrial priming was highest in undifferentiated cells and decreased gradually with each additional day of differentiation (Figure 2.10B). We further showed that two other hESC lines were more primed than their differentiated progeny (Figure 2.10A), suggesting that the correlation between priming and pluripotency is not limited to one specific hESC line.

What might lead to high mitochondrial priming in hESCs? We first tested whether p53 itself contributes to high priming in undifferentiated cells. Silencing
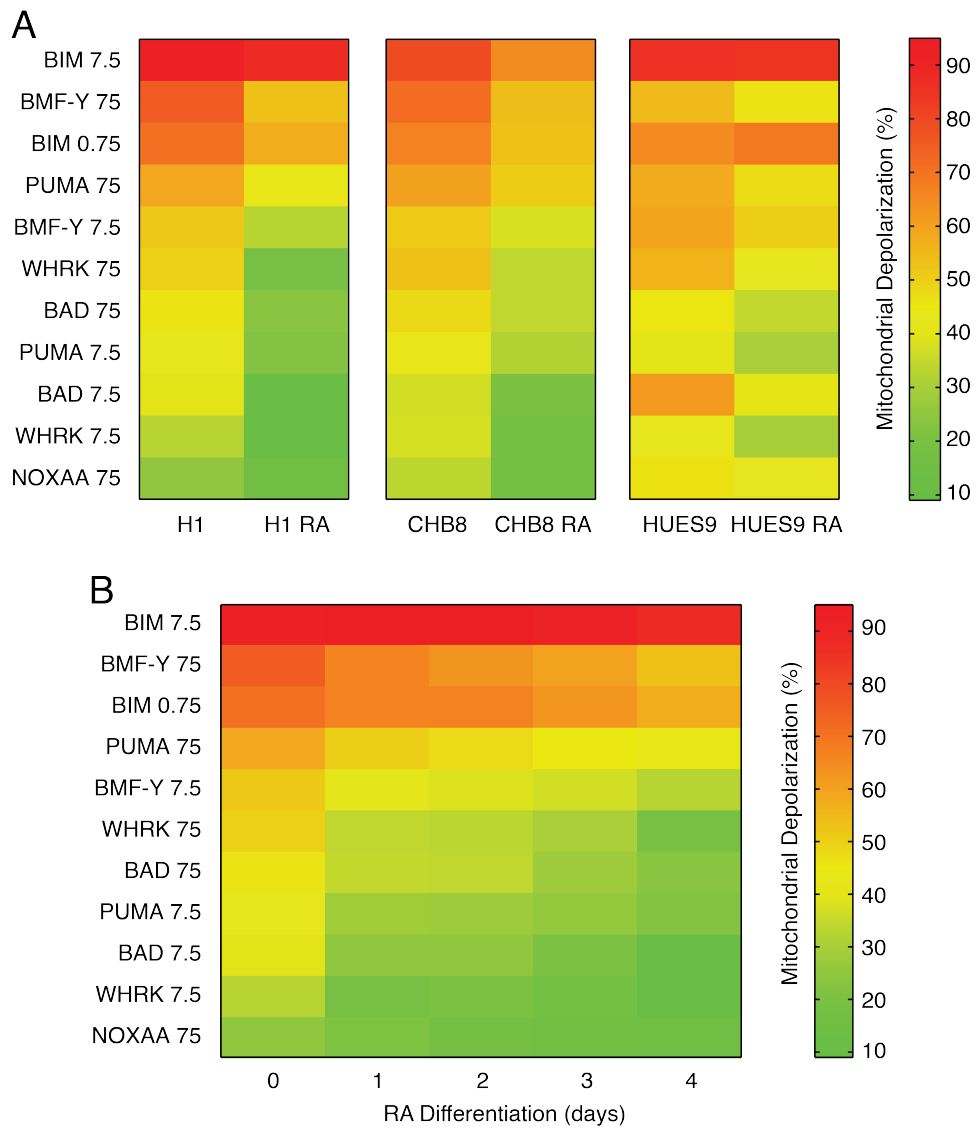
Figure 2.10: BH3 profiling reveals high priming of hESCs toward apoptosis.
(**A**). Heat map of mitochondrial depolarization (percentages indicated by colorbar) caused by BH3-only peptides at the indicated concentrations (μM) in hESCs and differentiated cells, for the three cell lines H1, CHB8, and HUES9. (**B**). Heat map of mitochondrial depolarization caused by BH3-only peptides in hESCs treated with 1 μM RA for 0, 1, 2, 3, and 4 days.

of p53 did not reduce priming; in fact, we found a slight increase in priming compared with hESCs expressing scramble shRNA (Figure 2.11A). Hence, hESCs can remain highly primed towards apoptosis independently of p53. Next, we sought to probe the status of the apoptotic machinery by measuring levels of pro- and anti- apoptotic proteins in hESCs and their differentiated progeny (Figure 2.11B). While most proteins showed comparable levels between undifferentiated and differentiated cells, we observed two differences that are consistent with the correlation between priming and pluripotency. Specifically, hESCs had lower levels of the anti-apoptotic protein Bcl-2 and higher levels of the pro-apoptotic protein PUMA (Figure 2.11B). Counterintuitively, undifferentiated cells showed higher levels of the anti-apoptotic protein Mcl-1. Taken together, these results suggest that Mcl-1 is not a major determinant of priming in hESCs; instead, the basal balance between other anti- and pro-apoptotic proteins, such as Bcl-2 and PUMA, contributes to the differential priming of undifferentiated and differentiated cells.

We next asked whether perturbing the balance between pro-and anti-apoptotic proteins can enable differentiated cells to activate apoptosis. We used ABT-263, a BH3-mimetic drug that binds and inhibits anti-apoptotic proteins including Bcl-2 (Tse et al., 2008), and we measured c-PARP after DNA damage. We found that differentiated cells treated with ABT-263 successfully activated apoptosis after damage (Figure 2.12A). This result suggests that the intrinsic balance of pro-apoptotic and anti-apoptotic proteins is closer to the apoptotic threshold in undifferentiated cells than it is in differentiated cells. Perturbation of this balance in differentiated cells changes their priming and leads to apoptosis. Notably, accumulation of c-PARP after damage in hESCs treated with ABT-263 did not exceed that in cells
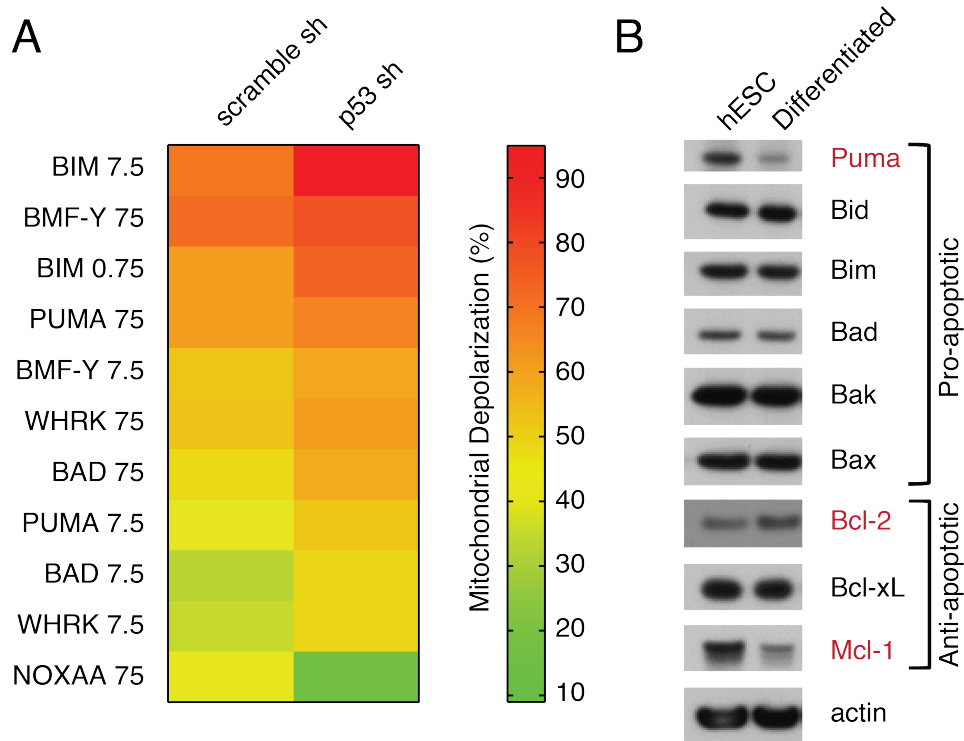
Figure 2.11: Priming in hESCs is dependent on the balance between anti- and pro-apoptotic proteins. (**A**). Heat map of mitochondrial depolarization caused by BH3-only peptides at the indicated concentrations (μм) in scramble shRNA and p53shRNA hESCs. (**B**). Immunoblots of pro- and anti-apoptotic proteins in hESCs and differentiated cells. Colored in red are proteins that show differential levels between hESCs and differentiated cells.

not treated with ABT-263 (lanes 2 and 4 of Figure 2.12A), suggesting that hESCs are already highly primed.

The observation that differentiated cells can trigger apoptosis when treated with ABT-263 suggests that p53 is fully functional in these cells. We have shown that apoptosis in undifferentiated cells results from p53 cytoplasmic activity. To determine whether cytoplasmic p53 is active only in hESCs and not in differentiated cells, we tested the localization of p53 in differentiated cells and the ability of cytoplasmic p53 to activate apoptosis in differentiated cells treated with ABT-263. First, we found that a small fraction of p53 was also localized to the cytoplasm in differentiated cells (Figure 2.12B). Next, we differentiated hESCs silenced for p53 and infected them with cytop53 and wtp53. Differentiated cells expressing the exogenous wtp53 showed behavior similar to that of their parental cells; they did not die after damage unless treated with ABT-263 (Figure 2.12C). Interestingly, differentiated cells expressing cytop53 also induced apoptosis after DNA damage under ABT-263 treatment, showing that cytoplasmic p53 is functional in differentiated cells, but lower mitochondrial priming in these cells prevents the activation of apoptosis in response to DNA damage.

In summary, we have shown that p53 exhibits similar apoptosis-inducing behavior in both undifferentiated and differentiated cells. However, differentiated cells are far from the apoptotic threshold, and p53 is unable to overcome this barrier. Only when the balance of pro- to anti-apoptotic proteins is altered in differentiated cells can p53 push cells toward apoptosis. In contrast, p53 can successfully push hESCs past the apoptotic threshold due to their highly primed state (Figure 2.13).
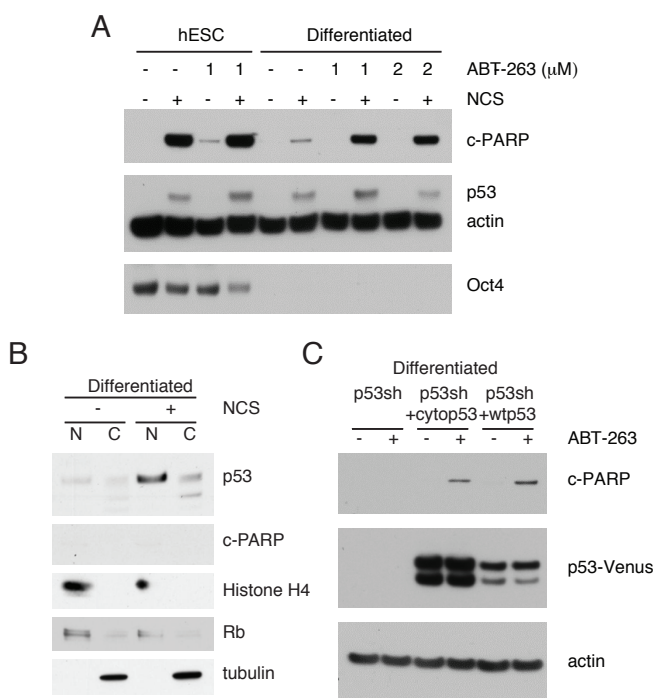
Figure 2.12: Increasing priming in differentiated cells leads to apoptosis after damage. (**A**). Immunoblot of c-PARP, p53, and Oct4 in hESCs and differentiated cells, untreated, treated with 100 ng/ml NCS for 3 hours, or treated with the indicated concentration of ABT-263 for 4 hours (1 hour pre-treatment when combined with NCS). (**B**). Immunoblot of p53 and c-PARP in the nuclear and cytoplasmic fractions of hESCs and differentiated cells. Cells were undamaged or damaged with NCS for 3 hours. Histone H4 and the transcription factor Rb serve as nuclear markers, and tubulin as a cytoplasmic marker. N = nuclear, C = cytoplasmic. (**C**). Immunoblot of c-PARP, p53, and Oct4 in cells differentiated from p53shRNA hESCs (p53sh), and where indicated, infected with wtp53 and cytop53 constructs. Prior to infection, cells were differentiated with 1 μM RA then passaged twice, maintaining RA in the media. All cells were treated with NCS for 3 hours, and where indicated, pre-treated with 1 μM ABT-263 for 1 hour before NCS addition.
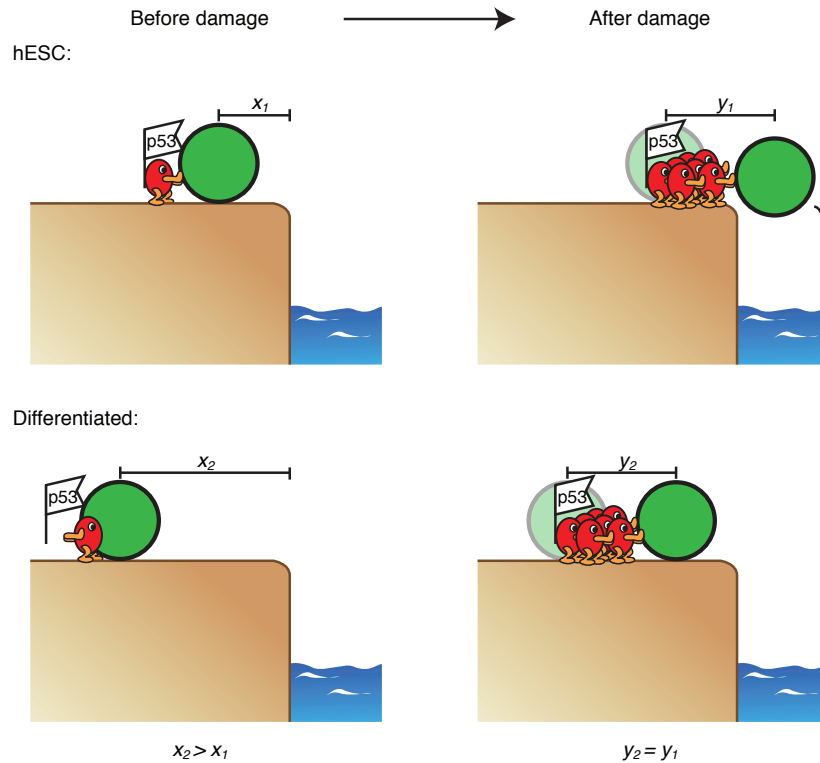
Figure 2.13: The proximity of hESCs, unlike differentiated cells, to the apoptotic threshold makes them sensitive to increased p53 after damage. Mitochondrial priming is depicted as proximity to the cliff's edge (the apoptotic threshold). A cell, shown as a green ball, is at distance x_1 from the edge if it is an hESC, and at distance x_2 from the edge if it is differentiated, where $x_2 > x_1$. Prior to damage, basal low levels of p53, represented as a red cartoon, are insufficient to push either an hESC or a differentiated cell over the cliff. Damage causes p53 to accumulate in both hESCs and differentiated cells to similar levels, with similar functions. The distance that p53 pushes the cell towards the cliff is represented by the displacement y_1 for the hESC and y_2 for the differentiated cell, where $y_1 = y_2$. For an hESC, $y_1 > x_1$, sufficing to push the cell over the cliff, crossing the apoptotic threshold and leading to cell death. In contrast, a differentiated cell is too far away from the edge ($y_2 < x_2$), so p53 function is insufficient to push the cell beyond the apoptotic threshold, allowing the cell to survive after damage.

2.4 DISCUSSION

A cell's decision among different cell fates is especially critical in response to challenging inputs such as DNA damage. Different cell types meet this challenge in a variety of ways. In cell types where maintenance of genomic integrity is crucial, such as hESCs, one might expect that signaling pathways are poised to cope with DNA damage aggressively by selecting terminal cell fates such as apoptosis. Here we show that hESCs use multiple pathways to ensure apoptosis is induced after damage, including activation of p53 transcription and cytoplasmic functions and high mitochondrial priming. We have shown that in hESCs p53's transcriptional activity is not required to induce apoptosis; rather, cytoplasmic p53 is sufficient for induction of apoptosis without transcription of downstream p53 target genes. Yet pro-apoptotic p53 target genes such as PUMA, NOXA, and APAF1 are up-regulated after damage in a p53-dependent manner, suggesting that hESCs may use the p53 transcriptional pathway as a second line of defense to ensure cell death in case cytoplasmic p53 fails to do so.

We have shown here that cytoplasmic p53 contributes to induction of apoptosis in hESCs. However, the mechanisms by which cytoplasmic p53 exerts its function remain open. A recent study showed that hESCs maintain active Bax that rapidly localizes from the Golgi to the mitochondria after damage, and that this translocation is p53-dependent (Dumitru et al., 2012). The role of p53 in generating the translocation of active Bax, however, remains unclear. Interestingly, this mechanism was employed to various extents by different hESC lines; the cell line primarily used in our study, H1, did not show active Bax under basal conditions (Dumitru et al., 2012). Yet we show here that H1 cells also undergo rapid apoptosis after DNA damage, suggesting cytoplasmic p53 can trigger the same end result

via other mechanisms.

While we have shown that the levels of the anti-apoptotic protein Bcl-2 and the pro-apoptotic protein PUMA are consistent with the high priming in hESCs in comparison with differentiated cells, the complete network that determines mitochondrial priming is likely to involve additional players. Even for apoptosis-regulating proteins that show similar levels in undifferentiated and differentiated cells (Figure 4C), specific modifications, localization, and protein interactions might affect their function and therefore generate differential priming. Furthermore, the relationship between priming and pluripotency might depend on other networks. For example, pluripotency is known to be linked to rapid cell cycle progression (Filipczyk et al., 2007), which may directly or indirectly affect the apoptotic machinery. Complete understanding of the mechanisms controlling priming will require global analysis of protein function and interaction in multiple pathways.

2.5 MATERIALS AND METHODS

Cell culture: Experiments were performed on H1 hESCs except where otherwise mentioned. H1 (also called WA01) was obtained from WiCell. CHB8, HUES9, and HUES9 p53-/- were kindly provided by George Daley, Doug Melton, and Yang Xu (Song et al., 2010) respectively. Cell culture was performed as previously described (Lerou et al., 2008). Briefly, hESCs were cultured feeder-free on plates treated with hESC-qualified Matrigel (BD Biosciences) in mTeSR-1 medium (Stemcell Technologies). The medium was changed daily, and cells were passaged every 4-6 days with 1 mg/ml Dispase (Stemcell Technologies). Differentiation of hESCs was induced by adding 1 μM RA (Sigma), with a fresh medium change daily.

Antibodies and reagents: Antibodies were used against p53 (DO1, Santa Cruz), actin (Sigma), Oct4 (Abcam), cleaved PARP-1 (Epitomics), PUMA (Cell Signaling), Histone H4 (Santa Cruz), tubulin (Developmental Studies Hybridoma Bank), ☐-H2AX (JBW301, Millipore), Bad (Santa Cruz), Bak (Millipore), Bax (Santa Cruz), Bid (Atlas), Bim (Cell Signaling), Mcl-1 (Cell Signaling), Bcl-2 (Santa Cruz), and Bcl-xL (Cell Signaling). Neocarzinostatin was obtained from Sigma and Nutlin-3a from Cayman Chemical.

Flow cytometry: Cell-cycle distributions were analyzed using propidium iodide. Annexin V measurements were performed using the Annexin V PE Apoptosis Detection Kit (eBioscience). Analysis was done in FlowJo and Matlab.

qRT-PCR: Total RNA was isolated using the RNeasy Mini Kit (Qiagen). cDNA was generated with the High-Capacity cDNA Reverse Transcription Kit (Applied Biosystems). For qPCR, reaction mixes were set up in triplicate using Power SYBR Green Master Mix (Applied Biosystems) and run using the CFX96 Real-Time System (Bio-Rad). mRNA levels were normalized to GAPDH expression, then relative expression calculated as fold-change from the untreated control.

Immunoblotting: Cells were harvested and protein extracts obtained by lysis in the presence of protease and phosphatase inhibitors. Total protein amount was quantified using the BCA assay (Pierce). Equal protein amounts were separated by electrophoresis on 4–12% Bis-Tris gradient gels (Invitrogen) and transferred to PVDF membranes by electroblotting. Membranes were blocked with 5% non-fat dried milk, incubated with primary antibody, washed, and incubated with secondary antibody coupled to horseradish peroxidase. Protein levels were detected using chemiluminescence (ECL 2, Pierce) after additional washing steps.

Immunofluorescence: hESC colonies were grown on Matrigel-coated glass cov-

erslips, fixed in 4% paraformaldehyde, permeabilized with 0.2% Triton X-100, and blocked in 3% BSA in PBS. Cells were incubated with primary antibody overnight at 40 C, washed, and incubated with Alexa Fluor-conjugated secondary antibody (Invitrogen) and counterstained with DAPI (Life Technologies).

siRNA knockdown: hESCs were dissociated into single cells in the presence of 10 μM Y27632 (StemGent) with Accutase (Stemcell Technologies) and plated at a density of 2×10^5 cells per well of a 6-well plate. The following day, cells were transfected with 250 pmol siRNA (Dharmacon) per well using Dharmafect1 transfection reagent. Media was changed 24 hours post-transfection, and experiments were performed 48-72 hours post-transfection.

Cell line construction: The p53shRNA construct with a blasticidin resistance cassette was kindly provided by the Agami lab (Brummelkamp et al., 2002). The cytop53 and wtp53 constructs are resistant to this p53shRNA due to silent point mutations described further below. The lentiviral vectors for cytop53 and wtp53 were created using standard molecular biology techniques to include an upstream ubiquitin promoter, p53, and an mVenus tag. Point mutations for the K305A and R306A amino acid substitutions in the NLS region of p53 for the cytop53 construct were introduced using site-directed mutagenesis (Quikchange kit, Agilent).

293T cells were transfected with the Agami lab p53shRNA construct and viral packaging vectors using the Mirus-293 transfection reagent, and viral supernatant was collected and concentrated. For viral infection, hESCs were dissociated and plated as described above for siRNA transfection. The following day, cells were infected with virus in media containing HEPES and protamine sulfate. Cells were allowed to recover in nonselective media for one day. Cells were thereafter maintained in 2 μg/ml blasticidin (InvivoGen), and a clonal line was selected from a

single colony.

The cytop53 and wtp53 constructs are resistant to the aforementioned p53shRNA, as their cDNA sequences contain the following 7 silent point mutations preserving the amino acid sequence: C777T, T778A, C779G, A781T, G782C, T786A and T789C. These point mutations were introduced using site-directed mutagenesis (Quikchange kit, Agilent) with the following primers:

5'-cctcaccatcatcacactggaggatagctctggaaacctactgggacggaacagctttgag-3' and

5'-ctcaaagctgttccgtcccagtaggtttccagagctatcctccagtgtgatgatggtgagg-3'.

For the cytop53 construct, point mutations for the K305A and R306A amino acid substitutions in the NLS region of p53 were introduced (Quikchange) using the following primers:

5'-ctgcccccagggagcactgcggcagcactgcccaac-3' and

5'-gttgggcagtgctgccgcagtgctccctggggggcag-3'.

The same viral production and infection procedures were used as for the p53shRNA construct.

BH3 profiling: hESCs were dissociated with Accutase, counted, and suspended in DTEB buffer (135 mM trehalose, 10 mM HEPES, 50 mM KCl, 20 µM EDTA, 20 µM EGTA, 5 mM potassium succinate, final pH 7.5) at 2.67×10^6 cells/mL. The cells were then added to an equal volume of 4X staining mastermix (4 µM JC-1, 40 µg/mL oligomycin, 20 mM 2-mercaptoethanol, 100 µg/mL digitonin in DTEB buffer) and allowed to stain for 10 minutes at RT. 15 µL of stained cells were added to wells containing 15 µL of peptides at 2X final concentration in DTEB to yield the final profiling plate with 20000 cells/well. Fluorescence at 590 nm was monitored using 545 nm excitation on a Tecan Safire 2 at a controlled temperature of 30C with automated readings every five minutes. The area under each pep-

tide response curve was calculated using Graphpad Prism, and these areas were normalized to the internal FCCP and DMSO controls as Depolarization (%) = 1 − ([sample-FCCP]/[DMSO-FCCP]).

2.6 Manuscript information

This chapter is adapted from Liu et al., 2013:

Julia C. Liu, Xiao Guan, Jeremy A. Ryan, Ana G. Rivera, Caroline Mock, Vishesh Agrawal, Anthony Letai, Paul H. Lerou, and Galit Lahav. High Mitochondrial Priming Sensitizes hESCs to DNA-Damage-Induced Apoptosis. *Cell Stem Cell*, 133(44):48348-491, October 2013.

Author contributions: Julia C. Liu conducted the experiments and performed the analysis, with help from co-authors. In particular, the BH3 profiling experiments and analysis were performed by Jeremy A. Ryan. Julia C. Liu and Galit Lahav wrote the paper.

A model is a lie that helps you see the truth.

Howard Skipper

3

p53 regulation of cell fate in response to cisplatin

IN CANCER THERAPY, one important goal is to eradicate cancer cells while preserving healthy cells. While our understanding of the genes and pathways that are dysregulated in cancer cells is increasing, we for the most part still have not developed methods to reliably target only those cells with the abnormalities. One challenge is that cancer cells themselves are a heterogeneous population that do

not all respond in the same way to identical treatment. When treated with a drug, some fraction of cancer cells might die while others recover and survive. This resistant population can eventually lead to tumor regrowth and acquire new mutations conferring further resistance. Thus, understanding what determines differential responses to chemotherapy drugs and manipulating these responses to improve therapeutic efficacy will be crucial.

3.1 CELLULAR RESPONSES TO CISPLATIN

One of the most effective broad-spectrum cancer drugs, cisplatin was accidentally discovered to inhibit *Escherichia coli* bacterial growth and only later was found to have anti-tumor activity (Shen et al., 2012). The mechanism of action of this small-molecule platinum compound is the formation of crosslinks in DNA, both inter-strand and intra-strand, as well as protein-DNA crosslinks. DNA crosslinks pose threats to normal cellular function, as they can interfere with transcription and cause stalled replication forks (Ide et al., 2011, Vare et al., 2012). The DNA adducts are detected by various DNA damage-sensing and repair pathways, as well as several important signaling pathways such as the Akt, p53, and MAPK pathways (Wang and Lippard, 2005).

Cisplatin is commonly used as a part of the treatment regimen for many solid tumor types, including head and neck, testicular, ovarian, cervical, lung, and colorectal cancers (Shen et al., 2012). Despite its widespread use, cisplatin therapy has several limitations, including toxicity and both inherent and acquired resistance. Even when a patient has a good initial response to cisplatin, often the development of cisplatin resistance results in relapse and diminished effectiveness (Siddik, 2003). Moreover, given the heterogeneity of cancer cells within a tumor,

fractional killing can result in some surviving cells that can seed tumor repopulation. Hence, the question of how drug treatment can lead to differential cell fate outcomes is of critical importance.

As colon cancer is one of the types of cancer treated by platinum-based compounds in the clinic, we undertook our study in HCT116 colon cancer cells. To determine how cisplatin affects HCT116 cell viability, we generated a dose response curve. The response of HCT116 to different doses of cisplatin was determined using the CellTiter-Glo assay (Promega), which measures ATP content as a proxy for cell viability. The dose response curve showed that ATP content decreased with increasing levels of cisplatin, and reached its half-maximal value at a cisplatin concentration of 12.5 µM (Figure 3.1A). We further characterized how a population of cells responds to this IC50 concentration of cisplatin by imaging and tracking cells by microscopy for 72 hours. At 12.5 µM cisplatin, approximately half of the cells die and half survive. Of the cells that die, the median time of death was 35 hours. The Jarque-Bera test confirmed that death times were normally distributed, and hence it can be inferred that 95% of cells that undergo apoptosis will die within 72 hours (Figure 3.1B).

Cisplatin-treated cells show a marked decrease in cell divisions. Compared to cells not treated with cisplatin, most of which completed 3 cell divisions in 72 hours, cells treated with cisplatin rarely divided more than once (Figure 3.1C). In a replating assay (Purvis et al., 2012), in which cells were replated after the 72 hour period and observed each day for the following 5 days, untreated cells continued to divide, while cells that survived the cisplatin treatment did not divide (Figure 3.1D). They also spread out and became very large, with a high cytoplasmic to nuclear ratio. These features are characteristic of senescent cells. From

49
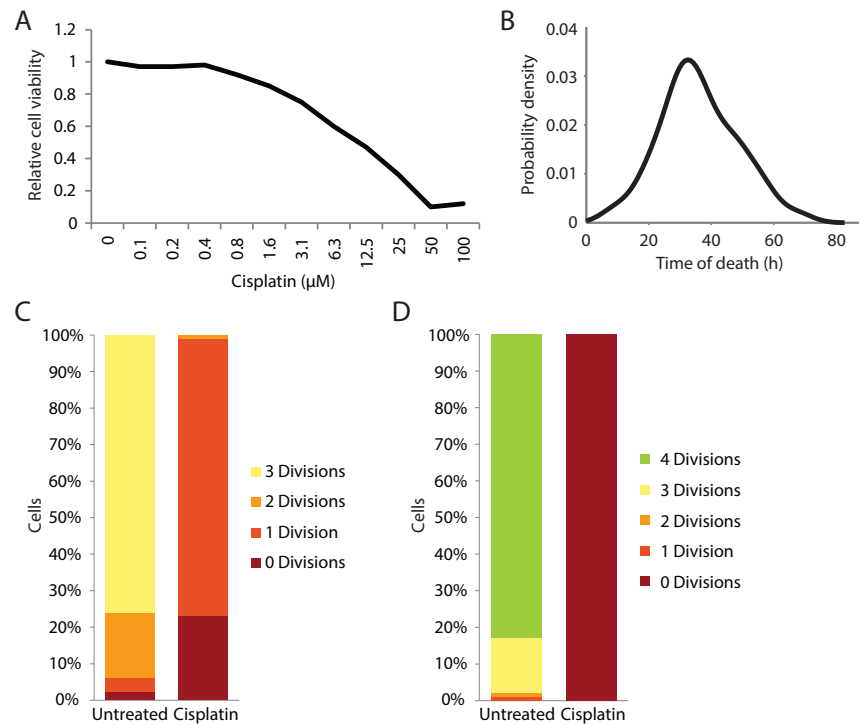
Figure 3.1: Cells treated with cisplatin undergo apoptosis or senescence. (**A**) ATP content, representing cell viability, as assayed by CellTiter-Glo on HCT116 cells treated with varying concentrations of cisplatin for 72 hours. (**B**) Probability density function for the distribution of death times of apoptotic cells after 12.5 μM cisplatin treatment. (**C**) Proportion of the cell population undergoing 0, 1, 2, or 3 divisions in 72 hours, untreated or after cisplatin. (**D**) Proportion of the cell population undergoing 0, 1, 2, 3, or 4 divisions in the 5 days after replating 72 hours after cisplatin treatment.

these data we infer that the half of the population that do not die instead enter senescence.

3.2 DEPENDENCY OF APOPTOSIS ON P53

Variation in tumor response to cisplatin is influenced by the genetic background of the tumor cells. As the tumor suppressor p53 is frequently mutated in cancer, many studies have evaluated the impact of its presence or absence on cisplatin sensitivity. While some studies suggest that p53 status has little effect on cellular response to cisplatin (Oliver et al., 2010), it has been found that wild-type p53 function in a National Cancer Institute (NCI) panel of 60 human cancer cell lines correlates positively with sensitivity to cisplatin (Vekris et al., 2004). Moreover, in ovarian cancer patients, p53 alterations correlate significantly with resistance to platinum-based chemotherapy, early relapse, and shortened overall survival (Reles et al., 2001). That p53 mutations may confer higher resistance to cancer cells implies that loss of p53 inhibits the transmission of the DNA damage signal to the apoptotic machinery (Siddik, 2003). Hence, p53 may play an active role in promoting apoptosis or other terminal cell fates in cells damaged by cisplatin. We therefore investigated post-cisplatin p53 behavior and function in the HCT116 cell line, which is wild type for p53.

To survey the p53 response to cisplatin in single living cells, we measured p53 using a fluorescent reporter construct. In our HCT116 background, the fluorescent protein mVenus was inserted at the 3' end of exon 12 of one allele of p53. The second p53 allele was unaltered. This HCT116 knock-in reporter cell line was treated with cisplatin and the level of p53 represented by the intensity of mVenus fluorescence was monitored by long-term time-lapse fluorescence microscopy ev-

ery 30 minutes for 72 hours. We verified that the HCT116 p53-mVenus knock-in (HCT116p53VKI) cell line showed similar dynamics of cell death after cisplatin treatment as the wild-type HCT116 line (Figure 3.2A). Moreover, we verified that post-cisplatin induction of apoptosis is to an extent dependent on p53, as HCT116 p53-/- cells were more resistant to cisplatin treatment. To test that the Venus reporter for p53 was faithful to the endogenous p53, we measured protein levels in the HCT116p53VKI cell line treated with cisplatin and confirmed that p53-mVenus dynamics resembled those of endogenous p53 (Figure 3.2B). p53 levels increase gradually after cells are treated with cisplatin, indicating that the p53 pathway is responsive to cisplatin-caused damage. On the single cell level, we observed that the dynamics of p53 accumulation were highly variable across cells. This spread suggests that p53 dynamics in individual cells could contribute to the decision between different downstream outcomes, as approximately half of the cells undergo apoptosis while the other half undergo senescence.

Several models have been suggested for how activation of p53 might induce differential downstream outcomes. The affinity model proposes that p53 might have different affinities for the promoters of downstream target genes effecting different outcomes, such as cell cycle arrest and apoptosis (Inga et al., 2002). Thus, if cell cycle arrest genes have promoters with high p53 affinity, they will be upregulated even with low p53 expression, whereas apoptotic genes with promoters with low p53 affinity will not be expressed until p53 accumulates to a high level. If this model were true, one would expect that low p53 induction would lead to expression of only cell cycle arrest target genes and not apoptotic target genes. In contrast to the affinity model, the threshold model does not rely on differences in p53 binding affinity but rather hypothesizes that the different types of p53
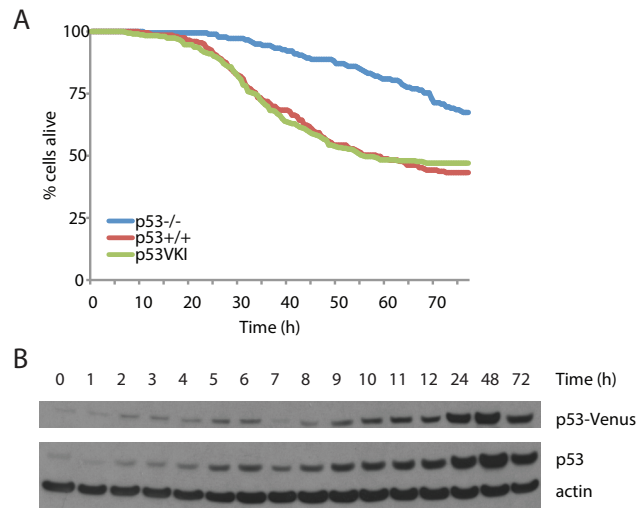
Figure 3.2: HCT116 expressing p53-Venus reliably represent wild-type HCT116. (**A**) Percentage of cells remaining alive as measured by microscopy after cisplatin treatment in three cell lines, HCT116 p53-/-, HCT116 p53+/+ (wild-type), and HCT116 with p53-mVenus knock-in (p53VKI). (**B**) Immunoblot of HCT116VKI protein levels at the indicated times after treatment with 12.5 μM cisplatin. Actin serves as a loading control.

target genes are concurrently expressed to the degree to which p53 is expressed (Kracikova et al., 2013). Low levels of p53 and hence low levels of its arrest and apoptotic targets will not cross the apoptotic threshold, but high levels of p53 for a long duration will result in increased expression of all target genes, including apoptotic ones, and eventually will cross the apoptotic threshold.

Analysis of the traces of p53 in cells that died after cisplatin treatment and cells that survived for at least 72 hours showed that the maximal level reached by p53 was similar in both groups (Figure 3.3A). Binning cells by their maximal p53 levels revealed no trend in the proportion of cells undergoing apoptosis (Fig-
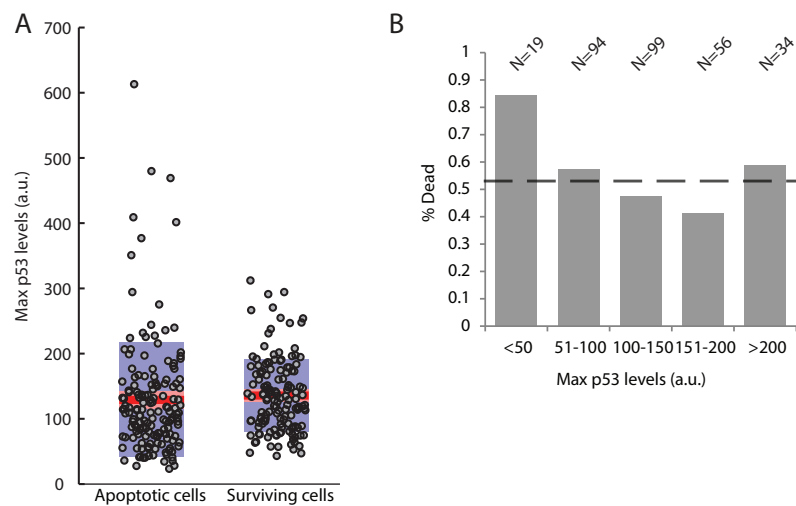
Figure 3.3: Maximal levels of p53 do not distinguish apoptotic from surviving cells. (**A**) The maximal p53 value of each cell is plotted as an open circle, with the red line denoting the mean, the pink the standard error of the mean, and the lavender the standard deviation. (**B**) Cells were binned by maximal p53 levels and the percentage of apoptotic cells was plotted for each bin.
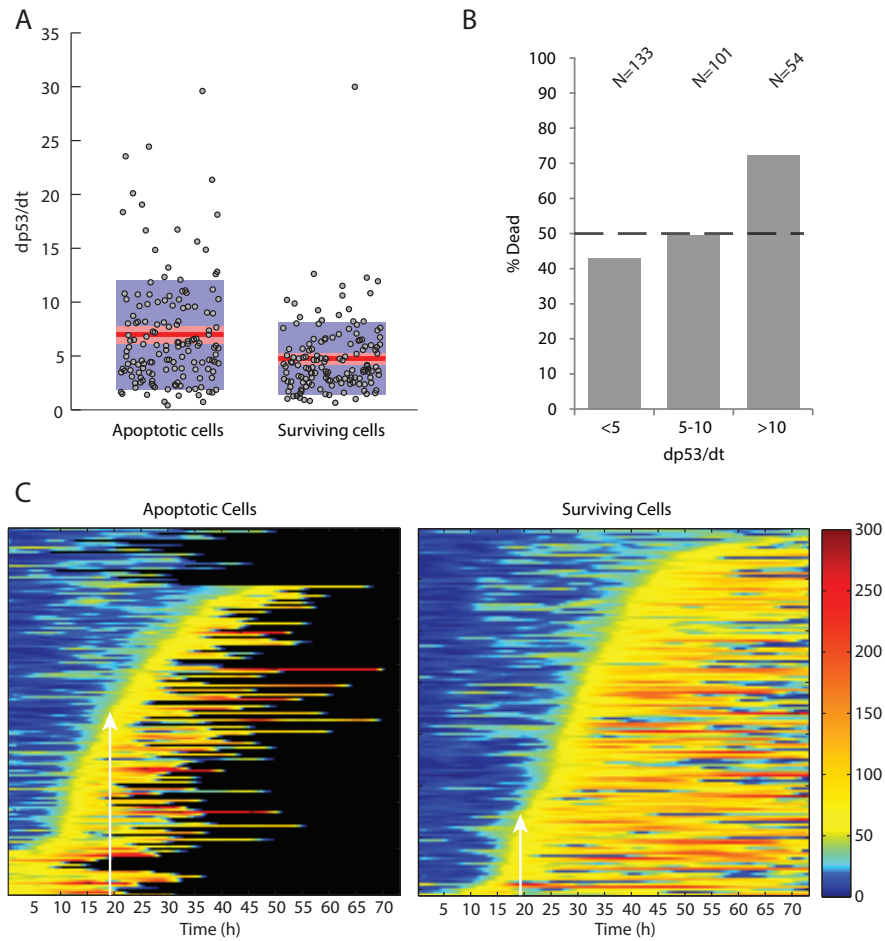
Figure 3.4: Rate of p53 accumulation differs in apoptotic and surviving cells.
(**A**) The rate of p53 increase (slope of p53 from 50% to 90% of max) of each cell is plotted as an open circle, with the red line denoting the mean, the pink the standard error of the mean, and the lavender the standard deviation. (**B**) Cells were binned by p53 accumulation rates and the percentage of apoptotic cells was plotted for each bin. (**C**) The p53 levels over time (x-axis) for individual cells (rows) plotted as a heat map, with the colorbar as indicated (a.u.) White arrow delineates the time point at which half of the apoptotic cells (left) have induced p53.

ure 3.3B), suggesting that cells with higher p53 are not more likely to undergo apoptosis. This implies that the decision between death and survival cannot be made based only on p53 levels, as is proposed in both the affinity and the threshold models. Instead we observed that the rate of p53 accumulation, measured by the slope from the half-maximal value of p53 to the point when p53 reaches 90% of its maximal value, was faster in the cells that underwent apoptosis (Figure 3.4A). This difference in p53 induction rate between dying and surviving cells was significant ($p < 0.0001$), and binning cells by p53 induction rate showed an increasing trend of greater proportion of apoptosis in cells that induce p53 faster (Figure 3.4B). When the individual traces of p53 expression of apoptotic and surviving cells were plotted in a heat map and sorted by time of p53 induction, we observed that the apoptotic cells tended to accumulate p53 earlier (Figure 3.4C). Shortly before 20 hours, when p53 levels had risen in half of the apoptotic cells, p53 had been induced in only a small fraction of the surviving cells.

Altering the dose of cisplatin changed the rate of p53 accumulation and the choice of cell fate. At half the concentration of cisplatin, 6.25 μM, we observed a longer lag before p53 accumulated, and only 23.5% of cells died (Figure 3.5A). Consistently, at double the concentration of cisplatin, 25 μM, the timing of p53 increase occurred earlier, and almost all cells (94.7%) died. For each concentration, the maximal p53 level reached was only slightly different between apoptotic and surviving cells (Figure 3.5B), with the exception at the highest cisplatin dose, where the sample size of surviving cells was small. While the maximal p53 level was not predictive of cell fate, p53 was induced earlier with increasing cisplatin concentration, correlating with higher proportion of apoptotic cells (Figure 3.5C).

Figure 3.5 *(following page)*: **Increasing concentrations of cisplatin promotes faster p53 increase and increased death.** (**A**) The p53 levels over time (x-axis) for individual cells (rows) plotted as heat maps, with the colorbar as indicated (a.u.) Top, 6.25 µM cisplatin. Middle, 12.5 µM cisplatin. Bottom, 25 µM cisplatin. (**B**) Maximal p53 levels reached for apoptotic and surviving cells at the indicated dose of cisplatin. (**C**) Time at which cells reached their half-maximal p53 value, for each dose of cisplatin. (**D**) Time at which cells reached their half-maximal p53 value, for each dose of cisplatin, separated between apoptotic and surviving cells. Error bars represent standard deviation.

58
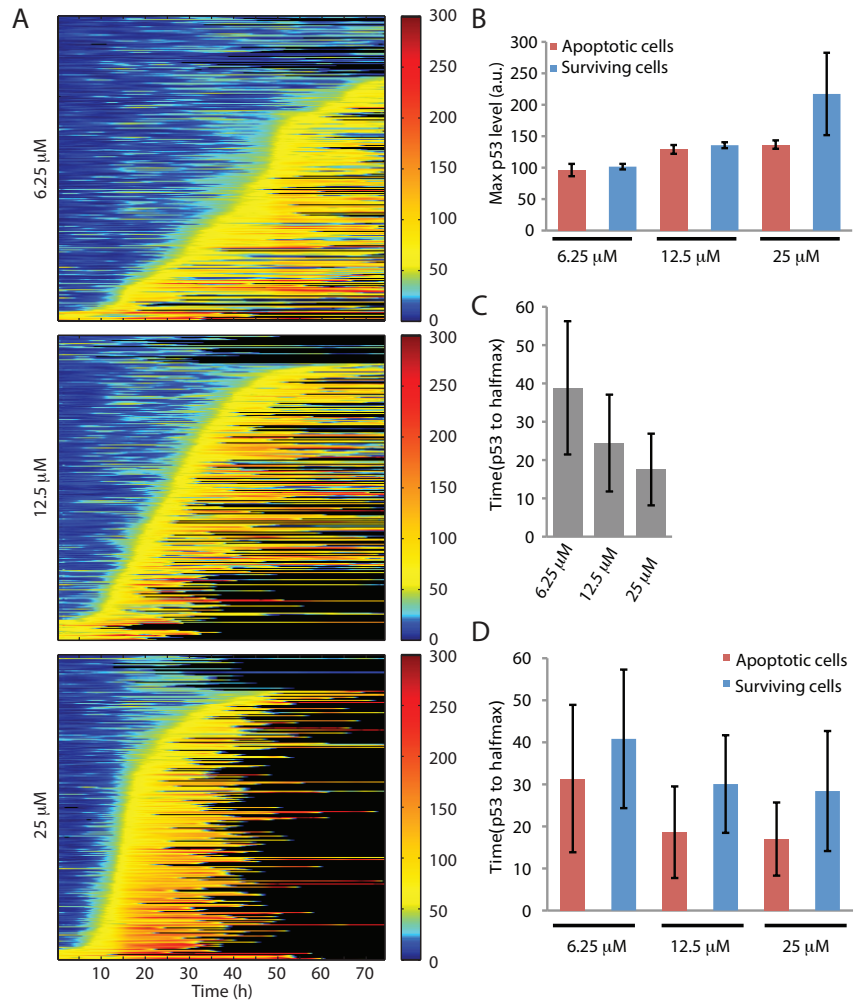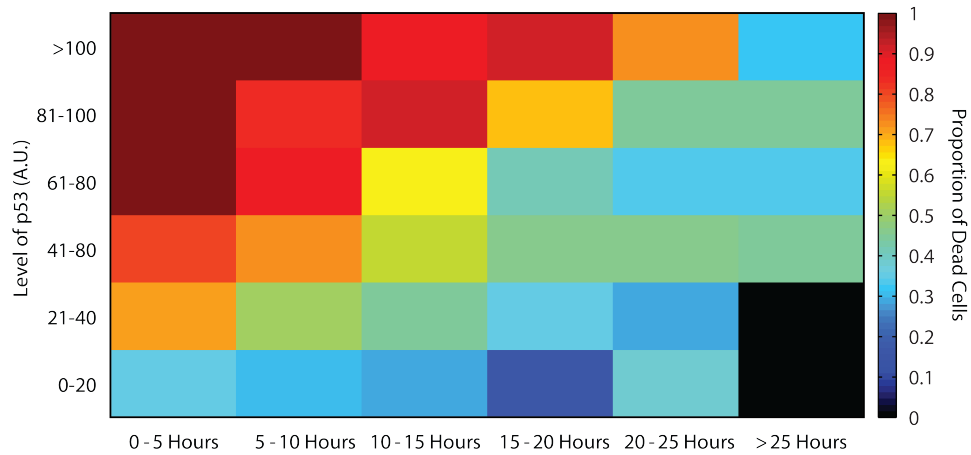
Figure 3.6: Dynamic threshold model of p53-induced apoptosis. Single-cell traces of p53 levels after 12.5 μM cisplatin treatment were divided into time windows, then binned by the maximal p53 value reached in each time window. Each bin was colored by the proportion of cells from that bin that eventually underwent apoptosis.

Indeed, consistent with Figure 3.4, at each cisplatin concentration the apoptotic cells activated p53 earlier than the surviving cells (Figure 3.5D). These data suggest that higher doses of damage cause more cells to induce p53 earlier, and earlier induction of p53 leads to a higher probability of cell death.

3.3 A MODEL FOR P53-MEDIATED APOPTOSIS

We analyzed the probability that a cell eventually will die given the maximal level of p53 reached within a certain time window. This probability was computed by first dividing up the initial 25 hours after 12.5 μM cisplatin treatment into 5-hour time windows (the time elapsed from 25 hours onwards was grouped into one window). For each segment of time, the p53 traces were binned by the maximal p53 value reached within that timeframe. The bins were then colored in a heatmap representing the proportion of cells from that bin that eventually un-

derwent apoptosis. The resulting matrix shows that as time progresses, the level of p53 at which cells become likely to undergo apoptosis progressively increases (Figure 3.6). Stated another way, if a cell's p53 level has not crossed the apoptotic threshold in one window, then in the following window it will have to surpass an even higher threshold for the cell to die. This suggests that there may be a threshold for triggering apoptosis, but that the threshold changes and becomes increasingly high over time. We named this the dynamic threshold model.

The dynamic threshold model suggests that forcing a faster increase of p53 at early times after cisplatin treatment should increase the proportion of dying cells relative to surviving cells. In contrast, further increase in p53 at later time points should lead to a smaller increase in apoptotic cells. To test this hypothesis, at different times after cisplatin treatment we also added Nutlin-3a (nutlin), the aforementioned small molecule that disrupts Mdm2 binding to p53 and thus facilitates p53 accumulation (Vassilev et al., 2004). Adding nutlin and causing p53 levels to increase early, at 3 hours after cisplatin, dramatically increases the proportion of cells undergoing apoptosis rather than surviving (Figure 3.7). In contrast, adding nutlin at 30 hours raises p53 to similarly high levels, yet a much smaller increase in the number of dying cells results. These findings indicate that the timing of p53 elevation is crucial for the decision to enter apoptosis.

As p53 dynamics play a role in regulating cell fate via differential activation of downstream target genes (Purvis et al., 2012), we hypothesized that faster p53 accumulation might lead to increase in expression of pro-apoptotic p53 target genes, or that slower p53 might allow cells to prevent apoptosis due to expression of p53 target genes that trigger cell cycle arrest, which could antagonize apoptosis.
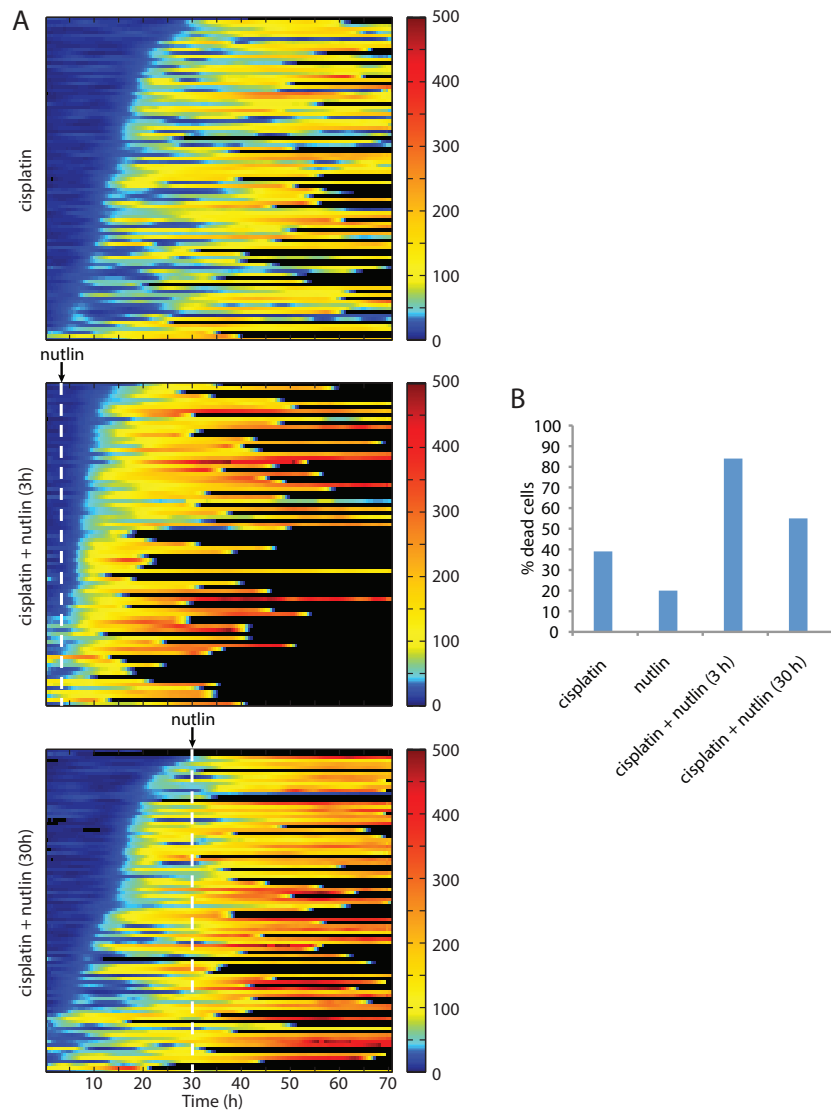
Figure 3.7: Addition of nutlin at different times after cisplatin influences cell fate. (**A**) The p53 levels over time (*x*-axis) for individual cells (rows) plotted as heat maps, with the colorbar as indicated (a.u.) Top, cisplatin only. Middle, cisplatin with 2 μM nutlin addition at 3 hours (indicated by white dashed line). Bottom, cisplatin with nutlin addition at 30 hours (white dashed line). (**B**). The percentage of apoptotic cells observed in the indicated conditions (cisplatin only, nutlin only, cisplatin with nutlin addition at 3 hours, and cisplatin with nutlin addition at 30 hours).
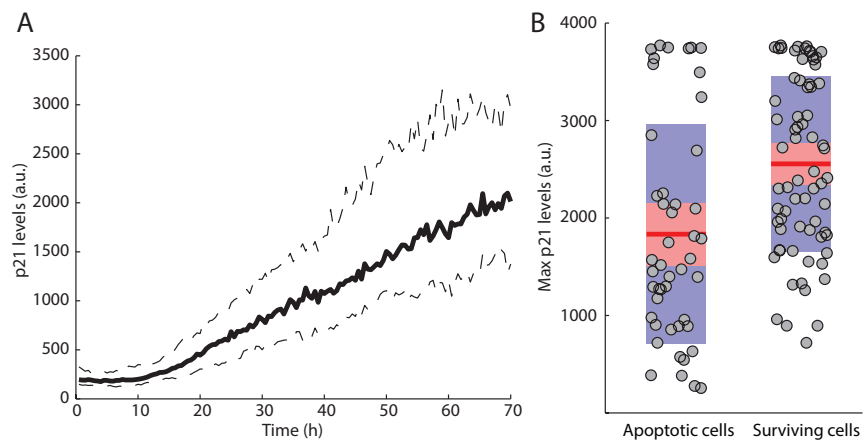
Figure 3.8: p21 levels increase after cisplatin treatment. (**A**) Median p21p-CFP trace (solid) of HCT116p53VKI-p21p-CFP cells after cisplatin treatment. Dashed lines show the 25th and 75th percentiles.(**B**) The maximal p21 value of each cell is plotted as an open circle, with the red line denoting the mean, the pink the standard error of the mean, and the lavender the standard deviation.

The p53 target p21 is known to play a role in arrest, and cells with disrupted p21 genes have been shown to be more sensitive to cisplatin (Fan et al., 1997). The increased apoptosis due to loss of p21 suggests that p21 has a protective effect and promotes survival. To measure the downstream effects of p53 induction, we employed a p21 promoter construct that contains the p53-responsive elements from the p21 promoter driving the expression of the fluorescent protein CFP. Incorporating this p21p-CFP construct into HCT116 p53VKI cells via lentiviral infection allowed us to monitor the p53-dependent mRNA expression of p21. We observed that p21 expression increased robustly in cisplatin-treated cells (Figure 3.8A). Surviving cells appeared to have higher maximal p21 levels than apoptotic cells (Figure 3.8B).

These data led us to consider a quantitative model in which the outcome of p53

signaling, either apoptosis or survival, depends on the rate of p53 accumulation. As p53 is induced, it will upregulate transcription of some apoptotic targets, for instance PUMA, that promote apoptosis. At the same time but with some delay, p53 will upregulate p21, which will promote arrest and senescence while inhibiting apoptosis, rescuing the cell from death (Figure 3.9A). Such a delay in p53-induced p21 expression can be generated with a coherent feed forward loop through a putative molecule X (Mangan and Alon, 2003). Expanding a previously published model (Batchelor et al., 2008), we modeled the system with delayed differential equations as the following:

$$\frac{dp53}{dt} = \beta_{p53} \tag{3.1}$$

$$\frac{dPUMA}{dt} = \beta_{PUMA}p53(t - \tau_{PUMA}) - \alpha_{PUMA}PUMA \tag{3.2}$$

$$\frac{dX}{dt} = \beta_{X}p53(t - \tau_{X}) - \alpha_{X}X \tag{3.3}$$

$$\frac{dp21}{dt} = \beta_{p21}p53(t - \tau_{p21})X(t - \tau_{p21}) - \alpha_{p21}p21 \tag{3.4}$$

$$\frac{dApop}{dt} = \beta_{Apop}PUMA - \alpha_{Apop}p21 \tag{3.5}$$

where *p53*, *PUMA*, *X*, *p21*, and *Apop* are the species, each with production terms with constants β and first order degradation terms with constants α. The equation for *p53* does not have degradation because it acts more as a driving function for the system and is independent of the other components. *Apop* is a variable that loosely represents the apoptotic signal in the cell, with the assumption that when *Apop* crosses a threshold the cell is committed to death. The equation for *Apop* also does not have first order degradation, as instead its degradation depends on *p21*.
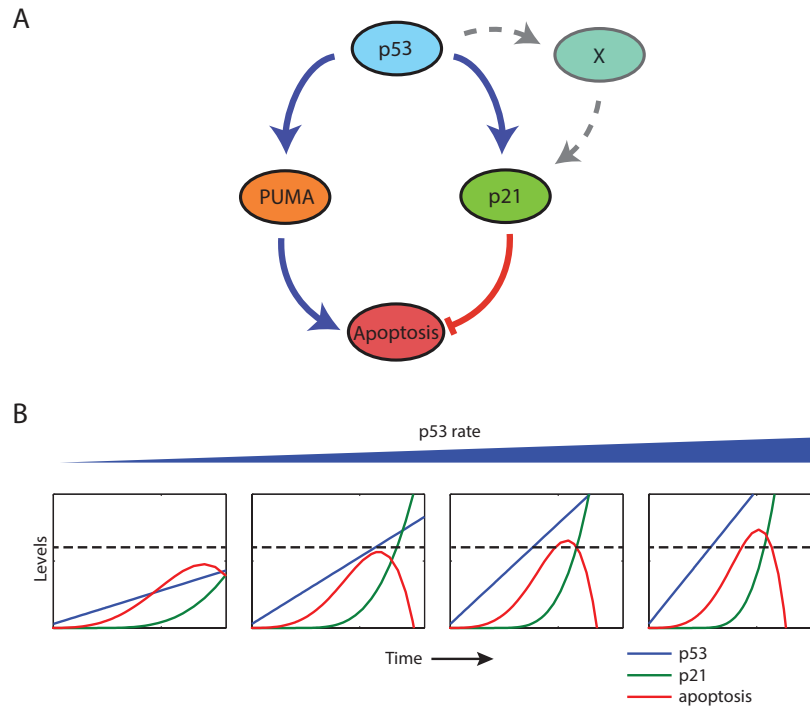
Figure 3.9: A model of the p53 network in response to cisplatin. (**A**) A diagram showing p53 induction of PUMA, which activates apoptosis. Also, p53 induces p21, which represses apoptosis. To create a delay in p53-induced p21 expression, a feed-forward loop connects p53 to p21 via a putative molecule X. (**B**) With increasing rates of p53 accumulation, the variable representing apoptosis reaches higher levels, triggering cell death when it crosses a threshold (dashed line).

With the very simplistic condition that p53 is linearly increasing (Equation 3.1), parameters can be found such that the variable representing apoptosis will cross a threshold with a fast p53 increase but not with a slow p53 increase (Figure 3.9B). This model predicts that p21 expression follows p53 expression but varies nonlinearly, so that after a delay, p21 is expected to increase much faster at higher rates of p53 accumulation (Figure 3.9B). However, for the rightmost two cells with high p53 rate in (Figure 3.9B), the apoptosis variable crosses the threshold at a point when p21 level is still low. The leftmost two cells with low p53 rate survive and in these cells p21 accumulates to high levels. This explains the difference in the maximal levels of p21 observed between apoptotic and surviving cells. Larger datasets and further analysis of individual cell traces of p21 expression will be needed to substantiate the dynamics of p21 predicted by the model.

3.4 DISCUSSION

The quantitative model can be expanded and improved in a number of ways. The linear increase in p53 is an over-simplification, and should be modified so that p53 levels increase after some delay. Furthermore, p53 levels should eventually plateau, since we observe that apoptotic cells that accumulate p53 quickly have similar maximal p53 levels as the surviving cells that accumulate p53 slowly. That the cells with fast-increasing p53 die, however, should be considered; because once the cell dies, the p53 level at later time points as predicted by the model is irrelevant, it may not be essential to explicitly write a limit for p53 into the equations. The model should also be adjusted to more accurately reflect the dynamic threshold for p53 activation of apoptosis; for instance, whether or not the molecule representing apoptosis crosses its threshold should correspond to whether p53 has

crossed its time-dependent increasing threshold. Further possible geometries of the p53 network should be explored in greater depth. Because cell death and survival are also only probabilistically predicted by p53 dynamics (Figure 3.6), one might also consider stochastic models for this system.

What regulates the choice between death and survival downstream of p53 is still not completely understood. Multiple pro-apoptotic or pro-arrest p53 target genes may be important for this cell fate decision. The dynamics of p21, for instance, are potentially one mechanism set in place to rescue the cell from apoptosis if the apoptotic signal is not strong enough. Such a hypothesis would suggest that one or more pro-apoptotic p53 target genes follow p53 dynamics quite faithfully, such that when p53 increases early and rapidly, target gene expression also increases and triggers apoptosis before p21 has had a chance to accumulate. When p53 accumulation is slower, the pro-apoptotic target genes also follow, but p21 continues to build up and thus prevents apoptosis. One might also imagine that the increase in p21 after cisplatin provides a natural source for the proposed dynamic threshold model; as time goes on, any p53-dependent apoptotic signal must overcome higher and higher levels of p21.

We currently are planning further experiments to verify that p21 is a factor that inhibits apoptosis and promotes survival. We are generating cells lacking p21 due to stable expression of p21 shRNA and will evaluate cisplatin-induced cell fate in these cells, expecting that p21 knockdown should increase the proportion of apoptotic cells. Based upon the model, a search for the putative molecule X could start with p53 target genes that may also influence expression of p21, though perhaps not directly. The p53 target HIC1 is a potential candidate that may positively regulate p53 transcriptional activity (Chen et al., 2005). Further

testing will be required for any candidate genes. We are additionally building a fluorescent reporter similar to the p21 reporter to measure expression from the promoter of the p53 pro-apoptotic gene PUMA. PUMA is a candidate for a p53 target involved in promoting apoptosis after cisplatin treatment, since like p21 its gene expression increases after cisplatin treatment as measured by qPCR. PUMA dynamics will potentially shed light on how the behavior of p53 after cisplatin regulates pro-apoptotic target genes.

Greater insight into how p53 dynamics influence cell fate decisions in cells treated with cisplatin will prompt the development of methods to manipulate those dynamics. The ability to modulate the dynamics of such network regulators and predict the cellular outcomes has direct clinical relevance. Moreover, given the wide use of chemotherapy to treat cancer, it is important to understand how the function of drugs like cisplatin may vary in different conditions and cancer cell types. Only with such understanding will we be able to predict how effective various therapies will be and perhaps how best to use them in combination.

3.5 MATERIALS AND METHODS

Cell culture: All HCT116 cell lines were grown in McCoy's media with 10% fetal calf serum, 100 U/ml penicillin, 100 μg/ml streptomycin, and 250 ng/ml fungizone. HCT116p53-/- cells were kindly provided by Bert Vogelstein. HCT116p53VKI cells were generated by Alexander Loewer via homologous recombination. Lentiviral infection and clonal selection were used to generate HCT116p53VKI cells with p21p-CFP with the protocol described in Chapter 2.

Antibodies and reagents: Antibodies were used against p53 (DO1, Santa Cruz) and actin (Sigma). Cisplatin (Sigma) was stored as a solid, dissolved in DMSO at a high

concentration then further diluted in water and rapidly added to cells. Nutlin-3a was obtained from Cayman Chemical. The CellTiter-Glo assay was performed according to manufacturer's instructions (Promega).

Immunoblotting: Western blots were performed as described in Chapter 2.

Microscopy: Two days prior to microscopy, cells were grown in RPMI media lacking riboflavin and phenol red to reduce medium autofluoresence in poly-D-lysine-coated glass-bottom plates (MatTek). Cells were imaged on a Nikon Eclipse TE2000-E inverted fluorescence microscope in which the stage was surrounded by a custom enclosure to maintain constant temperature, CO_2 concentration, and humidity. Images were acquired with MetaMorph software (Molecular Devices). Data were analyzed in MATLAB (Mathworks).

Computational modeling: Numerical integration was performed in MATLAB (Mathworks). The source code is available upon request. The parameters shown in Figure 3.9B are presented in the following table.

Parameter	Description	Value
β_{p53}	$p53$ production rate	0.5-2
β_{PUMA}	$PUMA$ production rate	0.4
τ_{PUMA}	Time delay in $PUMA$ production	0.5
α_{PUMA}	$PUMA$ degradation rate	0.2
β_X	X production rate	0.6
τ_X	Time delay in X production	0.5
α_X	X degradation rate	0.3
β_{p21}	$p21$ production rate	0.3
τ_{p21}	Time delay in $p21$ production	2
α_{p21}	$p21$ degradation rate	0.3
β_{Apop}	$Apop$ production rate	1
α_{Apop}	$Apop$ degradation rate	1.5

3.6 MANUSCRIPT INFORMATION

Author contributions: Andrew L. Paek conducted the experiments. Alexi Kedves and Bill Forrester provided the data for (Figure 3.1A). Andrew L. Paek and Julia C. Liu performed the experimental analysis. Julia C. Liu performed the computational modeling and wrote this chapter.

There is still the conspicuous asymmetry between molecular biology and, say, the therapy of lung cancer.

Lewis Thomas

4

Conclusion

THE QUESTION OF HOW CELLS SENSE AND RESPOND appropriately to diverse stimuli has broad implications in health and in disease. The signaling networks that regulate cell fate decisions have interactions with other networks, including those maintaining cell state and identity. These interactions can give rise to heterogeneous outcomes between different cell types as well as within a cell population. Understanding how cells and tissues are poised to respond to stimuli will help us to interpret and rectify alterations of these signaling networks in diseases such as

cancer.

In particular, cancer is often characterized by faulty cellular signal processing. Among the hallmarks of cancer are continual retention of proliferative signaling and the evasion of growth suppressive and cell death signals (Hanahan and Weinberg, 2011). However, the nature of regulatory network dysregulation is not uniform across cancer tissues and cell types. In part this can be attributed to the abundance of different mutations that give rise to cancerous cells. Nonetheless, even in the same cell line, variance in the dynamics of regulatory networks can lead to different downstream outcomes. As we discussed in Chapter 3, differences in p53 dynamics across single cells correlate with alternative cell fates, apoptosis and senescence.

The tissue of origin also plays a role in heterogeneity, as cells from different tissues often have very different responses to stimuli. This variation becomes clinically relevant as the DNA damage responses in different tissues can vary and thus confer differential sensitivity to radiation or chemotherapy (Gudkov and Komarova, 2003). The underlying mechanisms conferring sensitivity or resistance and how they vary with cell type are still open questions. Human embryonic stem cells (hESCs) have a uniquely sensitive DNA damage response, which we characterized in Chapter 2. While apoptotic death in hESCs after damage is dependent on p53, we showed that it is hESCs' proximity to the apoptotic threshold that makes them vulnerable to p53 signaling (Liu et al., 2013). BH3 profiling of hESCs in the process of differentiation reveals that as the cells differentiate, their priming gradually decreases, suggesting that high mitochondrial priming in hESCs is closely linked to pluripotency.

4.1 Causes of high mitochondrial priming in hESCs

How the highly primed state is created and maintained in hESCs is still an open question. One potential mechanism is by controlling the balance between pro- and anti-apoptotic proteins. Compared with differentiated cells, hESCs have lower levels of the anti-apoptotic protein Bcl-2 and higher levels of the pro-apoptotic protein Puma, consistent with the higher priming of hESCs. Yet other apoptosis-regulating proteins, including Bid, Bim and Bcl-xL, showed similar levels in undifferentiated and differentiated cells (Liu et al., 2013). It is unclear whether specific modifications, localization, or protein interactions might affect how these proteins contribute to priming. As mentioned, some hESC lines maintain basally activated Bax, which provides a quick and direct route to apoptosis. This close proximity to the apoptotic threshold is found only in undifferentiated cells, as just two days of differentiation of these hESCs into embryoid bodies were sufficient for activated Bax to disappear, and for the cells to no longer undergo apoptosis after damage (Dumitru et al., 2012). Thus, pluripotency seems to regulate the state of the cell to keep it highly primed and sensitive to damage, but our understanding of the nature of this regulation is still limited.

The relationships between the molecular players in the pluripotency and the priming networks could be complex and depend on other networks (Figure 4.1). The cell cycle network, for instance, appears to be uniquely modified in hESCs. It is well known that hESCs have a rapid cell cycle and an abbreviated G1 phase (Becker et al., 2006). Rapid cell cycle progression in hESCs has been shown to be tied to pluripotency, and slowing down the cell cycle by lengthening G1 through inhibition of Cdk2 causes hESCs to differentiate (Filipczyk et al., 2007, Neganova et al., 2009). Moreover, some of the canonical pluripotency proteins, such as Nanog,

have been directly implicated in regulating the cell cycle of hESCs. Nanog over-expression was found to shorten the transition time between G1 and S phase by directly binding to the regulatory regions of Cdk6 and Cdc25A (Zhang et al., 2009). Given how closely connected the pluripotency and cell cycle networks are, it is possible that priming and pluripotency are linked via cell cycle machinery.

Mitochondrial morphology itself could be a factor in determining priming. It has long been known that mitochondria can exist in a fused tubular state or a fragmented state, and they can convert between these states through fission and fusion processes (Bereiter-Hahn and Voth, 1994, Lewis and Lewis, 1914). More recent work has demonstrated that these dynamical changes are coordinated with cellular processes, such as cell proliferation and differentiation (Mitra, 2013). For instance, in somatic cells, mitochondria reach a fused state during the G1-S transition, which is associated with downregulation of Drp1, a mitochondrial fission-promoting GTPase (Mitra et al., 2009). Reduced Drp1 leads to elevation of cyclin E, promoting S phase entry and proliferation (Mitra et al., 2009). However, despite their high proliferative capacity, hESCs are known to have mitochondria that are fragmented, morphologically immature, and deficient at oxidative phosphorylation (Facucho-Oliveira and St. John, 2009, Prigione et al., 2010), suggesting that hESCs' relatively rapid G1-S transition might be differentially regulated. Indeed, as hESCs differentiate, they not only undergo cell cycle elongation but also develop more connected, complex, and metabolically active mitochondria (Prigione et al., 2010, Varum et al., 2011). Mitochondrial dynamics may play a role in reprogramming as well; blocking fission using a Drp1 inhibitor leads to a decrease in reprogramming efficiency of over 95%, suggesting that

Figure 4.1 *(following page)*: Proximity to the apoptotic threshold depends on a combination of factors that differ between hESCs and differentiated cells. hESCs (left) and differentiated cells (right) are represented as hot air balloons floating over lava (death). In this analogy, the size of the balloon envelope is the length of the cell cycle; a longer G1 phase in differentiated cells allows them to float higher, conferring protection from death. The burners that generate hot air for the balloons are represented by the mitochondria; fused mitochondria in differentiated cells provide better propulsion (shown as a larger flame) than fragmented mitochondria associated with hESCs. Finally, pro-apoptotic proteins are shown as sand bags that weigh the balloon down, and anti-apoptotic proteins are portrayed as scissors. In hESCs the sand bags outnumber the scissors, while in differentiated cells the scissors are able to cut off more of the sand bags. Summed together, the hESC balloon is in greater danger of sinking toward death than the differentiated cell balloon.

Figure 4.1: (continued)
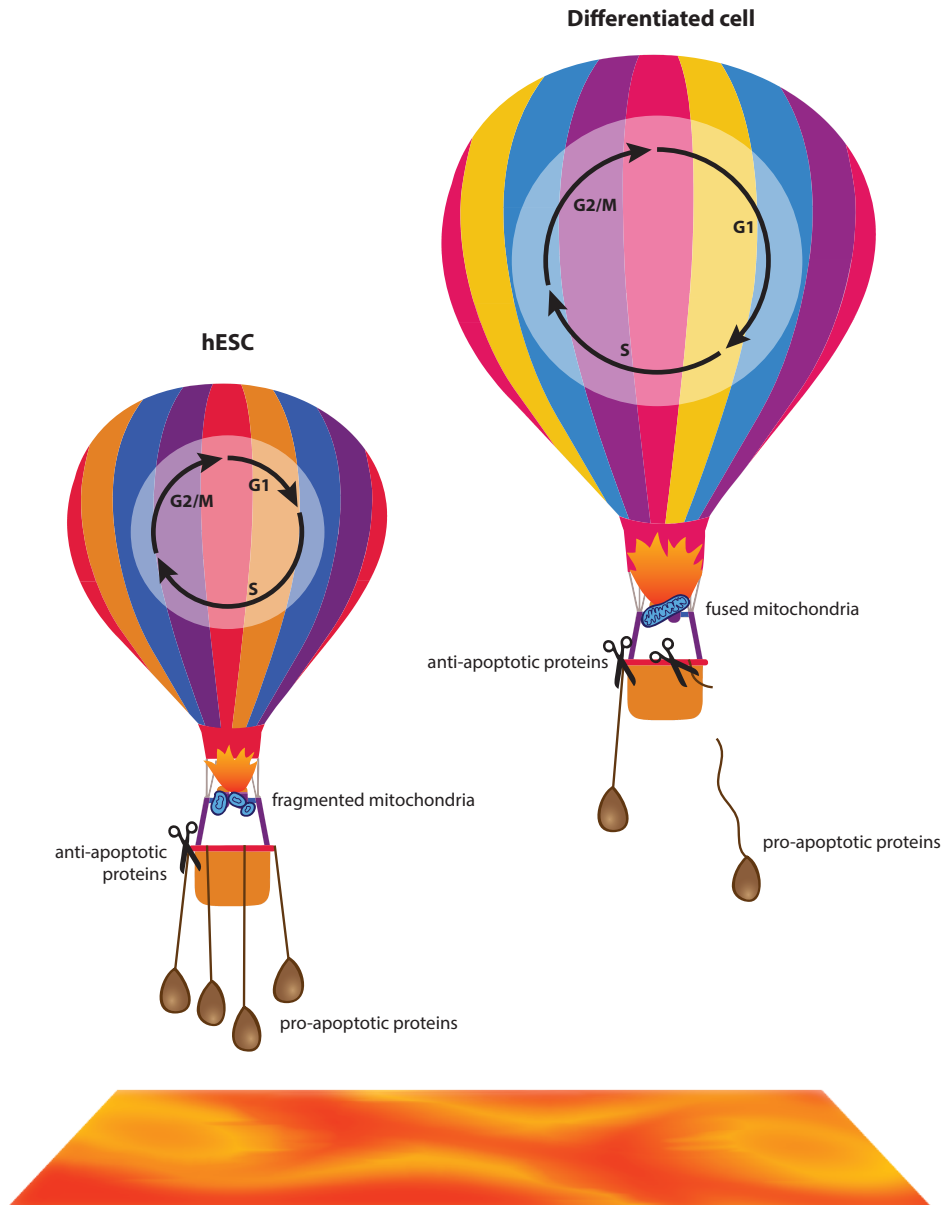
mitochondrial fission may be a critical feature of pluripotency (Vazquez-Martin et al., 2012). Moreover, it has been suggested that mitochondrial connectivity might have protective effects on cell survival, and conversely, conditions of mitochondrial fragmentation could facilitate apoptosis (Karbowski and Youle, 2003). Thus, the unique mitochondrial morphology associated with the pluripotent state could have both direct and indirect (via cell cycle) impact on priming. Deciphering the interactions between the various players in these networks continues to be a challenge, and most likely will require further studies looking at multiple systems and the interconnections between them in the same cell.

4.2 DNA DAMAGE SENSITIVITY IN ADULT STEM CELLS

Adult tissues have reserves of multipotent stem cells, which perform important roles in homeostasis and recovery after injury. In general, adult stem cells tend to be more resistant to damage than hESCs, though direct comparisons are difficult to make in human tissues. Many adult stem cell experiments have been performed in mice, where adult stem cell populations can be isolated and sorted using established label-retaining protocols. In several mouse tissues, the most primitive stem cells are relatively more resistant to damage. For instance, in comparison to more committed progenitors, purified hematopoietic stem cells (HSCs) are resistant to ionizing radiation (Mohrin et al., 2010). Similarly, mammary stem cells (MaSCs) show resistance to X-ray-induced apoptosis, in contrast to progenitor cells from mammospheres (Insinga et al., 2013). Skin is very sensitive to ionizing radiation, but in human epidermis slow-cycling keratinocyte stem cells (KSCs) undergo post-damage cell death to a lesser extent than their direct progeny, the keratinocyte progenitors (Rachidi et al., 2007). Conversely, candidate stem cells

toward the base of the small intestinal crypt are more sensitive to irradiation than small intestine progenitors higher up in the crypt (Qiu et al., 2008).

Variation in sensitivity to DNA damage among adult stem cells can be attributed to at least three underlying causes. One factor could be the duration of p53 activation, which was recently shown to affect cellular outcomes in cancer cells (Purvis et al., 2012). Differential p53 dynamics might also play a role in cell fate decisions of stem cells in tissues in which p53 is induced. Indeed, hair follicle bulge stem cells exhibit transient p53 activation after ionizing radiation and are more resistant to cell death, compared with other cells of the epidermis (Sotiropoulou et al., 2010). Long-term reconstituting HSCs are resistant to X-ray irradiation and show a greatly attenuated p53 response (Insinga et al., 2013). Interestingly, though short-term reconstituting HSCs do upregulate p53, they are also radioresistant, perhaps because p53 is activated to a lesser extent than in the more sensitive committed progenitor cells (Insinga et al., 2013). A second potential cause for the variation in sensitivity is differential mitochondrial priming as was discussed in the previous section, including disparities in the expression of pro-apoptotic or anti-apoptotic proteins. For instance, due to their higher levels of Bcl-2, colon stem cells tend to be more resistant to irradiation than small intestine stem cells (Merritt et al., 1995), which may explain the higher frequency of colon cancers compared with cancers of the small intestine. A third possible reason for variation in sensitivity is cell cycle duration. An important difference between hESCs and their adult counterparts is that in normal conditions many adult stem cells do not cycle rapidly but instead are largely quiescent, resting in the G0 phase of the cell cycle. Hence, while hESCs exhibit rapid cell cycle progression and have high sensitivity to DNA damage, slower cycling in tissue-specific stem cells may

contribute to increased resistance to damage. Variation in sensitivity among stem cells from different tissues correlates with this trend. As aforementioned, slow-cycling HSCs and KSCs are relatively resistant after irradiation. Actively cycling stem cells from the small intestine, however, undergo apoptosis after even low doses of irradiation. Thus quiescence appears to have a protective effect on stem cell survival.

Damage sensitivity also depends on the balances between competing signaling pathways, such as DNA repair versus apoptosis. Which mode of damage response is dominant in various tissues is still incompletely understood. Moreover, different cell types employ diverse DNA repair pathways, complicating our ability to understand and predict how each system will respond to DNA damage (Blanpain et al., 2011). For instance, the relatively resistant, quiescent stem cells that repair DNA after damage enter the cell cycle in G1 and hence use the error-prone non-homologous end joining pathway. Consistently, studies have shown that quiescent stem cells accumulate DNA damage with age and their function becomes progressively limited (Rossi et al., 2007). Thus cell cycle and DNA repair are interlinked factors that affect the decision between sensitivity and resistance, with subsequent effects that are compounded during aging.

4.3 Cell sensitivity or resistance in therapy

Cancer cells tend to have higher rates of cell proliferation. If a relationship between faster proliferation and greater radiosensitivity is reliable, it could potentially be exploited for therapeutic purposes. In a recent study, BH3 profiling was applied to predict the effects of chemotherapy in patients with acute myeloid leukemia (AML) (Vo et al., 2012). Mitochondrial priming was a determinant

of response to chemotherapy – the leukemia cells that were more primed were the cells more likely to respond. Normal HSCs were less primed than the AML myeloblasts of patients cured by chemotherapy. In AML patients who had responded poorly to chemotherapy, the myeloblasts were even less primed than the HSCs, showing that the relative priming of HSCs and leukemia cells characterized a boundary in clinical outcome. Moreover, BH3 profiling demonstrated that the AML myeloblasts tended to depend on Bcl-2 for survival, while the HSCs were selectively more dependent on Mcl-1. Hence, combining chemotherapy with the addition of Bcl-2-inhibiting drugs could potentially increase priming of the leukemia cells, improving the efficacy of the treatment.

Understanding how damage response pathways and intrinsic mitochondrial priming interact is clearly important for predicting the sensitivity of different tissues and the overall function and health of organisms. Regulated by interconnected networks including p53 signaling, cell cycle, and priming, stem cells must navigate the delicate balance between resistance and sensitivity. Resistance puts stem cells at risk of accumulating mutations that might lead to cancer, while sensitivity is important for genetic stability but may cause stem cell depletion, compromising function and contributing to aging. The line between resistance and sensitivity, as we have seen, is incompletely understood even in well-studied somatic cancer cell lines. The more we learn about how different cell types - from stem cells to cancer cells - respond to stress and damage, the better able we will be to predict these responses and potentially manipulate them for therapeutic purposes.

4.4   Manuscript information

This chapter is adapted from a publication in press:

Julia C. Liu, Paul H. Lerou, and Galit Lahav. How stem cells walk the fine line between resistance and sensitivity to DNA damage. *Trends in Cell Biology*, *in press*.

Life is pleasant. Death is peaceful. It's the transition that's troublesome.

Isaac Asimov

5

Appendix: a novel method to detect apoptosis and cell cycle

AS APOPTOSIS PLAYS IMPORTANT ROLES BOTH IN HOMEOSTASIS AND DISEASE, the ability to accurately measure the degree of apoptosis in cell populations is essential. Moreover, apoptosis is a multi-stage process, so ideally cellular progression through apoptosis should be detectable. Pinpointing cells in the early and late stages of apoptosis would enable the inference of the timing of commitment to

cell death after a given injury or damage.

Many cytotoxic agents also have effects on the cell cycle, and at higher concentrations can induce apoptosis. Dependent on the mechanism of drug action, apoptosis will occur from the cell cycle position in which the drug arrests the cells (Schimke et al., 1994). Some anti-cancer drugs, such as paclitaxel (taxol), exert their effects by inhibiting entry into or progression through mitosis and thus can cause cells to die in G2/M (Rieder and Maiato, 2004). Many DNA-damaging drugs impair DNA replication, for instance by inhibiting topoisomerase I (camptothecin, for instance (Liu et al., 2000)) or topoisomerase II (etoposide and doxorubicin, among others (Pommier et al., 2010)). These drugs tend to be most toxic in S phase, during which new DNA is synthesized. Identifying from which phase of the cell cycle damaged cells die is a step towards being able to manipulate the dose or timing of drugs or drug combinations to induce death or prevent it. Hence, it is useful to measure both cell cycle phase as well as apoptosis in a distribution of cells.

5.1 Methods to detect apoptosis

There are a variety of methods used to detect apoptosis using a large range of markers, such as morphology changes, caspase activation markers, membrane alterations, and DNA fragmentation (Elmore, 2007). Each of these methods has advantages and disadvantages in terms of specificity, time consumption, and cost. Some may detect different stages of apoptosis and be more or less appropriate for use in specific contexts. Because no one method is sufficient on its own to unequivocally demonstrate cell death, a combination of complementary yet unrelated techniques should be used (Galluzzi et al., 2009).

The gold standard for identifying apoptosis remains transmission electron microscopy (TEM), which can be used to detect changes in cell physiology directly (Robertson et al., 1978). The classification of apoptotic cells by definition requires certain morphological characterisitics, among which are nuclear fragmentation, disorganization of organelles, intact cell membrane even late in disintegration, blebbing, and apoptotic bodies. TEM is able to detect these morphological changes accurately. However, it is also costly, time-consuming, and limited to small regions, making it particularly unsuitable for high-throughput experiments. Furthermore, TEM is not optimal for detecting cells in the earliest stages of apoptosis.

Annexin V staining is a common method to detect early and late apoptosis (Koopman et al., 1994). During apoptosis, phosphatidylserine is transferred from the inner leaflet of the plasma membrane to the outer membrane. This exposure of phosphatidylserine to the outside surface serves as a signal for phagocytosis and also allows it to be detected by Annexin V. A recombinant phosphatidylserine-binding protein, Annexin V stains dying cells before the membrane is completely permeabilized. Hence, it is often combined with a live-cell-impermeant dye such as propidium iodide (PI) which only stains dead cells. When used in this combination, the Annexin V-positive, PI-negative cells are generally regarded as early apoptotic and Annexin V-positive, PI-positive cells are thought to be late apoptotic. While widely used and accepted as an apoptosis assay, Annexin V staining does not provide information about cell cycle stage.

The TUNEL (Terminal dUTP Nick End-Labeling) method detects apoptosis based on DNA fragmentation (Gavrieli et al., 1992, Kressel and Groscurth, 1994). This assay uses terminal deoxynucleotidyl transferase (TdT) to enzymatically la-

bel the DNA strand breaks generated by endonuclease cleavage during apoptosis. TdT adds labeled dUTP to the 3'-end of DNA fragments; the UTP can be labeled with a variety of probes such as biotin or BrdU. Once incorporated into DNA, the label can be detected with antibodies or other binding molecules. In some applications, these antibodies can be fluorescent, so as to be detectable by microscopy or flow cytometry. When used in conjunction with a DNA-labeling dye such as PI or DAPI (4',6-diamidino-2-phenylindole), TUNEL can visualize the cell cycle stage of the population of cells, including live and apoptotic cells. Hence, it is a standard method to demonstrate correlation of induction of apoptosis with cell cycle phase. However, it requires fixation of the cells and incubation with the TdT enzyme and whichever antibody is used to detect the labeled DNA ends, as well as various washing steps between the incubations.

Antibodies against active caspases, such as cleaved caspase 3, and caspase cleavage products, including cleaved PARP, are also popular for detecting apoptosis. Caspase activation and/or cleaved substrates can be detected in a variety of ways, including immunoblotting and immunohistochemistry. In the same manner as the TUNEL assay, when used for flow cytometry, antibodies against cleaved caspases or cleaved PARP can be combined with a DNA-labeling dye to concurrently assess cell cycle stage and apoptosis.

5.2 A NOVEL ASSAY TO CONCURRENTLY DETECT ARREST AND APOPTOSIS

YOPRO-1 was identified as a live-cell-impermeant nuclear dye specific for apoptotic cells (Idziorek et al., 1995). It is excluded from healthy cells and accurately
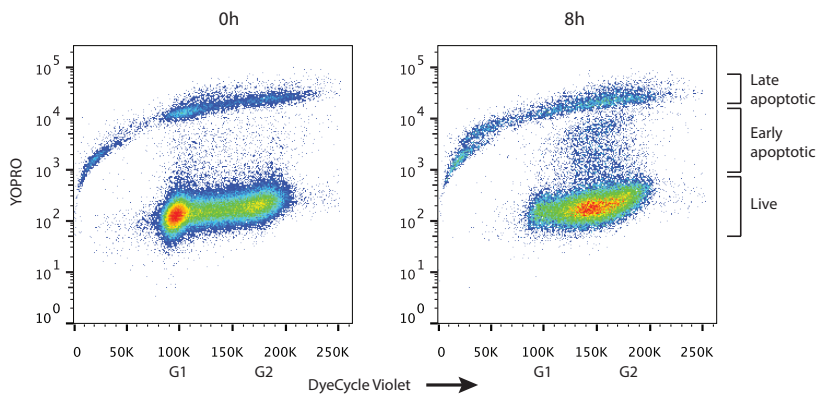
Figure 5.1: Camptothecin induces S phase arrest and apoptosis in EL-4 cells.
(**A**) EL-4 cells were treated with 0.125 μM camptothecin for 8 hours, then collected for the DCV/YOPRO flow cytometry assay. Stages of apoptosis are demarcated by incorporation of YOPRO, while cell cycle is measured by DCV (G1 and G2 peaks are indicated).

stains the fraction of the population with morphological features of apoptosis, such as nuclear shrinkage and fragmentation. Because it is used without permeabilization, a fixation step is not required and the protocol becomes substantially easier and more robust. Cells can be stained quickly, without fixation, in media, though prompt staining and analysis after the desired treatment are necessary. YOPRO-1 or its counterpart YOPRO-3 (hereafter YOPRO) can be combined with a live cell DNA stain such as Hoechst to simultaneously extract information about cell cycle phase. For applications using flow cytometers, in which laser sources that excite Hoechst are rare, Vybrant DyeCycle Violet (DCV) can be substituted for Hoechst (Telford, 2010). Like Hoechst, DCV is a cell-permeable DNA binding dye with a similar structure to Hoechst. After binding DNA, DCV emits fluorescence that is proportional to DNA mass, allowing for cell cycle analysis. Combined, DCV and YOPRO can help determine after a given treatment whether cells arrest
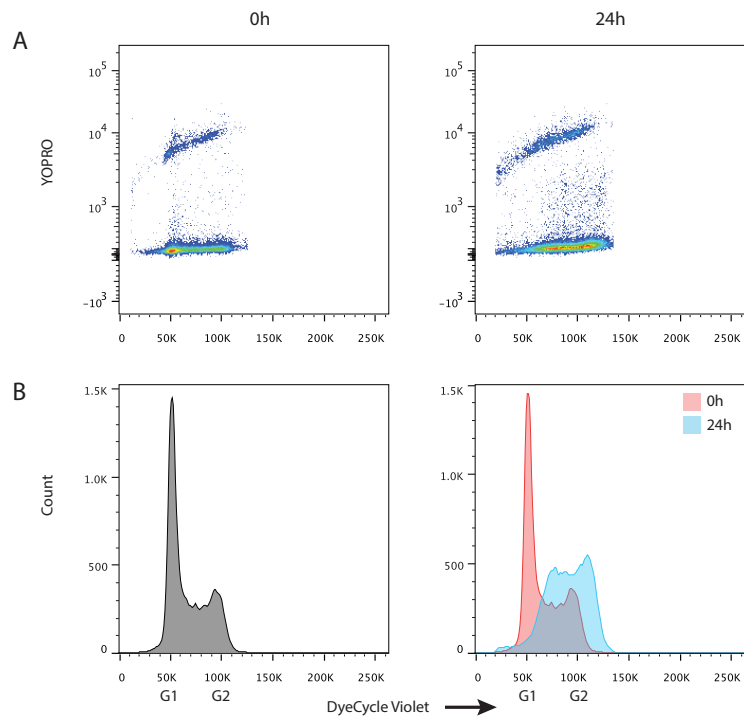
Figure 5.2: Camptothecin induces S/G2 arrest and apoptosis in 293T cells.
(**A**) 293T cells were treated with 0.5 μM camptothecin for 24 hours, then collected
for the DCV/YOPRO flow cytometry assay. (**B**) Histogram of DCV distribution
of untreated cells (left) and overlay of the distributions of untreated (pink) and
camptothecin-treated (blue) cells (right).
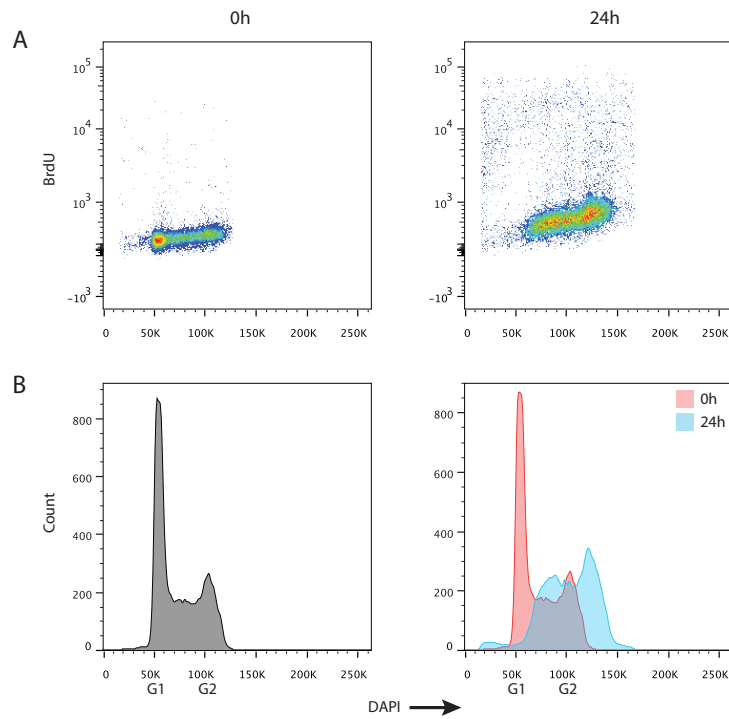
Figure 5.3: TUNEL confirms camptothecin-induced S/G2 arrest and apoptosis. (**A**) 293T cells were treated as in (Figure 5.2), then fixed for the Apo-BrdU TUNEL assay. (**B**) Histogram of DAPI distribution of untreated cells (left) and overlay of the distributions of untreated (pink) and camptothecin-treated (blue) cells (right).

and in what cell cycle stage, and from which stage they undergo apoptosis. We developed an assay we term DCV/YOPRO for use in flow cytometry.

We tested the DCV/YOPRO protocol on EL-4 mouse T lymphocyte cells, a lymphoma suspension cell line. In response to treatment with camptothecin, these cells undergo apoptosis after arresting in S phase of the cell cycle (Johnson et al., 1997). YOPRO staining appears to distinguish three classes of cells: low YOPRO staining indicates live healthy cells, medium YOPRO staining marks cells in the process of apoptosis, and high YOPRO staining is reserved for cells in the late stages of apoptosis, where DNA fragmentation (lower DCV staining) becomes common (Figure 5.1).

The DCV/YOPRO assay can be used on not only suspension cells but also trypsinized adherent cells. Human embryonic kidney (HEK) 293T cells also arrest after camptothecin treatment and a small fraction of cells die (Figure 5.2A,B). The arrest can be clearly seen by a histogram along the DCV axis, which reports the cell cycle profile of the population (Figure 5.2B). To compare our results to a known apoptosis assay, we performed TUNEL using the Apo-BrdU kit (Life Technologies). Similarly to the DCV/YOPRO assay, apoptosis (in this case BrdU staining) is on the y-axis and cell cycle (in this case DAPI) is on the x-axis (Figure 5.3A,B). The agreement between the two assays is fairly good, though YOPRO detects more late-stage apoptotic cells. The differences are potentially due to the different morphological changes used as marks of apoptosis: while YOPRO detects membrane changes, TUNEL reports DNA fragmentation, which is thought to be a later stage of apoptosis. Thus, TUNEL may have better resolution of nearly dead cells but miss some earlier events in apoptosis.

The DCV/YOPRO assay can potentially also be used to assess differences in
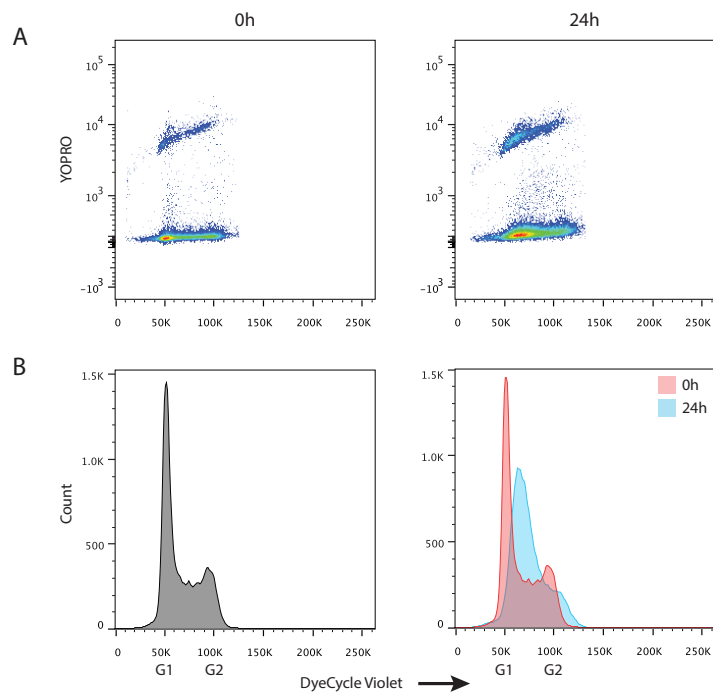
Figure 5.4: Aphidicolin induces S-phase arrest and apoptosis in 293T cells.
(**A**) 293T cells were treated with 1 µg/ml aphidicolin for 24 hours, then collected for
the DCV/YOPRO flow cytometry assay. (**B**) Histogram of DCV of untreated cells
(left) and overlay of untreated (pink) and aphidicolin-treated (blue) cells (right).
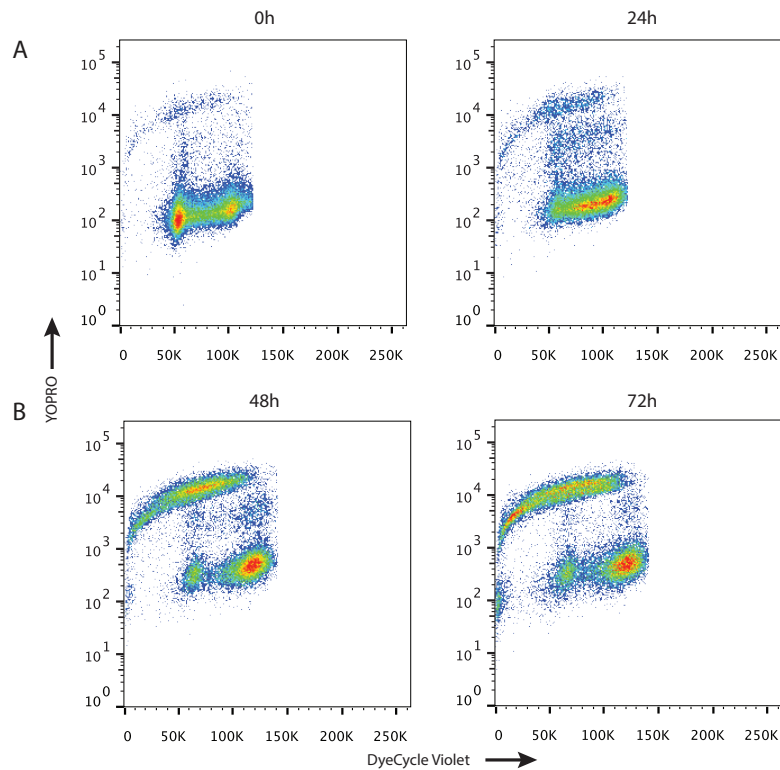
Figure 5.5: Cisplatin induces S/G2 arrest and apoptosis in HCT116 cells.
HCT116 cells were treated with 12.5 μM cisplatin and at the indicated times after
damage were collected for the DCV/YOPRO assay.

responses to various drugs. For instance, 293T cells treated with aphidicolin, an
inhibitor of DNA polymerases α and δ and hence a blocker of replicative DNA syn-
thesis, also arrest in S-phase with some S-phase-specific apoptosis (Figure 5.4A,B).
Distinct from camptothecin-induced arrest, aphidicolin-induced arrest is more
specific to early S-phase (Figure 5.4B). The DCV/YOPRO assay can potentially
be scaled up to be suited for high-throughput analyses of the effects of different
drugs at different doses and timescales, on the same cell line or across different

cell lines.

The DCV/YOPRO assay can also be used to analyze arrest and apoptosis with more temporal depth for a particular cell line or treatment. As discussed in Chapter 3, cisplatin treatment at its IC50 dose causes half of the population of HCT116 cells to undergo apoptosis while the other half senesce. Performing the DCV/YOPRO assay on cisplatin-treated HCT116 reveals cells in the early stages of apoptosis at 24 hours and late-stage apoptotic cells comprising about half the population by 72 hours (Figure 5.5), in close agreement with the microscopy data shown in Chapter 3. This flow cytometry method allows further characterization of divergent cell fate decisions in populations due to its ability to easily measure large populations but at single cell resolution.

5.3 Modification of the DCV/YOPRO assay for a variety of cell types

Human embryonic stem cells (hESCs), as discussed in Chapter 2, are exquisitely sensitive to DNA damage. They exhibit spontaneous apoptosis in culture, as is observed in the untreated condition. After treatment with the radiomimetic DNA-damaging drug neocarzinostatin (NCS), hESCs undergo cell death which has been previously characterized as apoptosis (Filion et al., 2009, Grandela et al., 2008, Liu et al., 2013, Qin et al., 2006). The DCV/YOPRO assay confirms that un-differentiated hESCs undergo rapid apoptosis after damage is induced with NCS (Figure 5.6A). Additionally, this assay reveals that damage-induced apoptosis of hESCs occurs fairly evenly from all stages in the cell cycle, without significant arrest.

When the DCV/YOPRO assay was performed on hESCs that had been differen-
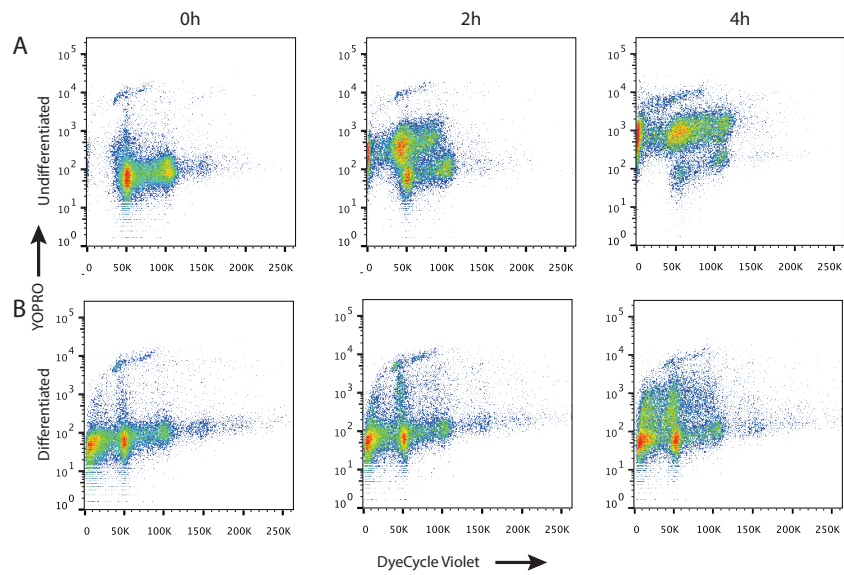
Figure 5.6: Undifferentiated cells undergo apoptosis after damage while differentiated cells exclude DCV. (**A**) Undifferentiated cells were treated with 200 ng/ml of NCS and at the indicated times after damage were collected for the DCV/YOPRO assay. (**B**) Cells differentiated with RA for 4 days were concurrently treated with NCS as in (**A**) and collected for the DCV/YOPRO assay.
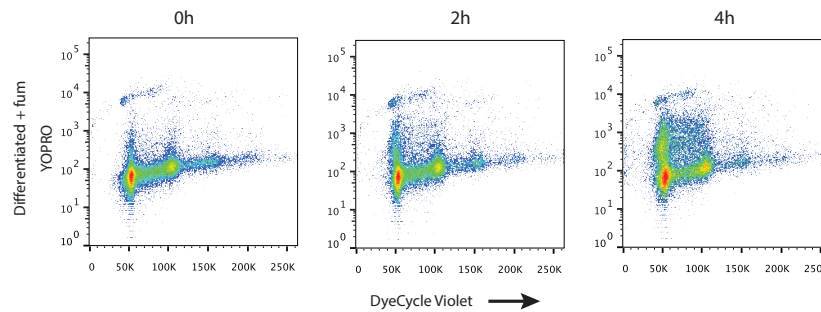
Figure 5.7: Inhibition of ABCG2 transport by fumitremorgin restores the normal cell cycle profile of differentiated cells. As in Figure 5.6, RA-differentiated cells were treated with 200 ng/ml of NCS and at the indicated times after damage were collected for DCV/YOPRO assay; fumitremorgin was added 30 minutes before collection.

tiated with retinoic acid (RA) for 4 days, then damaged with the same NCS treatment, we observed a peculiar shift of all cells leftward toward the hypodiploid region of the axis, even in the untreated control (Figure 5.6B). As almost all cells were alive, given the low amount of cell death even after NCS treatment, we suspected that this phenomenon occurred not as a result of DNA fragmentation (in the absence of apoptosis) but instead arose from a problem with DCV staining in this cell type.

We hypothesized that one reason that DCV incorporation and DNA binding would be impaired is if the cells were to pump out the dye. Certain cell types are known to express transporters that can pump out a wide range of drugs and other small molecules. For instance, the ATP-binding cassette (ABC) transporters comprise several subfamilies of efflux pumps with broad drug specificity. While little is known about the function of these transporters *in vivo* (van de Wetering and Sapthu, 2012, Vlaming et al., 2009), increased expression or activity of such

93

multidrug efflux pumps are known to contribute to multidrug resistance in cancer cells by lowering intracellular drug concentrations (Gottesman et al., 2002). Chemotherapy drugs known to be affected include vinblastine, vincristine, doxorubicin, daunorubicin, actinomycin-D, and paclitaxel (Ambudkar et al., 1999).

Moreover, some cell types have been identified based on exclusion of the DNA-binding Hoechst dye. The first cells so described, named side population (SP) cells because of their low Hoechst profile on flow cytometry, were a subset of adult mouse bone marrow with enriched hematopoietic stem cells (HSCs) (Goodell et al., 1996). Cells from multiple other tissues and cancer cell types that exclude Hoechst and its close relative DCV have since been shown to correspond to adult stem cell and tumor-initiating cancer cell populations (Mathew et al., 2009, Telford, 2010, Telford et al., 2007). Efflux of Hoechst was attributed to the ABC family of membrane transporters, and specifically shown to be dependent on ABCG2 (breast cancer resistance protein, BCRP1) (Scharenberg et al., 2002, Zhou et al., 2001), initially identified in multidrug-resistant breast cancer cells. We therefore investigated whether impaired DCV incorporation in RA-differentiated cells was due to ABCG2-mediated efflux of DCV.

To demonstrate that RA-differentiated cells indeed excluded DCV due to the activity of ABCG2, we employed fumitremorgin, a potent and specific inhibitor of ABCG2 (Mathew et al., 2009). Addition of fumitremorgin to differentiated cell samples restored the normal DCV/YOPRO profile of differentiated cells (Figure 5.7. This suggested that ABCG2 was active in differentiated cells. We therefore assessed the expression of ABCG2 in both undifferentiated and differentiated cells. A recent study had shown that hESCs have very low ABCG2 protein levels (Padmanabhan et al., 2012), but RA could potentially differentiate hESCs into
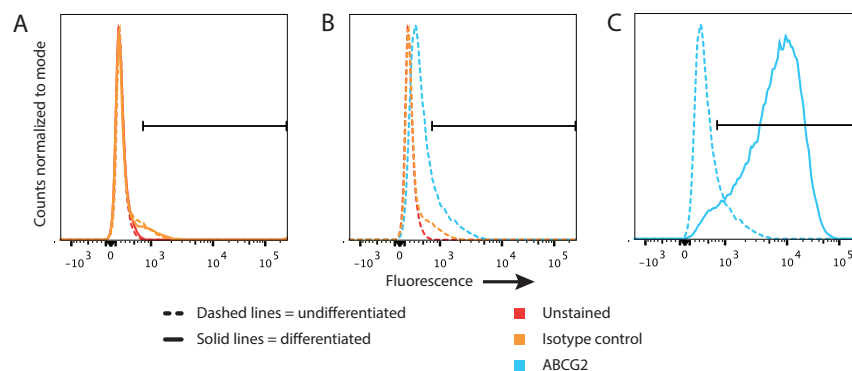
Figure 5.8: Differentiated cells express the ABCG2 pump. (**A**). Negative controls for ABCG2 staining, including unstained cells (red) and isotype control (orange), for undifferentiated (dashed lines) and differentiated cells (solid lines). (**B**). Undifferentiated cells stained with ABCG2 (cyan) compared to unstained and isotype control conditions. (**C**). ABCG2 staining in undifferentiated and differentiated cells. Horizontal line in all plots is an estimation of ABCG2-positive staining.

an intermediate state that might correspond to an adult stem or progenitor cell. Staining with an anti-ABCG2 monoclonal antibody that specifically recognizes an extracellular epitope of ABCG2 revealed little expression in undifferentiated cells and a drastic increase in ABCG2 expression in differentiated cells (Figure 5.8). We thereby determined that DCV staining was incomplete in RA-differentiated cells due to ABCG2 pump activity; however, the DCV/YOPRO assay can still be used when ABCG2 is inhibited.

5.4 Discussion

There are many techniques to detect various features of apoptosis, all with some advantages and some limitations. If we wish to additionally extract information about the cell cycle stage of the living and dying cells, there are fewer options.

We developed the DCV/YOPRO assay to address the need for a method to concurrently assess cell cycle stage and apoptosis that can be quickly and easily performed. DCV/YOPRO is a simple yet powerful tool that because of its ease of use can be scaled up to sample across different drugs, dosages, and cell lines as well as provide thorough temporal resolution of a few conditions. It is important, however, to confirm the analysis of apoptosis with at least one independent experimental approach which ideally should rely on a different parameter associated with apoptosis other than membrane permeability (Galluzzi et al., 2009).

5.5 MATERIALS AND METHODS

Cell culture: EL-4 and 293T cells were grown in DMEM with 10% fetal calf serum (FCS), 100 U/ml penicillin, 100 µg/ml streptomycin, and 250 ng/ml fungizone. HCT116 cells were grown in McCoy's media with the same supplements. hESCS (H1 line) culture and retinoic acid (RA) differentiation were performed as described in Chapter 2.

Antibodies and reagents: Unlabeled ABCG2 antibody (clone 5D3) and the corresponding mouse IgG1 kappa isotype control were obtained from eBioscience Inc. Secondary antibody labeling was performed with anti-mouse Alexa-488 (Life Technologies). Reagents used are as follows: camptothecin (Sigma), aphidicolin (Santa Cruz Biotechnologies), cisplatin (Sigma), neocarzinostatin (Sigma), and fumitremorgin C (Enzo Life Technologies).

Flow cytometry: Cells were dissociated when needed with trypsin or Accutase (Stemcell Technologies) and centrifuged. For the DCV/YOPRO assay, cells were resuspended in media at a concentration of 1×10^6 cells/ml. Vybrant DyeCycle Violet (Life Technologies) was added to a final concentration of 5-10 µM, and cells

were incubated for 20 minutes at 37C. YOPRO-3 (Life Technologies) was added to a final concentration of 0.1-0.5 µM, and cells were incubated for 15 minutes at room temperature, then analyzed on a BD LSRII flow cytometer and data were analyzed in FlowJo. YOPRO was detected in the DsRed channel, and DyeCycle Violet in the Pacific Blue channel. The TUNEL assay was performed with the Apo-BrdU TUNEL kit (Life Technologies), according to the manufacturer's suggested protocol.

5.6 Manuscript information

Author contributions: Julia C. Liu and Jodene K. Moore conducted the experiments and performed the analysis. Characterization of hESCs and differentiated cells with DCV/YOPRO and ABCG2 staining was performed by Julia C. Liu. Julia C. Liu wrote this chapter.

Bibliography

Devrim Acehan, Xuejun Jiang, David Gene Morgan, John E Heuser, Xiaodong Wang, and Christopher W Akey. Three-dimensional structure of the apoptosome: implications for assembly, procaspase-9 binding, and activation. *Molecular cell*, 9(2):423–432, February 2002. ISSN 1097-2765. PMID: 11864614.

S V Ambudkar, S Dey, C A Hrycyna, M Ramachandra, I Pastan, and M M Gottesman. Biochemical, cellular, and pharmacological aspects of the multidrug transporter. *Annual review of pharmacology and toxicology*, 39:361–398, 1999. ISSN 0362-1642. doi: 10.1146/annurev.pharmtox.39.1.361. PMID: 10331089.

P W Andrews. Retinoic acid induces neuronal differentiation of a cloned human embryonal carcinoma cell line in vitro. *Developmental biology*, 103(2):285–293, June 1984. ISSN 0012-1606. PMID: 6144603.

Eric Batchelor, Caroline S Mock, Irun Bhan, Alexander Loewer, and Galit Lahav. Recurrent initiation: a mechanism for triggering p53 pulses in response to DNA damage. *Molecular cell*, 30(3):277–289, May 2008. ISSN 1097-4164. doi: 10. 1016/j.molcel.2008.03.016. PMID: 18471974.

Eric Batchelor, Alexander Loewer, Caroline Mock, and Galit Lahav.

Stimulus-dependent dynamics of p53 in single cells. *Molecular Systems Biology*, 7, May 2011. ISSN 1744-4292. doi: 10.1038/msb.2011.20. URL `http://www.nature.com/doifinder/10.1038/msb.2011.20`.

Klaus A. Becker, Prachi N. Ghule, Jaclyn A. Therrien, Jane B. Lian, Janet L. Stein, Andre J. van Wijnen, and Gary S. Stein. Self-renewal of human embryonic stem cells is supported by a shortened g1 cell cycle phase. *Journal of Cellular Physiology*, 209(3):883–893, December 2006. ISSN 0021-9541, 1097-4652. doi: 10.1002/jcp.20776. URL `http://doi.wiley.com/10.1002/jcp.20776`.

J. Bereiter-Hahn and M. Voth. Dynamics of mitochondria in living cells: Shape changes, dislocations, fusion, and fission of mitochondria. *Microscopy Research and Technique*, 27(3):198–219, February 1994. ISSN 1059-910X, 1097-0029. doi: 10.1002/jemt.1070270303. URL `http://doi.wiley.com/10.1002/jemt.1070270303`.

Cedric Blanpain, Mary Mohrin, Panagiota A. Sotiropoulou, and Emmanuelle Passegué. DNA-Damage response in tissue-specific and cancer stem cells. *Cell Stem Cell*, 8(1):16–29, January 2011. ISSN 19345909. doi: 10.1016/j.stem.2010.12.012. URL `http://linkinghub.elsevier.com/retrieve/pii/S1934590910007071`.

Michael Certo, Victoria Del Gaizo Moore, Mari Nishino, Guo Wei, Stanley Korsmeyer, Scott A. Armstrong, and Anthony Letai. Mitochondria primed by death signals determine cellular addiction to antiapoptotic BCL-2 family members. *Cancer Cell*, 9(5):351–365, May 2006. ISSN 15356108. doi: 10.1016/j.ccr.2006.03.027. URL `http://linkinghub.elsevier.com/retrieve/pii/S1535610806001139`.

Wen Yong Chen, David H Wang, Raywhay Chiu Yen, Jianyuan Luo, Wei Gu, and
Stephen B Baylin. Tumor suppressor HIC1 directly regulates SIRT1 to modu-
late p53-dependent DNA-damage responses. *Cell*, 123(3):437–448, November
2005. ISSN 0092-8674. doi: 10.1016/j.cell.2005.08.011. PMID: 16269335.

Jerry E Chipuk, Tomomi Kuwana, Lisa Bouchier-Hayes, Nathalie M Droin, Don-
ald D Newmeyer, Martin Schuler, and Douglas R Green. Direct activation of bax
by p53 mediates mitochondrial membrane permeabilization and apoptosis. *Sci-
ence (New York, N.Y.)*, 303(5660):1010–1014, February 2004. ISSN 1095-9203.
doi: 10.1126/science.1092734. PMID: 14963330.

Jerry E Chipuk, Lisa Bouchier-Hayes, Tomomi Kuwana, Donald D Newmeyer, and
Douglas R Green. PUMA couples the nuclear and cytoplasmic proapoptotic
function of p53. *Science (New York, N.Y.)*, 309(5741):1732–1735, September
2005. ISSN 1095-9203. doi: 10.1126/science.1114297. PMID: 16151013.

Jerry E. Chipuk, Tudor Moldoveanu, Fabien Llambi, Melissa J. Parsons, and Dou-
glas R. Green. The BCL-2 family reunion. *Molecular Cell*, 37(3):299–310,
February 2010. ISSN 10972765. doi: 10.1016/j.molcel.2010.01.025. URL
`http://linkinghub.elsevier.com/retrieve/pii/S1097276510000791`.

Jing Deng, Nicole Carlson, Kunihiko Takeyama, Paola Dal Cin, Margaret Shipp,
and Anthony Letai. BH3 profiling identifies three distinct classes of apop-
totic blocks to predict response to ABT-737 and conventional chemotherapeu-
tic agents. *Cancer cell*, 12(2):171–185, August 2007. ISSN 1535-6108. doi:
10.1016/j.ccr.2007.07.001. PMID: 17692808.

Grant Dewson and Ruth M Kluck. Mechanisms by which bak and bax permeabilise

mitochondria during apoptosis. *Journal of cell science*, 122(Pt 16):2801–2808, August 2009. ISSN 0021-9533. PMID: 19795525 PMCID: PMC2736138.

Raluca Dumitru, Vivian Gama, B. Matthew Fagan, Jacquelyn J. Bower, Vijay Swahari, Larysa H. Pevny, and Mohanish Deshmukh. Human embryonic stem cells have constitutively active bax at the golgi and are primed to undergo rapid apoptosis. *Molecular Cell*, 46(5):573–583, June 2012. ISSN 10972765. doi: 10.1016/ j.molcel.2012.04.002. URL http://linkinghub.elsevier.com/retrieve/ pii/S1097276512002687.

P J Duriez and G M Shah. Cleavage of poly(ADP-ribose) polymerase: a sensitive parameter to study cell death. *Biochemistry and cell biology = Biochimie et biologie cellulaire*, 75(4):337–349, 1997. ISSN 0829-8211. PMID: 9493956.

Susan Elmore. Apoptosis: A review of programmed cell death. *Toxicologic Pathology*, 35(4):495–516, June 2007. ISSN 0192-6233. doi: 10.1080/ 01926230701320337. URL http://tpx.sagepub.com/cgi/doi/10.1080/ 01926230701320337.

J. M. Facucho-Oliveira and J. C. St. John. The relationship between pluripotency and mitochondrial DNA proliferation during early embryo development and embryonic stem cell differentiation. *Stem Cell Reviews and Reports*, 5(2):140–158, April 2009. ISSN 1550-8943, 1558-6804. doi: 10.1007/s12015-009-9058-0. URL http://link.springer.com/10.1007/ s12015-009-9058-0.

S Fan, J K Chang, M L Smith, D Duba, Jr Fornace, A J, and P M O'Connor. Cells lacking CIP1/WAF1 genes exhibit preferential sensitivity to cisplatin and nitro-

gen mustard. *Oncogene*, 14(18):2127–2136, May 1997. ISSN 0950-9232. doi:
10.1038/sj.onc.1201052. PMID: 9174048.

Tera M. Filion, Meng Qiao, Prachi N. Ghule, Matthew Mandeville, Andre J. van
Wijnen, Janet L. Stein, Jane B. Lian, Dario C. Altieri, and Gary S. Stein. Survival
responses of human embryonic stem cells to DNA damage. *Journal of Cellular
Physiology*, 220(3):586–592, September 2009. ISSN 00219541, 10974652. doi:
10.1002/jcp.21735. URL http://doi.wiley.com/10.1002/jcp.21735.

Adam A Filipczyk, Andrew L Laslett, Christine Mummery, and Martin F Pera. Dif-
ferentiation is coupled to changes in the cell cycle regulatory apparatus of hu-
man embryonic stem cells. *Stem cell research*, 1(1):45–60, October 2007. ISSN
1876-7753. doi: 10.1016/j.scr.2007.09.002. PMID: 19383386.

H Fujimoto, N Onishi, N Kato, M Takekawa, X Z Xu, A Kosugi, T Kondo, M Ima-
mura, I Oishi, A Yoda, and Y Minami. Regulation of the antioncogenic chk2
kinase by the oncogenic wip1 phosphatase. *Cell death and differentiation*, 13(7):
1170–1180, July 2006. ISSN 1350-9047. doi: 10.1038/sj.cdd.4401801. PMID:
16311512.

L Galluzzi, S A Aaronson, J Abrams, E S Alnemri, D W Andrews, E H Baehrecke,
N G Bazan, M V Blagosklonny, K Blomgren, C Borner, D E Bredesen, C Bren-
ner, M Castedo, J A Cidlowski, A Ciechanover, G M Cohen, V De Laurenzi,
R De Maria, M Deshmukh, B D Dynlacht, W S El-Deiry, R A Flavell, S Fulda,
C Garrido, P Golstein, M-L Gougeon, D R Green, H Gronemeyer, G Hajnóczky,
J M Hardwick, M O Hengartner, H Ichijo, M Jäättelä, O Kepp, A Kimchi, D J
Klionsky, R A Knight, S Kornbluth, S Kumar, B Levine, S A Lipton, E Lugli,
F Madeo, W Malorni, J-Cw Marine, S J Martin, J P Medema, P Mehlen,

G Melino, U M Moll, E Morselli, S Nagata, D W Nicholson, P Nicotera, G Nuñez, M Oren, J Penninger, S Pervaiz, M E Peter, M Piacentini, J H M Prehn, H Puthalakath, G A Rabinovich, R Rizzuto, C M P Rodrigues, D C Rubinsztein, T Rudel, L Scorrano, H-U Simon, H Steller, J Tschopp, Y Tsujimoto, P Vandenabeele, I Vitale, K H Vousden, R J Youle, J Yuan, B Zhivotovsky, and G Kroemer. Guidelines for the use and interpretation of assays for monitoring cell death in higher eukaryotes. *Cell Death and Differentiation*, 16(8):1093–1107, April 2009. ISSN 1350-9047, 1476-5403. doi: 10.1038/cdd.2009.44. URL `http://www.nature.com/doifinder/10.1038/cdd.2009.44`.

Y Gavrieli, Y Sherman, and S A Ben-Sasson. Identification of programmed cell death in situ via specific labeling of nuclear DNA fragmentation. *The Journal of cell biology*, 119(3):493–501, November 1992. ISSN 0021-9525. PMID: 1400587.

N. Geva-Zatorsky, E. Dekel, E. Batchelor, G. Lahav, and U. Alon. Fourier analysis and systems identification of the p53 feedback loop. *Proceedings of the National Academy of Sciences*, 107(30):13550–13555, July 2010. ISSN 0027-8424, 1091-6490. doi: 10.1073/pnas.1001107107. URL `http://www.pnas.org/cgi/doi/10.1073/pnas.1001107107`.

M A Goodell, K Brose, G Paradis, A S Conner, and R C Mulligan. Isolation and functional properties of murine hematopoietic stem cells that are replicating in vivo. *The Journal of experimental medicine*, 183(4):1797–1806, April 1996. ISSN 0022-1007. PMID: 8666936.

Michael M. Gottesman, Tito Fojo, and Susan E. Bates. Multidrug resistance in cancer: role of ATP-dependent transporters. *Nature Reviews Cancer*, 2(1):

48–58, January 2002. ISSN 14741768. doi: 10.1038/nrc706. URL `http://www.nature.com/doifinder/10.1038/nrc706`.

C. Grandela, M.F. Pera, and E.J. Wolvetang. p53 is required for etoposide-induced apoptosis of human embryonic stem cells. *Stem Cell Research*, 1(2):116–128, June 2008. ISSN 18735061. doi: 10.1016/j.scr.2007.10.003. URL `http://linkinghub.elsevier.com/retrieve/pii/S1873506107000104`.

Douglas R Green and Guido Kroemer. Cytoplasmic functions of the tumour suppressor p53. *Nature*, 458(7242):1127–1130, April 2009. ISSN 1476-4687. doi: 10.1038/nature07986. PMID: 19407794.

M S Greenblatt, W P Bennett, M Hollstein, and C C Harris. Mutations in the p53 tumor suppressor gene: clues to cancer etiology and molecular pathogenesis. *Cancer research*, 54(18):4855–4878, September 1994. ISSN 0008-5472. PMID: 8069852.

Andrei V Gudkov and Elena A Komarova. The role of p53 in determining sensitivity to radiotherapy. *Nature reviews. Cancer*, 3(2):117–129, February 2003. ISSN 1474-175X. doi: 10.1038/nrc992. PMID: 12563311.

J. Han, L. A. Goldstein, W. Hou, B. R. Gastman, and H. Rabinowich. Regulation of mitochondrial apoptotic events by p53-mediated disruption of complexes between antiapoptotic bcl-2 members and bim. *Journal of Biological Chemistry*, 285(29):22473–22483, April 2010. ISSN 0021-9258, 1083-351X. doi: 10.1074/jbc.M109.081042. URL `http://www.jbc.org/cgi/doi/10.1074/jbc.M109.081042`.

Douglas Hanahan and Robert A. Weinberg. Hallmarks of cancer: The next gen-

eration. *Cell*, 144(5):646–674, March 2011. ISSN 00928674. doi: 10.1016/j.
cell.2011.02.013. URL http://linkinghub.elsevier.com/retrieve/pii/
S0092867411001279.

Thomas Helleday, Eva Petermann, Cecilia Lundin, Ben Hodgson, and Ricky A.
Sharma. DNA repair pathways as targets for cancer therapy. *Nature Reviews
Cancer*, 8(3):193–204, March 2008. ISSN 1474-175X, 1474-1768. doi: 10.1038/
nrc2342. URL http://www.nature.com/doifinder/10.1038/nrc2342.

D C Huang and A Strasser. BH3-only proteins-essential initiators of apoptotic
cell death. *Cell*, 103(6):839–842, December 2000. ISSN 0092-8674. PMID:
11136969.

Hiroshi Ide, Mahmoud I Shoulkamy, Toshiaki Nakano, Mayumi
Miyamoto-Matsubara, and Amir M H Salem. Repair and biochemical ef-
fects of DNA-protein crosslinks. *Mutation research*, 711(1-2):113–122,
June 2011. ISSN 0027-5107. doi: 10.1016/j.mrfmmm.2010.12.007. PMID:
21185846.

T Idziorek, J Estaquier, F De Bels, and J C Ameisen. YOPRO-1 permits cytoflu-
orometric analysis of programmed cell death (apoptosis) without interfering
with cell viability. *Journal of immunological methods*, 185(2):249–258, Septem-
ber 1995. ISSN 0022-1759. PMID: 7561136.

Alberto Inga, Francesca Storici, Thomas A Darden, and Michael A Resnick. Dif-
ferential transactivation by the p53 transcription factor is highly dependent
on p53 level and promoter target sequence. *Molecular and cellular biology*, 22
(24):8612–8625, December 2002. ISSN 0270-7306. PMID: 12446780 PMCID:
PMC139870.

Alessandra Insinga, Angelo Cicalese, Mario Faretta, Barbara Gallo, Luisa Albano, Simona Ronzoni, Laura Furia, Andrea Viale, and Pier Giuseppe Pelicci. DNA damage in stem cells activates p21, inhibits p53, and induces symmetric self-renewing divisions. *Proceedings of the National Academy of Sciences of the United States of America*, 110(10):3931–3936, March 2013. ISSN 1091-6490. doi: 10.1073/pnas.1213394110. PMID: 23417300.

N Johnson, T T Ng, and J M Parkin. Camptothecin causes cell cycle perturbations within t-lymphoblastoid cells followed by dose dependent induction of apoptosis. *Leukemia research*, 21(10):961–972, October 1997. ISSN 0145-2126. PMID: 9403007.

M Karbowski and R J Youle. Dynamics of mitochondrial morphology in healthy cells and during apoptosis. *Cell Death and Differentiation*, 10(8):870–880, August 2003. ISSN 13509047, 14765403. doi: 10.1038/sj.cdd.4401260. URL `http://www.nature.com/doifinder/10.1038/sj.cdd.4401260`.

Lloyd Kelland. The resurgence of platinum-based cancer chemotherapy. *Nature Reviews Cancer*, 7(8):573–584, July 2007. ISSN 1474-175X, 1474-1768. doi: 10.1038/nrc2167. URL `http://www.nature.com/doifinder/10.1038/nrc2167`.

J F Kerr, A H Wyllie, and A R Currie. Apoptosis: a basic biological phenomenon with wide-ranging implications in tissue kinetics. *British journal of cancer*, 26(4):239–257, August 1972. ISSN 0007-0920. PMID: 4561027 PMCID: PMC2008650.

Hyungjin Kim, Mubina Rafiuddin-Shah, Ho-Chou Tu, John R Jeffers, Gerard P Zambetti, James J-D Hsieh, and Emily H-Y Cheng. Hierarchical regulation of

mitochondrion-dependent apoptosis by BCL-2 subfamilies. *Nature cell biology*, 8(12):1348–1358, December 2006. ISSN 1465-7392. doi: 10.1038/ncb1499. PMID: 17115033.

E. A. Komarova. Transgenic mice with p53-responsive lacZ: p53activity varies dramatically during normal development and determines radiation and drug sensitivity invivo. *The EMBO Journal*, 16(6):1391–1400, March 1997. ISSN 14602075. doi: 10.1093/emboj/16.6.1391. URL http://www.nature.com/doifinder/10.1093/emboj/16.6.1391.

G Koopman, C P Reutelingsperger, G A Kuijten, R M Keehnen, S T Pals, and M H van Oers. Annexin v for flow cytometric detection of phosphatidylserine expression on b cells undergoing apoptosis. *Blood*, 84(5):1415–1420, September 1994. ISSN 0006-4971. PMID: 8068938.

M Kracikova, G Akiri, A George, R Sachidanandam, and S A Aaronson. A threshold mechanism mediates p53 cell fate decision between growth arrest and apoptosis. *Cell Death and Differentiation*, 20(4):576–588, January 2013. ISSN 1350-9047, 1476-5403. doi: 10.1038/cdd.2012.155. URL http://www.nature.com/doifinder/10.1038/cdd.2012.155.

M Kressel and P Groscurth. Distinction of apoptotic and necrotic cell death by in situ labelling of fragmented DNA. *Cell and tissue research*, 278(3):549–556, December 1994. ISSN 0302-766X. PMID: 7850865.

Galit Lahav, Nitzan Rosenfeld, Alex Sigal, Naama Geva-Zatorsky, Arnold J Levine, Michael B Elowitz, and Uri Alon. Dynamics of the p53-mdm2 feedback loop in individual cells. *Nature genetics*, 36(2):147–150, February 2004. ISSN 1061-4036. doi: 10.1038/ng1293. PMID: 14730303.

D P Lane. p53, guardian of the genome. *Nature*, 358(6381):15–16, July 1992. ISSN 0028-0836. doi: 10.1038/358015a0. PMID: 1614522.

Paul H Lerou, Akiko Yabuuchi, Hongguang Huo, Justine D Miller, Leah F Boyer, Thorsten M Schlaeger, and George Q Daley. Derivation and maintenance of human embryonic stem cells from poor-quality in vitro fertilization embryos. *Nature protocols*, 3(5):923–933, 2008. ISSN 1750-2799. doi: 10.1038/nprot. 2008.60. PMID: 18451800.

J I-Ju Leu, Patrick Dumont, Michael Hafey, Maureen E Murphy, and Donna L George. Mitochondrial p53 activates bak and causes disruption of a bak-mcl1 complex. *Nature cell biology*, 6(5):443–450, May 2004. ISSN 1465-7392. doi: 10.1038/ncb1123. PMID: 15077116.

M. R. Lewis and W. H. Lewis. Mitochondria in tissue culture. *Science*, 39 (1000):330–333, February 1914. ISSN 0036-8075, 1095-9203. doi: 10. 1126/science.39.1000.330. URL http://www.sciencemag.org/cgi/doi/10. 1126/science.39.1000.330.

Julia C. Liu, Xiao Guan, Jeremy A. Ryan, Ana G. Rivera, Caroline Mock, Vishesh Agarwal, Anthony Letai, Paul H. Lerou, and Galit Lahav. High mitochondrial priming sensitizes hESCs to DNA-damage-induced apoptosis. *Cell Stem Cell*, 13(4):483–491, October 2013. ISSN 19345909. doi: 10.1016/ j.stem.2013.07.018. URL http://linkinghub.elsevier.com/retrieve/ pii/S1934590913003639.

L F Liu, S D Desai, T K Li, Y Mao, M Sun, and S P Sim. Mechanism of action of camptothecin. *Annals of the New York Academy of Sciences*, 922:1–10, 2000. ISSN 0077-8923. PMID: 11193884.

Alexander Loewer, Eric Batchelor, Giorgio Gaglia, and Galit Lahav. Basal dynamics of p53 reveal transcriptionally attenuated pulses in cycling cells. *Cell*, 142(1): 89–100, July 2010. ISSN 1097-4172. doi: 10.1016/j.cell.2010.05.031. PMID: 20598361.

Alexander Loewer, Ketki Karanam, Caroline Mock, and Galit Lahav. The p53 response in single cells is linearly correlated to the number of DNA breaks without a distinct threshold. *BMC Biology*, 11(1):114, 2013. ISSN 1741-7007. doi: 10.1186/1741-7007-11-114. URL http://www.biomedcentral.com/1741-7007/11/114.

Xiongbin Lu, Bonnie Nannenga, and Lawrence A Donehower. PPM1D dephospho-rylates chk1 and p53 and abrogates cell cycle checkpoints. *Genes & development*, 19(10):1162–1174, May 2005. ISSN 0890-9369. doi: 10.1101/gad.1291305. PMID: 15870257 PMCID: PMC1132003.

Markus Löbrich, Atsushi Shibata, Andrea Beucher, Anna Fisher, Michael Ensminger, Aaron A Goodarzi, Olivia Barton, and Penny A Jeggo. gammaH2AX foci analysis for monitoring DNA double-strand break repair: strengths, limitations and optimization. *Cell cycle (Georgetown, Tex.)*, 9(4):662–669, February 2010. ISSN 1551-4005. PMID: 20139725.

S Mangan and U Alon. Structure and function of the feed-forward loop network motif. *Proceedings of the National Academy of Sciences of the United States of America*, 100(21):11980–11985, October 2003. ISSN 0027-8424. doi: 10.1073/pnas.2133841100. PMID: 14530388 PMCID: PMC218699.

Grinu Mathew, Jr Timm, Earl A, Paula Sotomayor, Alejandro Godoy, Viviana P Montecinos, Gary J Smith, and Wendy J Huss. ABCG2-mediated DyeCycle vi-

olet efflux defined side population in benign and malignant prostate. *Cell cycle (Georgetown, Tex.)*, 8(7):1053–1061, April 2009. ISSN 1551-4005. PMID: 19270533.

A J Merritt, C S Potten, A J Watson, D Y Loh, K Nakayama, K Nakayama, and J A Hickman. Differential expression of bcl-2 in intestinal epithelia. correlation with attenuation of apoptosis in colonic crypts and the incidence of colonic neoplasia. *Journal of cell science*, 108 (Pt 6):2261–2271, June 1995. ISSN 0021-9533. PMID: 7673346.

Motohiro Mihara, Susan Erster, Alexander Zaika, Oleksi Petrenko, Thomas Chittenden, Petr Pancoska, and Ute M Moll. p53 has a direct apoptogenic role at the mitochondria. *Molecular cell*, 11(3):577–590, March 2003. ISSN 1097-2765. PMID: 12667443.

Kasturi Mitra. Mitochondrial fission-fusion as an emerging key regulator of cell proliferation and differentiation: Prospects & overviews. *BioEssays*, pages n/a–n/a, August 2013. ISSN 02659247. doi: 10.1002/bies.201300011. URL `http://doi.wiley.com/10.1002/bies.201300011`.

Kasturi Mitra, Christian Wunder, Badrinath Roysam, Gang Lin, and Jennifer Lippincott-Schwartz. A hyperfused mitochondrial state achieved at g1-s regulates cyclin e buildup and entry into s phase. *Proceedings of the National Academy of Sciences of the United States of America*, 106(29):11960–11965, July 2009. ISSN 1091-6490. doi: 10.1073/pnas.0904875106. PMID: 19617534.

Mary Mohrin, Emer Bourke, David Alexander, Matthew R. Warr, Keegan Barry-Holson, Michelle M. Le Beau, Ciaran G. Morrison, and Emmanuelle

Passegué. Hematopoietic stem cell quiescence promotes error-prone DNA repair and mutagenesis. *Cell Stem Cell*, 7(2):174–185, August 2010. ISSN 19345909. doi: 10.1016/j.stem.2010.06.014. URL `http://linkinghub.elsevier.com/retrieve/pii/S1934590910003292`.

Olga Momcilovic, Leah Knobloch, Jamie Fornsaglio, Sandra Varum, Charles Easley, and Gerald Schatten. DNA damage responses in human induced pluripotent stem cells and embryonic stem cells. *PLoS ONE*, 5(10):e13410, October 2010. ISSN 1932-6203. doi: 10.1371/journal.pone.0013410. URL `http://dx.plos.org/10.1371/journal.pone.0013410`.

M Müller, S Wilder, D Bannasch, D Israeli, K Lehlbach, M Li-Weber, S L Friedman, P R Galle, W Stremmel, M Oren, and P H Krammer. p53 activates the CD95 (APO-1/Fas) gene in response to DNA damage by anticancer drugs. *The Journal of experimental medicine*, 188(11):2033–2045, December 1998. ISSN 0022-1007. PMID: 9841917.

K Nakano and K H Vousden. PUMA, a novel proapoptotic gene, is induced by p53. *Molecular cell*, 7(3):683–694, March 2001. ISSN 1097-2765. PMID: 11463392.

I Neganova, X Zhang, S Atkinson, and M Lako. Expression and functional analysis of g1 to s regulatory components reveals an important role for CDK2 in cell cycle regulation in human embryonic stem cells. *Oncogene*, 28(1):20–30, January 2009. ISSN 1476-5594. doi: 10.1038/onc.2008.358. PMID: 18806832.

Triona Ni Chonghaile, Kristopher A Sarosiek, Thanh-Trang Vo, Jeremy A Ryan, Anupama Tammareddi, Victoria Del Gaizo Moore, Jing Deng, Kenneth C Anderson, Paul Richardson, Yu-Tzu Tai, Constantine S Mitsiades, Ursula A Matulonis, Ronny Drapkin, Richard Stone, Daniel J Deangelo, David J McConkey,

Stephen E Sallan, Lewis Silverman, Michelle S Hirsch, Daniel Ruben Carrasco, and Anthony Letai. Pretreatment mitochondrial priming correlates with clinical response to cytotoxic chemotherapy. *Science (New York, N.Y.)*, 334(6059): 1129–1133, November 2011. ISSN 1095-9203. doi: 10.1126/science.1206727. PMID: 22033517.

D W Nicholson. Caspase structure, proteolytic substrates, and function during apoptotic cell death. *Cell death and differentiation*, 6(11):1028–1042, November 1999. ISSN 1350-9047. doi: 10.1038/sj.cdd.4400598. PMID: 10578171.

H Niwa, J Miyazaki, and A G Smith. Quantitative expression of oct-3/4 defines differentiation, dedifferentiation or self-renewal of ES cells. *Nature genetics*, 24(4): 372–376, April 2000. ISSN 1061-4036. doi: 10.1038/74199. PMID: 10742100.

E Oda, R Ohki, H Murasawa, J Nemoto, T Shibue, T Yamashita, T Tokino, T Taniguchi, and N Tanaka. Noxa, a BH3-only member of the bcl-2 family and candidate mediator of p53-induced apoptosis. *Science (New York, N.Y.)*, 288 (5468):1053–1058, May 2000a. ISSN 0036-8075. PMID: 10807576.

K Oda, H Arakawa, T Tanaka, K Matsuda, C Tanikawa, T Mori, H Nishimori, K Tamai, T Tokino, Y Nakamura, and Y Taya. p53AIP1, a potential mediator of p53-dependent apoptosis, and its regulation by ser-46-phosphorylated p53. *Cell*, 102(6):849–862, September 2000b. ISSN 0092-8674. PMID: 11030628.

K. O'Keefe, H. Li, and Y. Zhang. Nucleocytoplasmic shuttling of p53 is essential for MDM2-Mediated cytoplasmic degradation but not ubiquitination. *Molecular and Cellular Biology*, 23(18):6396–6405, August 2003. ISSN 0270-7306. doi: 10.1128/MCB.23.18.6396-6405.2003. URL http://mcb.asm.org/cgi/doi/10.1128/MCB.23.18.6396-6405.2003.

Trudy G Oliver, Kim L Mercer, Leanne C Sayles, James R Burke, Diana Mendus, Katherine S Lovejoy, Mei-Hsin Cheng, Aravind Subramanian, David Mu, Scott Powers, Denise Crowley, Roderick T Bronson, Charles A Whittaker, Arjun Bhutkar, Stephen J Lippard, Todd Golub, Juergen Thomale, Tyler Jacks, and E Alejandro Sweet-Cordero. Chronic cisplatin treatment promotes enhanced damage repair and tumor progression in a mouse model of lung cancer. *Genes & development*, 24(8):837–852, April 2010. ISSN 1549-5477. doi: 10.1101/gad.1897010. PMID: 20395368 PMCID: PMC2854397.

Raji Padmanabhan, Kevin G Chen, Jean-Pierre Gillet, Misty Handley, Barbara S Mallon, Rebecca S Hamilton, Kyeyoon Park, Sudhir Varma, Michele G Mehaffey, Pamela G Robey, Ronald D G McKay, and Michael M Gottesman. Regulation and expression of the ATP-binding cassette transporter ABCG2 in human embryonic stem cells. *Stem cells (Dayton, Ohio)*, 30(10):2175–2187, October 2012. ISSN 1549-4918. doi: 10.1002/stem.1195. PMID: 22887864.

E Christine Pietsch, J I-Ju Leu, Amanda Frank, Patrick Dumont, Donna L George, and Maureen E Murphy. The tetramerization domain of p53 is required for efficient BAK oligomerization. *Cancer biology & therapy*, 6(10):1576–1583, October 2007. ISSN 1555-8576. PMID: 17895645.

Yves Pommier, Elisabetta Leo, HongLiang Zhang, and Christophe Marchand. DNA topoisomerases and their poisoning by anticancer and antibacterial drugs. *Chemistry & biology*, 17(5):421–433, May 2010. ISSN 1879-1301. doi: 10.1016/j.chembiol.2010.04.012. PMID: 20534341.

Alessandro Prigione, Beatrix Fauler, Rudi Lurz, Hans Lehrach, and James Adjaye. The senescence-related Mitochondrial/Oxidative stress pathway is repressed in

human induced pluripotent stem cells. *STEM CELLS*, 28(4):721–733, March 2010. ISSN 10665099, 15494918. doi: 10.1002/stem.404. URL `http://doi.wiley.com/10.1002/stem.404`.

Jeremy E Purvis, Kyle W Karhohs, Caroline Mock, Eric Batchelor, Alexander Loewer, and Galit Lahav. p53 dynamics control cell fate. *Science (New York, N.Y.)*, 336(6087):1440–1444, June 2012. ISSN 1095-9203. doi: 10.1126/science.1218351. PMID: 22700930.

H. Qin, T. Yu, T. Qing, Y. Liu, Y. Zhao, J. Cai, J. Li, Z. Song, X. Qu, P. Zhou, J. Wu, M. Ding, and H. Deng. Regulation of apoptosis and differentiation by p53 in human embryonic stem cells. *Journal of Biological Chemistry*, 282(8):5842–5852, December 2006. ISSN 0021-9258, 1083-351X. doi: 10.1074/jbc.M610464200. URL `http://www.jbc.org/cgi/doi/10.1074/jbc.M610464200`.

Wei Qiu, Eleanor B. Carson-Walter, Hongtao Liu, Michael Epperly, Joel S. Greenberger, Gerard P. Zambetti, Lin Zhang, and Jian Yu. PUMA regulates intestinal progenitor cell radiosensitivity and gastrointestinal syndrome. *Cell Stem Cell*, 2(6):576–583, June 2008. ISSN 19345909. doi: 10.1016/j.stem.2008.03.009. URL `http://linkinghub.elsevier.com/retrieve/pii/S1934590908001227`.

Walid Rachidi, Ghida Harfourche, Gilles Lemaitre, Franck Amiot, Pierre Vaigot, and Michèle T Martin. Sensing radiosensitivity of human epidermal stem cells. *Radiotherapy and oncology: journal of the European Society for Therapeutic Radiology and Oncology*, 83(3):267–276, June 2007. ISSN 0167-8140. doi: 10.1016/j.radonc.2007.05.007. PMID: 17540468.

A Reles, W H Wen, A Schmider, C Gee, I B Runnebaum, U Kilian, L A Jones,

A El-Naggar, C Minguillon, I Schönborn, O Reich, R Kreienberg, W Lichtenegger, and M F Press. Correlation of p53 mutations with resistance to platinum-based chemotherapy and shortened survival in ovarian cancer. *Clinical cancer research: an official journal of the American Association for Cancer Research*, 7(10):2984–2997, October 2001. ISSN 1078-0432. PMID: 11595686.

Conly L. Rieder and Helder Maiato. Stuck in division or passing through: What happens when cells cannot satisfy the spindle assembly checkpoint. *Developmental Cell*, 7(5):637–651, November 2004. ISSN 15345807. doi: 10.1016/j.devcel.2004.09.002. URL http://linkinghub.elsevier.com/retrieve/pii/S1534580704003016.

Todd Riley, Eduardo Sontag, Patricia Chen, and Arnold Levine. Transcriptional control of human p53-regulated genes. *Nature Reviews Molecular Cell Biology*, 9 (5):402–412, May 2008. ISSN 1471-0072, 1471-0080. doi: 10.1038/nrm2395. URL http://www.nature.com/doifinder/10.1038/nrm2395.

A M Robertson, C C Bird, A W Waddell, and A R Currie. Morphological aspects of glucocorticoid-induced cell death in human lymphoblastoid cells. *The Journal of pathology*, 126(3):181–187, November 1978. ISSN 0022-3417. doi: 10.1002/path.1711260307. PMID: 745025.

A I Robles, N A Bemmels, A B Foraker, and C C Harris. APAF-1 is a transcriptional target of p53 in DNA damage-induced apoptosis. *Cancer research*, 61(18): 6660–6664, September 2001. ISSN 0008-5472. PMID: 11559530.

Derrick J Rossi, Jun Seita, Agnieszka Czechowicz, Deepta Bhattacharya, David Bryder, and Irving L Weissman. Hematopoietic stem cell quiescence attenuates DNA damage response and permits DNA damage accumulation during aging.

Cell cycle (Georgetown, Tex.), 6(19):2371–2376, October 2007. ISSN 1551-4005. PMID: 17700071.

Christian W Scharenberg, Michael A Harkey, and Beverly Torok-Storb. The ABCG2 transporter is an efficient hoechst 33342 efflux pump and is preferentially expressed by immature human hematopoietic progenitors. *Blood*, 99(2):507–512, January 2002. ISSN 0006-4971. PMID: 11781231.

R T Schimke, A Kung, S S Sherwood, J Sheridan, and R Sharma. Life, death and genomic change in perturbed cell cycles. *Philosophical transactions of the Royal Society of London. Series B, Biological sciences*, 345(1313):311–317, August 1994. ISSN 0962-8436. doi: 10.1098/rstb.1994.0111. PMID: 7846128.

Ding-Wu Shen, Lynn M Pouliot, Matthew D Hall, and Michael M Gottesman. Cisplatin resistance: a cellular self-defense mechanism resulting from multiple epigenetic and genetic changes. *Pharmacological reviews*, 64(3):706–721, July 2012. ISSN 1521-0081. doi: 10.1124/pr.111.005637. PMID: 22659329.

Y Shiloh, G P van der Schans, P H Lohman, and Y Becker. Induction and repair of DNA damage in normal and ataxia-telangiectasia skin fibroblasts treated with neocarzinostatin. *Carcinogenesis*, 4(7):917–921, 1983. ISSN 0143-3334. PMID: 6223717.

Sathyavageeswaran Shreeram, Oleg N Demidov, Weng Kee Hee, Hiroshi Yamaguchi, Nobuyuki Onishi, Calvina Kek, Oleg N Timofeev, Crissy Dudgeon, Albert J Fornace, Carl W Anderson, Yasuhiro Minami, Ettore Appella, and Dmitry V Bulavin. Wip1 phosphatase modulates ATM-dependent signaling pathways. *Molecular cell*, 23(5):757–764, September 2006. ISSN 1097-2765. doi: 10.1016/j.molcel.2006.07.010. PMID: 16949371.

Zahid H Siddik. Cisplatin: mode of cytotoxic action and molecular basis of resistance. *Oncogene*, 22(47):7265–7279, October 2003. ISSN 0950-9232. doi: 10.1038/sj.onc.1206933. PMID: 14576837.

Rajeshwar P. Sinha and Donat-P. Häder. UV-induced DNA damage and repair: a review. *Photochemical & Photobiological Sciences*, 1(4):225–236, April 2002. ISSN 1474905X, 14749092. doi: 10.1039/b201230h. URL http://xlink.rsc.org/?DOI=b201230h.

Mykyta V Sokolov, Irina V Panyutin, Igor G Panyutin, and Ronald D Neumann. Dynamics of the transcriptome response of cultured human embryonic stem cells to ionizing radiation exposure. *Mutation research*, 709-710:40–48, May 2011. ISSN 0027-5107. doi: 10.1016/j.mrfmmm.2011.02.008. PMID: 21376742.

Hoseok Song, Sun-Ku Chung, and Yang Xu. Modeling disease in human ESCs using an efficient BAC-Based homologous recombination system. *Cell Stem Cell*, 6(1):80–89, January 2010. ISSN 19345909. doi: 10.1016/j.stem.2009.11.016. URL http://linkinghub.elsevier.com/retrieve/pii/S1934590909006237.

Panagiota A. Sotiropoulou, Aurélie Candi, Guilhem Mascré, Sarah De Clercq, Khalil Kass Youssef, Gaelle Lapouge, Ellen Dahl, Claudio Semeraro, Geertrui Denecker, Jean-Christophe Marine, and Cédric Blanpain. Bcl-2 and accelerated DNA repair mediates resistance of hair follicle bulge stem cells to DNA-damage-induced cell death. *Nature Cell Biology*, 12(6):572–582, May 2010. ISSN 1465-7392, 1476-4679. doi: 10.1038/ncb2059. URL http://www.nature.com/doifinder/10.1038/ncb2059.

Daniel Speidel. Transcription-independent p53 apoptosis: an alternative route to death. *Trends in Cell Biology*, 20(1):14–24, January 2010. ISSN 09628924.

doi: 10.1016/j.tcb.2009.10.002. URL `http://linkinghub.elsevier.com/retrieve/pii/S0962892409002402`.

Rebecca C. Taylor, Sean P. Cullen, and Seamus J. Martin. Apoptosis: controlled demolition at the cellular level. *Nature Reviews Molecular Cell Biology*, 9(3): 231–241, March 2008. ISSN 1471-0072, 1471-0080. doi: 10.1038/nrm2312. URL `http://www.nature.com/doifinder/10.1038/nrm2312`.

William G Telford. Stem cell side population analysis and sorting using DyeCycle violet. *Current protocols in cytometry / editorial board, J. Paul Robinson, managing editor ... [et al.]*, Chapter 9:Unit9.30, January 2010. ISSN 1934-9300. doi: 10. 1002/0471142956.cy0930s51. PMID: 20069528.

William G Telford, Jolene Bradford, William Godfrey, Robert W Robey, and Susan E Bates. Side population analysis using a violet-excited cell-permeable DNA binding dye. *Stem cells (Dayton, Ohio)*, 25(4):1029–1036, April 2007. ISSN 1066-5099. doi: 10.1634/stemcells.2006-0567. PMID: 17185610.

Edward C Thornborrow, Sejal Patel, Anthony E Mastropietro, Elissa M Schwartzfarb, and James J Manfredi. A conserved intronic response element mediates direct p53-dependent transcriptional activation of both the human and murine bax genes. *Oncogene*, 21(7):990–999, February 2002. ISSN 0950-9232. doi: 10.1038/sj.onc.1205069. PMID: 11850816.

York Tomita, Natasha Marchenko, Susan Erster, Alice Nemajerova, Alexander Dehner, Christian Klein, Hongguang Pan, Horst Kessler, Petr Pancoska, and Ute M Moll. WT p53, but not tumor-derived mutants, bind to bcl2 via the DNA binding domain and induce mitochondrial permeabilization. *The Journal*

of biological chemistry, 281(13):8600–8606, March 2006. ISSN 0021-9258. doi: 10.1074/jbc.M507611200. PMID: 16443602.

Christin Tse, Alexander R Shoemaker, Jessica Adickes, Mark G Anderson, Jun Chen, Sha Jin, Eric F Johnson, Kennan C Marsh, Michael J Mitten, Paul Nimmer, Lisa Roberts, Stephen K Tahir, Yu Xiao, Xiufen Yang, Haichao Zhang, Stephen Fesik, Saul H Rosenberg, and Steven W Elmore. ABT-263: a potent and orally bioavailable bcl-2 family inhibitor. *Cancer research*, 68(9):3421–3428, May 2008. ISSN 1538-7445. doi: 10.1158/0008-5472.CAN-07-5836. PMID: 18451170.

Koen van de Wetering and Sunny Sapthu. ABCG2 functions as a general phytoestrogen sulfate transporter in vivo. *FASEB journal: official publication of the Federation of American Societies for Experimental Biology*, 26(10):4014–4024, October 2012. ISSN 1530-6860. doi: 10.1096/fj.12-210039. PMID: 22707564.

Daniel Vare, Petra Groth, Rickard Carlsson, Fredrik Johansson, Klaus Erixon, and Dag Jenssen. DNA interstrand crosslinks induce a potent replication block followed by formation and repair of double strand breaks in intact mammalian cells. *DNA repair*, 11(12):976–985, December 2012. ISSN 1568-7856. doi: 10.1016/j.dnarep.2012.09.010. PMID: 23099010.

Sandra Varum, Ana S. Rodrigues, Michelle B. Moura, Olga Momcilovic, Charles A. Easley, João Ramalho-Santos, Bennett Van Houten, and Gerald Schatten. Energy metabolism in human pluripotent stem cells and their differentiated counterparts. *PLoS ONE*, 6(6):e20914, June 2011. ISSN 1932-6203. doi: 10.1371/journal.pone.0020914. URL http://dx.plos.org/10.1371/journal.pone.0020914.

Lyubomir T Vassilev, Binh T Vu, Bradford Graves, Daisy Carvajal, Frank Podlaski, Zoran Filipovic, Norman Kong, Ursula Kammlott, Christine Lukacs, Christian Klein, Nader Fotouhi, and Emily A Liu. In vivo activation of the p53 pathway by small-molecule antagonists of MDM2. *Science (New York, N.Y.)*, 303(5659): 844–848, February 2004. ISSN 1095-9203. doi: 10.1126/science.1092472. PMID: 14704432.

Alejandro Vazquez-Martin, Sílvia Cufí, Bruna Corominas-Faja, Christina Oliveras-Ferraros, Luciano Vellon, and Javier A Menendez. Mitochondrial fusion by pharmacological manipulation impedes somatic cell reprogramming to pluripotency: new insight into the role of mitophagy in cell stemness. *Aging*, 4(6):393–401, June 2012. ISSN 1945-4589. PMID: 22713507.

Antoine Vekris, Delphine Meynard, Marie-Christine Haaz, Martine Bayssas, Jacques Bonnet, and Jacques Robert. Molecular determinants of the cytotoxicity of platinum compounds: the contribution of in silico research. *Cancer research*, 64(1):356–362, January 2004. ISSN 0008-5472. PMID: 14729645.

Andrea Ventura, David G Kirsch, Margaret E McLaughlin, David A Tuveson, Jan Grimm, Laura Lintault, Jamie Newman, Elizabeth E Reczek, Ralph Weissleder, and Tyler Jacks. Restoration of p53 function leads to tumour regression in vivo. *Nature*, 445(7128):661–665, February 2007. ISSN 1476-4687. doi: 10.1038/nature05541. PMID: 17251932.

Andreas Villunger, Ewa M Michalak, Leigh Coultas, Franziska Müllauer, Gunther Böck, Michael J Ausserlechner, Jerry M Adams, and Andreas Strasser. p53- and drug-induced apoptotic responses mediated by BH3-only proteins puma and

noxa. *Science (New York, N.Y.)*, 302(5647):1036–1038, November 2003. ISSN 1095-9203. doi: 10.1126/science.1090072. PMID: 14500851.

Maria L.H. Vlaming, Jurjen S. Lagas, and Alfred H. Schinkel. Physiological and pharmacological roles of ABCG2 (BCRP): recent findings in abcg2 knockout mice. *Advanced Drug Delivery Reviews*, 61(1):14–25, January 2009. ISSN 0169409X. doi: 10.1016/j.addr.2008.08.007. URL `http://linkinghub.elsevier.com/retrieve/pii/S0169409X08002536`.

Thanh-Trang Vo, Jeremy Ryan, Ruben Carrasco, Donna Neuberg, Derrick J. Rossi, Richard M. Stone, Daniel J. DeAngelo, Mark G. Frattini, and Anthony Letai. Relative mitochondrial priming of myeloblasts and normal HSCs determines chemotherapeutic success in AML. *Cell*, 151(2):344–355, October 2012. ISSN 00928674. doi: 10.1016/j.cell.2012.08.038. URL `http://linkinghub.elsevier.com/retrieve/pii/S0092867412011191`.

B Vogelstein, D Lane, and A J Levine. Surfing the p53 network. *Nature*, 408 (6810):307–310, November 2000. ISSN 0028-0836. doi: 10.1038/35042675. PMID: 11099028.

Karen H Vousden and David P Lane. p53 in health and disease. *Nature reviews. Molecular cell biology*, 8(4):275–283, April 2007. ISSN 1471-0072. doi: 10.1038/nrm2147. PMID: 17380161.

Dong Wang and Stephen J Lippard. Cellular processing of platinum anticancer drugs. *Nature reviews. Drug discovery*, 4(4):307–320, April 2005. ISSN 1474-1776. doi: 10.1038/nrd1691. PMID: 15789122.

Kitchener D Wilson, Ning Sun, Mei Huang, Wendy Y Zhang, Andrew S Lee,

Zongjin Li, Shan X Wang, and Joseph C Wu. Effects of ionizing radiation on self-renewal and pluripotency of human embryonic stem cells. *Cancer research*, 70(13):5539–5548, July 2010. ISSN 1538-7445. doi: 10.1158/0008-5472. CAN-09-4238. PMID: 20530673.

Wen Xue, Lars Zender, Cornelius Miething, Ross A Dickins, Eva Hernando, Valery Krizhanovsky, Carlos Cordon-Cardo, and Scott W Lowe. Senescence and tumour clearance is triggered by p53 restoration in murine liver carcinomas. *Nature*, 445(7128):656–660, February 2007. ISSN 1476-4687. doi: 10.1038/nature05529. PMID: 17251933.

Richard J Youle and Andreas Strasser. The BCL-2 protein family: opposing activities that mediate cell death. *Nature reviews. Molecular cell biology*, 9(1):47–59, January 2008. ISSN 1471-0080. doi: 10.1038/nrm2308. PMID: 18097445.

Xin Zhang, Irina Neganova, Stefan Przyborski, Chunbo Yang, Michael Cooke, Stuart P Atkinson, George Anyfantis, Stefan Fenyk, W Nicol Keith, Stacey F Hoare, Owen Hughes, Tom Strachan, Miodrag Stojkovic, Philip W Hinds, Lyle Armstrong, and Majlinda Lako. A role for NANOG in g1 to s transition in human embryonic stem cells through direct binding of CDK6 and CDC25A. *The Journal of Cell Biology*, 184(1):67–82, January 2009. ISSN 1540-8140. doi: 10.1083/jcb.200801009. PMID: 19139263.

R Zhao, K Gish, M Murphy, Y Yin, D Notterman, W H Hoffman, E Tom, D H Mack, and A J Levine. Analysis of p53-regulated gene expression patterns using oligonucleotide arrays. *Genes & Development*, 14(8):981–993, April 2000. ISSN 0890-9369. PMID: 10783169.

S Zhou, J D Schuetz, K D Bunting, A M Colapietro, J Sampath, J J Morris,

I Lagutina, G C Grosveld, M Osawa, H Nakauchi, and B P Sorrentino. The ABC transporter Bcrp1/ABCG2 is expressed in a wide variety of stem cells and is a molecular determinant of the side-population phenotype. *Nature medicine*, 7(9): 1028–1034, September 2001. ISSN 1078-8956. doi: 10.1038/nm0901-1028. PMID: 11533706.